



**30th GASEOUS
ELECTRONICS CONFERENCE**

EXECUTIVE COMMITTEE

F. C. Fehsenfeld, CHAIRMAN
NOAA ERL

W. P. Allis, HONORARY CHAIRMAN
Massachusetts Institute of Technology

J. R. Peterson, SECRETARY
SRI International

G. L. Rogoff, TREASURER
Westinghouse Research Laboratories

D. M. Benenson
State University of New York
at Buffalo

M. J. W. Boness
Avco Everett Research Laboratory

R. H. Bullis
United Technologies Research Center

J. H. Ingold
General Electric, Cleveland

O. P. Judd
Los Alamos Scientific Laboratory

J. T. Verdeyen
University of Illinois at
Urbana-Champaign

**A Topical Conference of the
American Physical Society**

Sponsored by:
**SRI International
American Physical Society
Division of Electron and Atomic Physics**

Assisted by:
Office of Naval Research

PROGRAM AND ABSTRACTS

Thirtieth Annual Gaseous Electronics Conference

18-21 October 1977

李隆吉

Long C. Lee
649 Maybell Ave.
Palo Alto, Ca. 94306

LOCAL COMMITTEE:

- M. J. Coggiola
- W. Cooke
- P. C. Cosby
- K. A. Cromwell
- T. D. Gaily
- T. F. Gallagher
- K. T. Gillen
- R. M. Hill
- D. L. Huestis
- M. V. McCusker
- J. T. Moseley
- R. P. Saxon

(415) 494-3217

CONTENTS

Program	1
Session AA: Rare Gas Halides	17
Session AB: LTE Arcs I	21
Session BA: Rare Gas Halides and Dimer Ion Spectroscopy	27
Session BB: LTE Arcs II	32
Session CA: Kinetics and Modeling of Rare Gas-Halide Lasers	36
Session CB: Electrode Effects and Vacuum Arcs	41
Session DA: Rare Gas-Halide Discharges	47
Session DB: Arcs and Flows	51
Session FA: Electron Attachment and Transport, and Negative Ions	56
Session FB: Metal-Halide, Metal-Rare Gas, and Other Diatomics	63
Session GA: Electron-Molecule Scattering	70
Session GB: Glow Discharges	75
Session HA: Electron-Atom Excitation and Ionization	81
Session HB: Discharges and Afterglows	88
Session JA: Rare Gas, Metal, and Group VI Kinetics and Spectroscopy	94
Session JB: Charge Transfer and Fast Beams	100
Session KA: Breakdown, Corona, and Boundary Effects	107
Session KB: Ion-Ion and Ion-Electron Recombination	112
Session LA: Processes in Various Lasers	117
Session LB: Reactions of Excited Species	124
Session MA: Photodissociation and Photodetachment	131
Session MB: Processes in CO ₂ Lasers	137
Session NA: Ion Molecule Reactions	142
Session NB: CO Lasers	149
Index to Abstracts	154

30th ANNUAL GASEOUS ELECTRONICS CONFERENCE

PROGRAM

OCTOBER 17, 1977

MONDAY EVENING, 7:30-10:00 p.m.

REGISTRATION AND MIXER (CASH BAR)

Foyer of the Palo Alto Room, Rickey's Hyatt House

SESSION AA: RARE GAS HALIDES Chairman: W. L. Nighan, United Technology	SESSION AB: LTE ARCS I Chairman: J. Uhlenbusch, Universität Dusseldorf
Room A	Room B
AA-1 ELECTRONIC STRUCTURE AND RADIATIVE PROPERTIES OF THE RARE GAS HALIDES P. J. Hay and T. H. Dunning (20 min)	AB-1 TRANSPORT PROPERTIES AND CONVECTION IN VERTICAL HIGH PRESSURE MERCURY ARCS R. J. Zollweg (20 min)
AA-2 DIATOMICS-IN-MOLECULES (DIM) CALCULATIONS ON THE TRIATOMIC RARE GAS HALIDES: Rg ₂ X N. E. Schlotter and D. L. Huestis (7 min)	AB-2 CATAPHORETIC SEGREGATION OF SODIUM IN A HIGH PRESSURE SODIUM DISCHARGE R. S. Bergman and J. H. Ingold (14 min)
AA-3 RADIATIVE LIFETIMES OF KrF* AND XeF* R. Burnham and S. K. Searles (7 min)	AB-3 MEASUREMENTS OF THE ELECTRON DENSITY IN A HIGH-PRESSURE Na-Xe DISCHARGE J. H. Waszink and H. J. Flinsenbergh (7 min)
AA-4 RADIATION LIFETIMES AND QUENCHING RATE CONSTANTS FOR KrF AND XeF G. P. Quigley and W. M. Hughes (7 min)	AB-4 DETERMINATION OF THE Na AND Hg VAPOUR PRESSURE IN HIGH PRESSURE Na-Hg DISCHARGES J. J. de Groot and J. A. J. M. van Vliet (7 min)
AA-5 PHOTOLYSIS OF XeF ₂ BY ArCl*: COLLISIONAL DEACTIVATION OF XeF*(B) J. G. Eden and R. W. Waynant (7 min)	AB-5 "D" LINE RADIATION IN AFTERGLOW OF HIGH PRESSURE SODIUM ARC E. F. Wyner (7 min)
AA-6 RADIATIVE LIFETIME AND QUENCHING KINETICS FOR THE XeF(B 1/2) STATE C. H. Fisher and R. E. Center (7 min)	AB-6 SPECTROSCOPIC INVESTIGATION OF K AND Rb ARC PLASMAS R. Bleekrode (7 min)
	AB-7 SPECTROSCOPIC MEASUREMENTS ON Dy/Cs/Hg/I-ARCS W. J. Van den Hoek and J. A. Visser (7 min)

COFFEE BREAK

OCTOBER 18, 1977

TUESDAY MORNING, 10:45 a.m.

SESSION BA; RARE GAS HALIDES AND DIMER ION SPECTROSCOPY Chairman: R. P. Saxon, SRI International	session AB continued
BA-1 ELECTRONIC STRUCTURE AND SPECTRAL PROPERTIES OF RARE-GAS DIMER IONS (Ne_2^+ , Ar_2^+ , Kr_2^+ , Xe_2^+) AND TRI-ATOMIC RARE-GAS FLUORIDES (Ar_2F , Kr_2F) W. R. Wadt, D. C. Cartwright, P. J. Hay and J. S. Cohen (7 min)	AB-8 THE COLLISIONAL BROADENING OF Li 4603 A IN DENSE PLASMAS A. J. Barnard and E. Kallne (7 min)
BA-2 PHOTODISSOCIATION OF NOBLE GAS DIMER IONS H. H. Michels and R. H. Hobbs (7 min)	AB-9 STATISTICAL ASPECTS OF PARTIALLY IONIZED SYSTEMS G. H. Ecker (20 min)
BA-3 PHOTOELECTRON SPECTRUM OF THE Xe_2 DIMER P. M. Dehmer and J. L. Dehmer (7 min)	SESSION BB: LTE ARCS II Chairman: R. J. Zollweg, Westinghouse Room B
BA-4 PHOTODISSOCIATION CROSS SECTIONS IN Ar_2^+ FOR THE Σ - Σ TRANSITION D. Katayama, J. F. Paulson and T. L. Rose (7 min)	BB-1 A COMPLEX IMPEDANCE MODEL OF AN ELECTRODELESS DISCHARGE P. Haugsjaa, W. McNeill, and R. Regan (7 min)
BA-5 PHOTODISSOCIATION CROSS SECTIONS OF Ar_2^+ , Kr_2^+ , AND Xe_2^+ FROM 6950 TO 8600 Å L. C. Lee, G. P. Smith, T. M. Miller, and P. C. Cosby (7 min)	BB-2 INTERACTION OF MICROWAVES WITH HIGH-PRESSURE DISCHARGES W. McNeill, P. Haugsjaa, and R. Regan (7 min)
BA-6 UV ABSORPTIONS OF RARE GAS IONS IN E-BEAM PUMPED RARE GASES R. O. Hunter, J. Oldenettel, C. Howton, and M. V. McCusker (7 min)	BB-3 SPECTROMETRIC GAS COMPOSITION MEASUREMENTS OF UF_6 RF PLASMAS W. C. Roman and M. F. Zabielski (7 min)
BA-7 ABSORPTION PROCESSES AND MOLECULAR ION KINETICS IN E-BEAM EXCITED RARE GAS PLASMAS J. B. West and W. H. Long, Jr. (7 min)	BB-4 THERMODYNAMIC AND TRANSPORT PROPERTIES OF UF_6 AND $\text{UF}_6 + \text{H}_2$ MIXTURES R. W. Liebermann and C. L. Chen (7 min)
BA-8 CF_2 ABSORPTION IN KrF DISCHARGE LASERS J. Goldhar and J. R. Murray (7 min)	BB-5 THERMODYNAMIC AND TRANSPORT PROPERTIES OF SF_6 R. W. Liebermann and C. L. Chen (7 min)

LUNCH - 12:15-1:45 P.M.

<p>SESSION CA: KINETICS AND MODELING OF RARE GAS-HALIDE LASERS Chairman: D. W. Setser, Kansas State University</p>	<p>Room A</p>	<p>Room B</p>
<p>CA-1 KINETIC MODEL OF AN XeF* LASER L. J. Palumbo, T. F. Finn, and L. F. Champagne (7 min)</p>		<p>SESSION CB: ELECTRODE EFFECTS AND VACUUM ARCS Chairman: G. Eckhardt, Hughes Research Laboratories</p>
<p>CA-2 FORMATION AND QUENCHING KINETICS OF XeF* IN E-BEAM PUMPED Ne/Xe/F₂ MIXTURES M. Rokni, J. H. Jacob, and J. A. Mangano (7 min)</p>		<p>CB-1 INITIATION PROCESSES OF CATHODE SPOTS IN VACUUM ARCS J. Mitterauer (20 min)</p>
<p>CA-3 ABSORPTION IN E-BEAM PUMPED XeF* LASER MEDIUM WITH Ne AND Ar DILUENTS M. Rokni, J. H. Jacob and J. A. Mangano (7 min)</p>		<p>CB-2 CALCULATED CHARACTERISTICS OF ISOLATED, STATIONARY CATHODE SPOTS ON COPPER ELECTRODES L. P. Harris (7 min)</p>
<p>CA-4 INVESTIGATIONS OF XeF LASER CHARACTERISTICS WITH Ne AND Ar DILUENTS J. Hsia, J. A. Mangano, M. Rokni, A. Hawryluk and J. H. Jacob (7 min)</p>		<p>CB-3 CATHODE SPOT PROPERTIES OF A DC MERCURY VACUUM ARC G. Eckhardt (7 min)</p>
<p>CA-5 MULTIATMOSPHERE OPERATION OF THE KrF LASER IN NEON DILUENT L. F. Champagne (7 min)</p>		<p>CB-4 EROSION PRODUCTS FROM THE CATHODE SPOT REGION OF A COPPER VACUUM ARC D. T. Tuma, C. L. Chen, and D. K. Davies (7 min)</p>
<p>CA-6 THEORETICAL MODEL FOR UV-PREIONIZED FAST TRANSVERSE DISCHARGE KrF LASERS A. E. Greene and C. A. Brau (7 min)</p>		<p>CB-5 MEASUREMENT OF THE ANGULAR DISTRIBUTION OF THE ION CURRENT FROM A VACUUM ARC J. V. R. Heberlein (7 min)</p>
<p>CA-7 PARAMETRIC AND SCALING STUDIES OF SPARK-PREIONIZED DISCHARGE-EXCITED RARE-GAS HALIDE LASERS D. E. Rothe (7 min)</p>		<p>CB-6 ANODE HEAT FLUXES DURING THE INITIAL PHASE OF PULSED HIGH INTENSITY ARCS D. Johnson and E. Pfender (7 min)</p>
<p>CA-8 ELECTRON KINETICS OF RARE GAS HALOGEN LASERS W. L. Morgan, R. A. Haas and R. D. Franklin (7 min)</p>		<p>CB-7 ION AND NEUTRAL EXCITED STATE DENSITIES IN A MULTI-CATHODE-SPOT VACUUM ARC R. Boxman and S. Goldsmith (7 min)</p>
		<p>CB-8 TEMPERATURE OF THE CATHODE REGION OF THE SURGE DISCHARGE IN VACUUM L. M. Burrage (7 min)</p>
		<p>CB-9 THE EFFECT OF ALUMINA INCLUSIONS ON THE BREAK-DOWN AND EMISSION PROPERTIES OF COPPER SURFACES IN VACUUM G. A. Farrall, F. G. Hudda and R. H. Johnston (7 min)</p>

COFFEE BREAK

OCTOBER 18, 1977

TUESDAY AFTERNOON, 3:45 p.m.

SESSION DA: RARE GAS-HALIDE DISCHARGES Chairman: J.G. Eden, Naval Research Laboratory		Room A	Room B
DA-1	PLASMA KINETICS IN KrF* LASER DISCHARGES W. L. Nighan (7 min)		DB-1 TEMPERATURE PROFILES AND FLUCTUATION LEVELS MEASURED IN AN ARC IN AN AXIAL GAS FLOW J. F. Driscoll, R. W. Anderson, K. P. Zondervan, and K. L. Zondervan (7 min)
DA-2	DISCHARGE STABILITY AND SCALING OF THE KrF LASER W. H. Long (7 min)		DB-2 EXPERIMENTAL AND THEORETICAL STUDY OF A DC ARC IN A CONSTANT DIAMETER NOZZLE FLOW H. T. Negamatsu (7 min)
DA-3	QUASI-STEADY OPERATION OF SELF-SUSTAINED RARE-GAS-HALIDE DISCHARGES G. L. Rogoff, L. E. Kline, J. L. Pack, and W. H. Kasner (7 min)		DB-3 DIELECTRIC RECOVERY RATE OF REPETITIVE DISCHARGES IN A TRANSVERSE GAS FLOW J. F. Driscoll (7 min)
DA-4	TIME-RESOLVED DISCHARGE DEVELOPMENT IN HIGH PRESSURE, GLOW-DISCHARGE EXCIMER LASERS W. J. Sarjeant, A. J. Alcock and K. E. Leopold (7 min)		DB-4 INVESTIGATIONS OF THE DIELECTRIC BREAKDOWN OF SF-6 AT HIGH TEMPERATURES B. Eliasson and E. Schade (7 min)
DA-5	HOLLOW CATHODE DISCHARGES IN ELECTRONEGATIVE GASES S. Griffin, M. Simmons, J. T. Verdeyen, and B. E. Cherrington (7 min)		DB-5 TRANSPORT MECHANISMS IN THE ANODE REGION OF HIGH INTENSITY ARCS C. H. Liu and E. Pfender (7 min)
			DB-6 CALCULATION AND EXPERIMENTAL PROCEDURES IN TURBULENT ARCS Y-K Chien and D. M. Benenson (7 min)
			DB-7 ACOUSTICAL RESONANCES IN CYLINDRICAL CESIUM ARCS H. L. Witting (7 min)

TUESDAY EVENING, 7:30 p.m.

SESSION E: WORKSHOP ON KINETIC PROCESSES IN RARE GAS-HALIDE LASERS Moderator: D.C. Lorents, SRI International		Room A
E-1	INTRODUCTION AND OVERVIEW - C. Brau (30 min)	
E-2	EXCITED STATE REACTION KINETICS - D. Setser (20 min)	
E-3	NEUTRAL KINETICS OF ArF - C. Chen (20 min)	
E-4	THREE-BODY ION RECOMBINATION - M. Flannery (15 min)	
	DISCUSSION OF XeF KINETICS (45 min)	

SESSION FA: ELECTRON ATTACHMENT AND TRANSPORT, AND NEGATIVE IONS		SESSION FB: METAL-HALIDE, METAL-RARE GAS, AND OTHER DIATOMICS	
Chairman: S. F. Wong, Yale University		Chairman: J. J. Ewing, Lawrence Livermore Labs	
Room A		Room B	
FA-1	ISOTOPICALLY SELECTIVE PHOTO-ENHANCED DISSOCIATIVE ATTACHMENT IN SF ₆ C. L. Chen and P. J. Chantry (20 min)	FB-1	HgCl* (B-X) EMISSIONS AT 560 NM FROM E-BEAM PUMPED Ar/Hg/Cl ₂ MIXTURES J. A. Margevicius, M. V. McCusker, D. L. Huestis, and D. C. Lorents (7 min)
FA-2	CALCULATION OF DISSOCIATIVE ATTACHMENT AND VIBRATIONAL EXCITATION IN F ₂ R. J. Hall and W. L. Nighan (7 min)	FB-2	REACTIVE QUENCHING OF Hg(SP _{1,0}) BY HALOGENS AND HALOGENATED MOLECULES T. Shay, J. E. Velazco and G. J. Collins (7 min)
FA-3	ATTACHMENT OF SLOW ELECTRONS TO Br ₂ AND HBr D. W. Trainor and M. J. W. Boness (7 min)	FB-3	EFFECT OF DISSOCIATIVE RECOMBINATION ON STEADY STATE EXCITED ATOM AND ELECTRON DENSITIES IN HIGH PRESSURE DISCHARGES A. V. Phelps, D. Leep, and A. Gallagher (7 min)
FA-4	ELECTRON ATTACHMENT TO POLYMERS OF NITROUS OXIDE AND CARBON DIOXIDE C. E. Klotz and R. N. Compton (7 min)	FB-4	HIGH-POWER DISCHARGES IN Na AND TI DOPED Xe H. Rothwell, D. Leep, and A. Gallagher (7 min)
FA-5	ELECTRON AFFINITIES OF STRONGLY POLAR MOLECULES W. R. Garrett (7 min)	FB-5	MODELS OF HIGH-POWER DISCHARGES IN Na-DOPED Xe. R. Shuker, W. L. Morgan, A. Gallagher and A. V. Phelps (7 min)
FA-6	THE DRIFT VELOCITY OF LOW ENERGY ELECTRONS IN OXYGEN I. D. Reid and R. W. Crompton (7 min)	FB-6	E-BEAM EXCITATION OF MIXTURES OF TI AND Xe L. A. Schlie and D. L. Drummond (7 min)
FA-7	ELECTRON DRIFT VELOCITIES IN FLUORINE-HELIUM MIXTURES S. R. Hunter, J. Fletcher, S. R. Foltyn, and K. J. Nygaard	FB-7	ANALYTICAL MODEL OF THALLIUM-MERCURY KINETICS R. P. Benedict, L. A. Schlie, and D. L. Drummond (7 min)
FA-8	ELECTRON ATTACHMENT IN FLUORINE-RARE GAS MIXTURES K. J. Nygaard, S. R. Hunter, S. R. Foltyn, and J. Fletcher (12 min)	FB-8	FLUORESCENCE YIELDS OF METAL HALIDE VAPORS EXCITED BY PHOTODISSOCIATION J. Maya (7 min)
FA-9	DRIFT VELOCITIES OF NEGATIVE FLUORINE IONS IN HELIUM J. Fletcher, S. R. Hunter, S. R. Foltyn, and K. J. Nygaard	FB-9	THE ELECTRONIC STATES OF ALKALI-RARE GAS DIATOMICS B. Laskowski, S. Langhoff, and J. Stallcop (7 min)
FA-10	TRANSPORT PARAMETERS OF A PULSED TOWNSEND DISCHARGE IN HYDROGEN AT ELEVATED SWARM ENERGIES S. R. Hunter, J. Fletcher, and H. A. Blevin (7 min)	FB-10	LASER CANDIDATE MOLECULES IN EXCITED STATES OF IONIC CHARACTER D. L. Huestis (7 min)
FA-11	PRODUCTION AND CONFINEMENT OF NEGATIVE HYDROGEN IONS IN LOW PRESSURE HYDROGEN PLASMA M. Bacal, E. Nicolopolou and H. J. Doucet (7 min)	FB-11	A PERIODIC TABLE FOR DIATOMIC MOLECULES R. Hefferlin (7 min)

COFFEE BREAK

OCTOBER 19, 1977

WEDNESDAY MORNING, 10:45 a.m.

SESSION GA: ELECTRON-MOLECULE SCATTERING Chairman: R.N. Crompton, Australian National University		SESSION GB: GLOW DISCHARGES Chairman: A. Garscadden, A. F. Aeropropulsion Lab	
Room A		Room B	
GA-1	EXCITATION OF MOLECULAR NITROGEN BY LOW-ENERGY ELECTRON IMPACT IN THE REGION OF THE DISSOCIATION THRESHOLD D. Spence, R. H. Huebner, and P. D. Burrow (12 min)	GB-1	MEASUREMENT OF TOWNSEND IONIZATION COEFFICIENT AND BREAKDOWN POTENTIALS FOR THE PENNING MIXTURES OF Ne AND Kr A. K. Bhattacharya (7 min)
GA-2	EXCITATION OF RYDBERG STATES IN THE ENERGY REGION OF THE SCHUMAN-RUNGE CONTINUUM OF O ₂ BY LOW-ENERGY ELECTRON IMPACT D. Spence and R. H. Huebner (7 min)	GB-2	CALCULATION OF TOWNSEND'S α AT HIGH E/p J. H. Ingold and R. S. Bergman (7 min)
GA-3	EXCITATION OF (2p π) (np σ) $1\sigma_g^+$ BY ELECTRON-H ₂ IMPACT F. A. Sharpton, R. L. Day and R. J. Anderson (7 min)	GB-3	THE NEGATIVE GLOW EFFICIENCY WITH RECOMBINATION W. P. Allis (7 min)
GA-4	RESONANCES IN ELECTRON SCATTERING FROM SUBSTITUTED BENZENE MOLECULES P. D. Burrow, J. A. Michejda and K. D. Jordan (7 min)	GB-4	PRE-BREAKDOWN DISCHARGES W. D. Parfitt and L. E. Kline (7 min)
GA-5	APPLICATION OF SEMICLASSICAL PERTURBATION SCATTERING THEORY TO e ⁻ + CO F. T. Smith and A. P. Hickman (7 min)	GB-5	IONIZATION PROCESSES IN THE LOW-PRESSURE Hg-Ar DISCHARGE R. A. J. Keijser, L. Vriens, F. A. S. Ligthart (7 min)
GA-6	MOMENTUM TRANSFER AND VIBRATIONAL EXCITATION CROSS SECTIONS FOR ELECTRON-CARBON MONOXIDE COLLISIONS IN THE RANGE 1-4 eV H. B. Milloy (7 min)	GB-6	THE INFLUENCE OF AC CURRENT WAVEFORM ON ULTRA-VIOLET OUTPUT OF LOW-PRESSURE MERCURY-NEON GAS DISCHARGE S. G. Johnson (7 min)
GA-7	RATE COEFFICIENTS AND INELASTIC MOMENTUM TRANSFER CROSS SECTIONS FOR ELECTRONIC EXCITATION OF N ₂ BY ELECTRONS D. C. Cartwright (7 min)	GB-7	MULTIVALUED V-I CHARACTERISTIC OF LOW PRESSURE Na-Ne DISCHARGES M. J. C. van Gemert and T. G. Verbeek (7 min)
GA-8	ABSOLUTE OSCILLATOR STRENGTHS (10-60 eV) FOR PHOTOABSORPTION, PHOTOIONISATION AND BREAKDOWN OF H ₂ C. E. Brion, K. H. Tan, Ph. E. Van der Leeuw, and M. J. Van der Wiel (7 min)	GB-8	A NEW THEORY FOR STRIATIONS WITH EXPERIMENTAL VERIFICATIONS E. E. Kempe (7 min)
		GB-9	AN EXACT THEORY OF IONIZATION WAVES IN NITROGEN W. H. Long, Jr. (7 min)

LUNCH 12:15 - 1:45 p.m.

SESSION HA: ELECTRON-ATOM EXCITATION AND IONIZATION Chairman: P. Burrow, University of Nebraska	SESSION HB: DISCHARGES AND AFTERGLOWS Chairman: L. Chanin, University of Minnesota
Room A HA-1 ELECTRON IMPACT EXCITATION OF SiIII W. D. Robb (7 min) HA-2 ELECTRON EXCITATION OF THE ALKALI RESONANCE LINES S. T. Chen and A. Gallagher (7 min) HA-3 ELECTRON IMPACT EXCITATION OF METASTABLE ARGON AND KRYPTON ATOMS H. A. Hyman (7 min) HA-4 ABSOLUTE DIFFERENTIAL CROSS SECTIONS FOR ELASTIC AND INELASTIC (P_1 , P_2) EXCITATION OF ATOMIC BARIUM BY ELECTRON IMPACT S. Jensen, D. Register, and S. Trajmar (10 min) HA-5 ELECTRON IMPACT SPECTROSCOPY OF LASER EXCITED BARIUM D. F. Register, S. W. Jensen, S. Trajmar, and R. T. Poe HA-6 ELECTRONIC COLLISIONAL TRANSFER BETWEEN HIGH RYDBERG LEVELS OF HELIUM J.-F. Delpech, J. Boulmer and F. Devos (7 min) HA-7 A NEW TECHNIQUE TO DIFFERENTIATE BE- TWEEN RESONANCE (NEGATIVE ION) AND DOUBLY-EXCITED AUTOIONIZING STATES IN THE IONIZATION CONTINUUM OF THE RARE GASES D. Spence HA-8 MEASUREMENT OF DOUBLY-EXCITED STATES IN Ne FROM SCATTERED ELECTRON SPECTRA D. Spence (14 min) HA-9 STUDIES OF POST-COLLISION INTERACTIONS IN Ne FROM SCATTERED ELECTRON SPECTRA D. Spence HA-10 ELECTRON PHOTON ANGULAR CORRELATION MEASUREMENT FOR THE 2^1P_1 STATE OF HELIUM V. C. Sutcliffe, N. Steph, G. N. Haddad and D. E. Golden (7 min) HA-11 TRIPLE-DIFFERENTIAL CROSS SECTION FOR LOW- ENERGY ELECTRON IMPACT IONIZATION OF ARGON S. P. Hong and E. C. Beay (7 min) HA-12 ELECTRON IMPACT DOUBLE IONIZATION CROSS SECTIONS OF K^+ IONS R. K. Feeney and W. E. Sayle (7 min)	Room B HB-1 STABILIZATION OF GLOW DISCHARGES BY SUPERSONIC FLOWS E. Wasserstrom, Y. Crispin and O. Biblarz (7 min) HB-2 THE MAXIMUM CONSTRICTION PHASE OF A WEAKLY IONIZED DISCHARGE IN HELIUM L. Oster (7 min) HB-3 PRESSURE AND VOLTAGE DEPENDENCE OF THE ELECTRON DENSITY IN A PULSED HELIUM DISCHARGE M. Stockton, M. J. Cleary, and S. A. Taylor (7 min) HB-4 ANALYSIS OF THE GLOW DISCHARGE IN OXYGEN J. W. Dettmer, W. F. Bailey, M. R. Stamm, and A. Garscadden (7 min) HB-5 OZONE BALANCE IN AN ELECTRON BEAM CONTROLLED DISCHARGE IN OXYGEN G. Fournier, R. Lucas, D. Pigache, and M. Lecuillier (7 min) HB-6 OPTO-GALVANIC SPECTROSCOPY OF GLOW DISCHARGES: IONIZATION PROCESSES K. C. Smyth and P. K. Schenck (7 min) HB-7 SOLAR RADIATION MAINTAINED OPTICAL DISCHARGE IN CESIUM A. J. Palmer (7 min) HB-8 THE EFFECT OF ELECTRON TEMPERATURE RELAXATION ON PLASMA AFTERGLOW PROCESSES G. L. Ogram, J-S Chang, J. G. Laframboise and R. M. Hobson (7 min) HB-9 THE PRODUCTION OF EXCITED CESIUM IONS IN HELIUM- CESIUM AFTERGLOWS C. P. de Vries and H. J. Oskam (7 min) HB-10 RELAXATION OF NEODYMIUM IN A WEAKLY IONIZED EXPANDING PLASMA H-L Chen, R. Bedford, C. Borzilleri, W. Brunner, and M. Hayes (7 min)

COFFEE BREAK

WEDNESDAY AFTERNOON, 4:00 p.m.

OCTOBER 19, 1977

SESSION I: WORKSHOP ON ELECTRON-EXCITED STATE COLLISIONS

Moderator: A. V. Phelps, JILA

Room A

A. Collisions of Electrons with Excited Atoms and Molecules

Contributions by: M. R. Flannery

A. Garscadden and M. L. Lake

M. J. W. Boness

J. A. Michejda

B. The Role of Electron Collisions with Excited Atoms in Discharges

Contributions by: B. E. Cherrington

W. L. Morgan and R. A. Haas

W. L. Nighan

J. Mangano

OCTOBER 20, 1977

THURSDAY MORNING, 8:30 a.m.

SESSION JA: RARE GAS, METAL, AND GROUP VI KINETICS AND SPECTROSCOPY		SESSION JB: CHARGE TRANSFER AND FAST BEAMS	
Chairman: J. Mangano, Avco		Chairman: N. Adams, University of Birmingham	
Room A	Room B		
<p>JA-1 RADIATIVE LIFETIMES AND REACTION RATES OF THE LOWEST BOUND MOLECULAR STATES IN KRYPTON AND KRYPTON-XENON MIXTURES F. H. K. Rambow, T. D. Bonifield, and G. K. Walters (7 min)</p> <p>JA-2 SPECTROSCOPIC STUDIES ON RECOMBINATION FED LINE EMISSIONS IN HIGH PRESSURE RARE GASES A. Szoke and E. V. George (7 min)</p> <p>JA-3 KINETICS AND SPECTRA OF E-BEAM EXCITED Ar/Xe MIXTURES H. T. Powell and A. Szoke (7 min)</p> <p>JA-4 PERFORMANCE OF RARE GAS EXCIMER LASER AND FLUORESCENCE SOURCES H. T. Powell, J. J. Ewing, R. D. Franklin and R. A. Haas (7 min)</p> <p>JA-5 RARE GAS EXCIMER RADIATION PUMPING FOR PHOTO-LYTIC LASER MEDIA R. A. Haas, R. D. Franklin, J. J. Ewing, C. W. Werner, and W. L. Morgan (7 min)</p> <p>JA-6 COLLISION-INDUCED PREDISSOCIATION OF Sr₂ MOLECULES R. R. Freeman and P. F. Liao (7 min)</p> <p>JA-7 MULTIPHOTON IONIZATION OF C₃ DIMERS THROUGH DISSOCIATIVE MOLECULAR STATES J. A. Anderson, C. B. Collins, D. Popescu, and I. Popescu (7 min)</p> <p>JA-8 SEQUENTIAL TWO-PHOTON IONIZATION OF Li₂ AND Na₂ G. Reck, B. P. Mathur and E. W. Rothe (7 min)</p> <p>JA-9 PHOTOLYTIC PRODUCTION OF S(1S) IN LIQUID Ar L. Abouaf, J. Margevicius, M. V. McCusker and D. C. Lorents (7 min)</p> <p>JA-10 OPTICAL EMISSIONS FROM DOPED CONDENSED RARE GASES EXCITED BY ELECTRONS J. Margevicius, L. Abouaf, M. V. McCusker, D. L. Huestis, and D. C. Lorents (7 min)</p>	<p>JB-1 SPIN DEPENDENT CHARGE TRANSFER IN LOW-ENERGY COLLISIONS BETWEEN HELIUM IONS AND CESIUM ATOMS (20 min) H. A. Schuessler</p> <p>JB-2 SPIN-CONSERVATION IN DOUBLE CHARGE TRANSFER COLLISIONS G. D. Myers, J. G. Ambrose, P. B. James and J. J. Leventhal (7 min)</p> <p>JB-3 FINE STRUCTURE IN LOW ENERGY CHARGE TRANSFER IN ARGON K. B. McAfee, W. E. Falconer, R. S. Hozaek and D. J. McClure (7 min)</p> <p>JB-4 ATOMIC ION-METAL ATOM CHARGE TRANSFER J. A. Rutherford and D. A. Vroom (7 min)</p> <p>JB-5 EXCITED HYDROGEN ATOM AND ARGON ATOM PRODUCTION BY CHARGE TRANSFER OF (Ar⁺)[*] IN H₂ H. L. Rothwell, R. C. Amme, and B. Van Zyl (7 min)</p> <p>JB-6 CHARGE TRANSFER REACTIONS OF EXCITED O⁺(²D) AND C⁺(⁴P) STATE IONS WITH NEUTRAL MOLECULES T. F. Moran and J. B. Wilcox (7 min)</p> <p>JB-7 ELECTRON TRANSFER IN COLLISIONS OF DOUBLY CHARGED ATOMIC IONS WITH RARE-GAS ATOMS FOR PRIMARY-ION ENERGIES BELOW 100 eV W. B. Maier (7 min)</p> <p>JB-8 ENERGY TRANSFER IN COLLISIONS OF He AND H ATOMS WITH N₂, CO, AND O₂ G. H. Bearman and J. J. Leventhal (7 min)</p> <p>JB-9 COLLISIONAL DISSOCIATION OF NO₃⁻ AND OF SOME SOLVATED HYDROXYL IONS J. F. Paulson (7 min)</p> <p>JB-10 IONIZING COLLISIONS BETWEEN MOLECULES IN THE NEAR-THRESHOLD ENERGY REGION N. G. Utterback and B. Van Zyl (7 min)</p>		

COFFEE BREAK

OCTOBER 20, 1977

THURSDAY MORNING, 10:45 a.m.

SESSION KA: BREAKDOWN, CORONA, AND BOUNDARY EFFECTS Room A Chairman: L. E. Kline, Westinghouse		Session JB continued
KA-1	CONTINUOUS CURRENT IN THE POSITIVE POINT-TO-PLANE CORONA M. Hirsh and M. Goldman (7 min)	JB-11 FORMATION OF UF_6^- BY IMPACT OF Cs ATOMS R. J. Warmack, J. A. D. Stockdale, and R. N. Compton (7 min)
KA-2	STREAMER PULSES AND THE SPARK TRANSITION IN POSITIVE POINT-TO-PLANE CORONA M. Hirsh and G. Hartmann (7 min)	SESSION KB: ION-ION AND ION-ELECTRON RECOMBINATION Chairman: T. M. Miller, SRI International Room B
KA-3	THE ROLE OF NEUTRAL DENSITY VARIATIONS IN THE FORMATION OF STREAMER INDUCED SPARK E. Marode, F. Bastien and M. Bakker (7 min)	KB-1 BINARY MUTUAL NEUTRALISATION RATE COEFFICIENTS DETERMINED IN A FLOWING AFTERGLOW D. Smith and M. J. Church (20 min)
KA-4	PREVENTION OF SPARK DEVELOPMENT IN INTENSE CORONA DISCHARGES M. J. Kofoid (7 min)	KB-2 MUTUAL NEUTRALIZATION OF NH_4^+ (NH_3) _n IONS WITH NO_2^- AND Cl^- M. J. Church, D. Smith, and T. M. Miller
KA-5	SURFACE ARCS G. H. Ecker (7 min)	KB-3 THEORY OF THREE BODY IONIC RECOMBINATION FOR DIFFERENT IONIC AND NEUTRAL PARTICLE MASSES J. M. Wadehra and J. N. Bardsley (7 min)
KA-6	A COLD CATHODE GLOW DISCHARGE ELECTRON GUN D. L. Jordan and G. G. Isaacs (7 min)	KB-4 THREE-BODY RECOMBINATION RATE FOR K^+e IN ARGON L. D. Schearer (7 min)
KA-7	SOLUTION OF THE COLLISIONLESS PLASMA-SHEATH EQUATION FOR ION EXTRACTION THROUGH AN APERTURE J. H. Wheaton and J. C. Whitson (7 min)	KB-5 MERGED BEAM STUDIES OF THE DISSOCIATIVE RECOMBINATION OF CH^+ J. B. A. Mitchell, J. W. McGowan and H. R. Froelich (7 min)
KA-8	INVESTIGATION OF THE VELOCITY DISTRIBUTION OF NEUTRALS IN THE WALL REGION OF LOW PRESSURE He-DISCHARGES J. Hackmann and J. Uhtenbusch (7 min)	KB-6 DISSOCIATIVE RECOMBINATION IN KRYPTON: DEPENDENCE OF THE TOTAL RATE COEFFICIENT AND EXCITED-STATE PRODUCTION ON ELECTRON TEMPERATURE Y-J Shiu and M. A. Biondi (7 min)
		KB-7 ELECTRON TEMPERATURE DEPENDENCE OF RECOMBINATION OF HYDRONIUM CLUSTER-IONS AND ELECTRONS C. M. Huang, M. Whitaker, M. A. Biondi, and R. Johnson (7 min)
Business Meeting, 12:15 - 12:45 p.m.		

LUNCH 12:45 - 2:15 P.M.

SESSION LA: PROCESSES IN VARIOUS LASERS Chairman: W. H. Long, Jr., Northrop		Room A	SESSION LB: REACTIONS OF EXCITED SPECIES Chairman: B. Van Zyl, Denver University		Room B
LA-1	PARAMETER STUDIES ON A CO REACTOR-EXCITED LASER AT ROOM TEMPERATURE D. A. McArthur	(7 min)	LB-1	COLLISIONAL RELAXATION OF IONIC $2p_{3/2}$ EXCITED STATES IN RARE GASES E. Weber and W. Buttler	(7 min)
LA-2	A NUCLEAR PUMPED LASER USING Ne-CO AND Ne-CO ₂ MIXTURES M. A. Prellas, J. H. Anderson, F. P. Boody, S. J. S. Nagalingam and G. H. Miley	(7 min)	LB-2	O(¹ S) PRODUCTION THROUGH COLLISIONAL ELECTRONIC ENERGY TRANSFER FROM TWO-PHOTON EXCITED Xe ATOMS D. Kligler, D. Pritchard, W. K. Bischel and C. K. Rhodes	(7 min)
LA-3	OPTICALLY PUMPED ATOMIC IRON LASER D. W. Trainor and S. A. Mani	(7 min)	LB-3	QUENCHING OF N ₂ (A ³ Σ _u ⁺) BY I ₂ A Mandl and J. J. Ewing	(7 min)
LA-4	POPULATION INVERSION FOR THE RESONANCE TRANSITIONS OF ATOMS IN RECOMBINING PLASMAS W. L. Bohn	(7 min)	LB-4	CHEMILUMINESCENCE STUDIES OF ALKALINE EARTH COLLISION WITH METASTABLE ARGON J. H. Goble, D. C. Hartman and J. S. Winn	(7 min)
LA-5	A TECHNIQUE FOR DETERMINING GAS TEMPERATURE AND ATOMIC DENSITY FROM ABSORPTION MEASUREMENTS L. H. Taylor, R. B. Feldman, D. W. Feldman and C. S. Liu	(7 min)	LB-5	EXCITATION REACTIONS OF He(2 ³ S) AND Ar(3 ² P _{0,2}) METASTABLE ATOMS WITH CH ₄ , C ₂ H ₄ , C ₂ H ₂ , Cyclo-C ₃ H ₆ , C ₆ H ₆ , C ₆ F ₆ AND C ₆ F ₅ H G. W. Taylor, R. S. F. Chang, and D. W. Setser	(7 min)
LA-6	TEMPORALLY RESOLVED Cu DENSITY MEASUREMENTS IN CONTINUOUSLY-PULSED CuBr LASER DISCHARGES C. S. Liu, D. W. Feldman and L. A. Weaver	(7 min)	LB-6	REACTION RATE MEASUREMENTS OF HELIUM METASTABLE SPECIES AT ATMOSPHERIC PRESSURES A. J. Cunningham and G. D. Myers	(7 min)
LA-7	DIFFUSION PROCESSES AND QUENCHING MECHANISMS IN METAL VAPOR LASERS B. G. Bricks, T. W. Karras, R. S. Anderson and R. J. Homsey	(7 min)	LB-7	ENERGY TRANSFER BETWEEN HELIUM METASTABLE PARTICLES AND NEON D. W. Ernie and H. J. Oskam	(7 min)
LA-8	CHARGE TRANSFER PUMPING OF THE HELIUM-NITROGEN LASER IN AN ELECTRICAL AVALANCHE DISCHARGE AT ATMOSPHERIC PRESSURES C. B. Collins, K. N. Taylor, and J. M. Carroll	(7 min)	LB-8	PENNING AND ASSOCIATIVE IONIZATION IN SYSTEMS OF TWO METASTABLE REACTANTS R. H. Neynaber and S. Y. Tang	(10 min)
LA-9	THE MODELLING OF He ⁺ + N ₂ LASER W. W. Jones and A. W. Ali	(7 min)	LB-9	CHARGE TRANSFER IN COLLISIONS OF He ⁺ WITH Ne [*] S. Y. Tang and R. H. Neynaber	(7 min)
LA-10	EXCITATION MECHANISM OF THE He-Se LASER W. L. Little, J. K. Boyer and G. J. Collins	(7 min)	LB-10	REACTIONS OF METASTABLE EXCITED IONS OF O, O ₂ , AND NO WITH O ₂ , N ₂ , CO, CO ₂ , NO, H ₂ AND Ar AT THERMAL ENERGIES J. Gosik, A. B. Rakshit, N. D. Twiddy, N. G. Adams, and D. Smith	(7 min)
LA-11	EXPERIMENTAL DETERMINATION OF THE COLLISIONAL EXCITATION AND DE-EXCITATION COEFFICIENTS OF THE UPPER LASER STATES OF Ar ⁺ J. Jolly and J. L. Delcroix	(7 min)	LB-11	FLOW-DRIFT TUBE STUDIES OF THE REACTIONS OF NO ⁺ WITH N ₂ , CO ₂ , CH ₄ , SO ₂ , AND Ar I. Dotan, D. L. Albritton, and F. C. Fehsenfeld	(7 min)

OCTOBER 20, 1977

THURSDAY EVENING, 5:00 p.m.

MOLECULAR PHYSICS CENTER OPEN HOUSE

5:00 - 6:30 p.m.

SOCIAL HOUR

International Building Courtyard, SRI

6:30 p.m.

BANQUET

International Building Dining Room, SRI

7:30 p.m.

GUEST SPEAKER

Dr. C. Barry Raleigh
U. S. Geological Survey

Topic: EARTHQUAKES AND EARTHQUAKE PREDICTION
IN THE U.S. AND CHINA

<p>SESSION MA: PHOTODISSOCIATION AND PHOTODETACHMENT Chairman: J. Laudenslager, Jet Propulsion Laboratory</p>	<p>SESSION MB: PROCESSES IN CO₂ LASERS Chairman: G. Fournier, O.N.E.R.A.</p>
<p>Room A</p>	<p>Room B</p>
<p>MA-1 PHOTOFRAGMENT SPECTROSCOPY OF OZONE IN THE UV REGION 270-310 nm AND AT 600 nm C. E. Fairchild, E. J. Stone and G. M. Lawrence (10 min)</p>	<p>MB-1 A 16 μm CO₂ LASER KINETICS MODEL L. H. Taylor, Y. S. Evangelista, D. W. Feldman, and W. H. Kasner (7 min)</p>
<p>MA-2 PHOTOFRAGMENT SPECTROSCOPY OF OC10 IN THE WAVELENGTH REGION 300-340 nm C. E. Fairchild and G. M. Lawrence</p>	<p>MB-2 MEGAWATT OPERATION OF AN (0, 0⁰, 2) → (1, 0⁰, 1) SEQUENCE-BAND HIGH-PRESSURE CO₂ LASER R. A. Fisher, B. J. Feldman, C. R. Pollock, S. W. Simons and R. G. Tercovich (7 min)</p>
<p>MA-3 PREDISSOCIATION AND PHOTOFRAGMENT SPECTROSCOPY OF QUARTET STATES OF O₂⁺ J. T. Moseley, M. Tadjeddine, B. A. Huber, R. Abouaf, and P. C. Cosby (7 min)</p>	<p>MB-3 ACOUSTIC INSTABILITY MODEL FOR HIGH POWER CWEDL LASERS D. Korff, S. L. Glickler, and J. D. Daugherty (20 min)</p>
<p>MA-4 PHOTODESTRUCTION OF IONS FORMED IN O₂/SO₂ GAS MIXTURES J. A. Vanderhoff (7 min)</p>	
<p>MA-5 PHOTODESTRUCTION CROSS SECTIONS OF ATMOSPHERIC NEGATIVE IONS G. P. Smith, L. C. Lee, P. C. Cosby, J. R. Peterson, and J. T. Moseley (7 min)</p>	
<p>MA-6 PHOTODISSOCIATION OF ATMOSPHERIC POSITIVE IONS P. C. Cosby, G. P. Smith, J. T. Moseley, and L. C. Lee (7 min)</p>	<p>MB-4 ATTACHMENT AND ELECTRODE SURFACE FIELD EFFECTS ON ARC FORMATION IN LASER GLOW DISCHARGES L. J. Denes, L. E. Kline, R. R. Mitchell, and R. J. Spreadbury (7 min)</p>
<p>MA-7 FORMATION AND PHOTODISSOCIATION OF PEROXY NO₃⁻ J. T. Moseley, P. C. Cosby, J. R. Peterson and G. P. Smith (7 min)</p>	<p>MB-5 PLASMA AND CHEMICAL PROCESSES IN CO₂ VOLUME DISCHARGES W. J. Sarjeant and C. Willis (7 min)</p>
<p>MA-8 ZERO CORE-CONTRIBUTION CALCULATION OF PHOTODETACHMENT OF ATOMIC NEGATIVE IONS HAVING AN OUTERMOST d-ORBITAL W. B. Clodius, R. M. Stehman, and S. B. Woo (10 min)</p>	<p>MB-6 A SIMULATED HIGH-REPETITION RATE TEA CO₂ LASER R. Turner and R. A. Murphy (7 min)</p>
<p>MA-9 ZERO CORE-CONTRIBUTION CALCULATION OF PHOTODETACHMENT OF O₂⁻ AND S₂⁻ R. M. Stehman and S. B. Woo</p>	<p>MB-7 CALCULATION OF THE TRANSPORT COEFFICIENTS OF MOLECULAR SPECIES IN LASER DISCHARGES R. M. Thomson (7 min)</p>
<p>MA-10 HIGH RESOLUTION PHOTODETACHMENT CROSS SECTION OF A DIPOLAR MOLECULAR ION P. L. Jones, S. E. Novick, J. H. Futrell, and W. C. Lineberger (7 min)</p>	

COFFEE BREAK

SESSION NA: ION MOLECULE REACTIONS Chairman: J. Leventhal, University of Missouri - St. Louis	SESSION NB: CO LASERS Chairman: R. Center, Mathematical Sciences Northwest
<p>NA-1 ION-MOLECULE REACTIONS AT THERMAL ENERGIES STUDIED USING THE SIFT N. G. Adams, D. Smith, and D. Grief (20 min)</p>	<p>NB-1 SPARK PHOTOIONIZATION OF NITRIC OXIDE AND ETHYLENE IN CARBON MONOXIDE LASER MIXTURES D. R. Suhre (7 min)</p>
<p>NA-2 A STUDY OF THE BINARY AND TERNARY REACTIONS OF CH₃⁺ IONS AT THERMAL ENERGIES D. Smith and N. G. Adams (7 min)</p>	<p>NB-2 UV-SUSTAINED CARBON MONOXIDE LASER PLASMA D. R. Suhre and S. A. Wutzke (7 min)</p>
<p>NA-3 SOME POSITIVE ION-MOLECULE REACTIONS OF STRATOSPHERIC INTEREST N. G. Adams, D. Smith, and T. M. Miller (7 min)</p>	<p>NB-3 V-I CHARACTERISTICS OF SELF-SUSTAINED CO LASER DISCHARGES R. R. Mitchell, L. E. Kline, D. R. Suhre, and S. A. Wutzke (7 min)</p>
<p>NA-4 THE REACTIONS OF O₂⁺, O₂ WITH CO₂, O₃ AND CH₄ AND O₂⁺, O₃ WITH CH₄ AND H₂O I. Dotan, F. C. Fehsenfeld, and D. L. Albritton (7 min)</p>	<p>NB-4 ELECTRICAL CHARACTERISTICS AND VIBRATIONAL EXCITATION IN A SUPERSONIC CO ELECTRIC DISCHARGE A. C. Stanton, R. K. Hanson, and M. Mitchner (7 min)</p>
<p>NA-5 THEORY OF He-X GAS MIXTURE PLASMA AFTERGLOW AND ITS APPLICATION TO ION-MOLECULE REACTION MEASUREMENTS BY A PULSED-FLOWING AFTERGLOW TECHNIQUE J-S Chang, R. M. Hobson, G. L. Ogram, R. H. Prince and A. Saleh (7 min)</p>	<p>NB-5 POKER-CONTROLLED PULSED DISCHARGES IN SUPERSONIC CO FLOWS W. M. Moeny and J. P. O'Loughlin (7 min)</p>
<p>NA-6 MEASUREMENT OF THE RATE COEFFICIENTS FOR THE BIMOLECULAR AND TERMOLECULAR CHARGE TRANSFER REACTIONS OF He₂⁺ C. B. Collins and F. W. Lee (7 min)</p>	<p>NB-6 PERFORMANCE OF A CW PULSER-SUSTAINER CARBON MONOXIDE ELECTRIC-DISCHARGE SUPERSONIC LASER D. J. Monson and G. Srinivasan (7 min)</p>
<p>NA-7 CHARGE TRANSFER STUDIES OF Ne-N₂ BY PROTON EXCITATION C. H. Chen, J. P. Judish, and M. G. Payne (7 min)</p>	<p>NB-7 PARAMETRIC EVALUATION OF COLLISIONAL PROCESSES IN AN E-BEAM SUSTAINED CO LASER D. J. Pistorosi and D. J. Nelson (7 min)</p>
<p>NA-8 PRODUCT DISTRIBUTIONS FOR SOME THERMAL ENERGY CHARGE TRANSFER REACTIONS OF RARE GAS IONS J. B. Laudenslager, V. G. Anichich, W. T. Huntress, Jr., and J. H. Futrell (7 min)</p>	<p>NB-8 EXPERIMENTAL FINDINGS ON THE GLOW-ARC TRANSITION IN DISCHARGES IN THE SUPERSONIC CO LASER M. F. Weisbach and D. J. Nelson (7 min)</p>
<p>NA-9 MEASUREMENTS OF ION-MOLECULE REACTION RATES IN A HIGH TEMPERATURE DRIFT TUBE-MASS SPECTROMETER APPARATUS A. K. Chen, R. Johnson, and M. A. Biondi (7 min)</p>	
<p>NA-10 REACTIONS OF CO₂⁺, CO₂⁺ AND COCO⁺ WITH THE OXIDES OF NITROGEN IN CO₂ J. L. Moruzzi and P. Coxon (7 min)</p>	
<p>NA-11 ION MOBILITY "RESONANCE" IN HIGH PRESSURE HELIUM PLASMAS PRODUCED BY BETA PARTICLES C. C. Leiby, Jr. (7 min)</p>	
<p>NA-12 ION MOBILITIES IN DENSE HELIUM VAPOR B. L. Henson (7 min)</p>	

SESSION AA

9:00 AM - 10:30 AM, Tuesday, October 18

Room A

RARE GAS HALIDES

Chairman: W. L. NIGHAN,
UNITED TECHNOLOGY

AA-1

Electronic Structure and Radiative Properties of the Rare Gas Halides.* P. J. HAY and T. H. DUNNING, Los Alamos Scientific Laboratory. -- The electronic states of the rare gas fluorides (ArF, KrF, XeF) and xenon halides (XeCl, XeBr, XeI) are investigated using ab initio configuration interaction techniques. Calculated emission wavelengths and lifetimes for the major bands in these systems are compared with existing experimental data. Simulations of the emission spectra are also reported based on the theoretically obtained quantities.

AA-2

Diatomics-in-Molecules (DIM) Calculations on the Triatomic Rare Gas Halides: Rg_2X .* N.E. SCHLOTTER and D.L. HUESTIS, Molecular Physics Center, SRI International --Emission spectra of the triatomic rare gas halides: Ar₂F (290 ± 25 nm), Kr₂F (400 ± 30 nm), Ar₂Cl (246 ± 14 nm), Kr₂Cl (325 ± 15 nm), and Xe₂Cl (450 ± 20 nm) have been observed.¹ We have performed DIM calculations including spin-orbit coupling on Ne₂F, Ar₂F, Kr₂F, and Kr₂Cl which support the $Rg_2^+X^- \rightarrow Rg_2X$ assignment. In the case of Ar₂F the DIM results are in close agreement with more elaborate calculations.^{2,3} DIM calculations, for a minimum of effort, supply the energy surfaces needed for calculating absorption and fluorescence spectra as well as molecular dynamics (although good potential curves are required for the ground and excited states of the constituent diatomics).

*Supported by DARPA through the U.S. Army BMDATC.

1. D.L. Huestis, D.C. Lorents, N.E. Schlotter, R.M. Hill, M.V. McCusker, and H.H. Nakano, 32nd Symposium on Molecular Spectroscopy, Columbus, OH 13-17 June 1977.
2. W.R. Wadt and P.J. Hay, Appl. Phys. Lett. 30, 573 (1977).
3. H.H. Michels & R.H. Hobbs, Chem. Phys. Lett. 48, 158 (1977).

AA-3

Radiative Lifetimes of KrF* and XeF*,[†] R.

BURNHAM and S. K. SEARLES, Naval Research Laboratory, Washington, D. C. 20375 - The radiative lifetimes of the upper laser levels of the krypton fluoride and xenon fluoride molecules which emit at 249 nm and 351 nm respectively have been measured using a pulsed laser photolysis technique. In our experiments the excited state of the rare-gas halide of interest is produced directly through dissociative photoexcitation of the parent rare-gas difluoride (KrF₂ or XeF₂) with radiation at 193 nm from a discharge pumped argon fluoride laser. The resulting fluorescence at 249 or 351 nm is found to follow a single exponential decay subsequent to the termination of the 10 nsec laser excitation pulse. The radiative lifetimes measured in this way are 9.0 ± 0.6 nsec for KrF* and 15.0 ± 0.8 nsec for XeF*.

[†]Work supported in part by DARPA

AA-4

RADIATION LIFETIMES AND QUENCHING RATE CONSTANTS FOR KrF AND XeF. G.P.Quigley & W.M.Hughes, Los Alamos Scientific Laboratory.

Excitation of atomic Xe or Kr in the presence of F₂ by a wavelength selective 2.5 ns long argon excimer photolytic source was used to initiate the reaction sequence resulting in the formation of excited KrF or XeF. The radiative lifetimes of the KrF and XeF laser transitions have been determined. For KrF* this was found to be 11 ns. This work constitutes the first such measurement of the KrF* lifetime. The results are in agreement with the calculated values¹ if an effective lifetime for the collisionally mixed II 3/2, III 1/2 electronic states¹ is invoked. The pressure and wavelength dependence of these lifetimes will be discussed. For KrF* the two body quenching by F₂ is 5.6×10^{-10} cm³/sec and the three body quenching by Kr is 3×10^{-31} cm⁶/sec. Similar results for XeF will be presented. The three body quenching of KrF* by Kr results in the formation of Kr₂F which emits a continuum centered near 415 nm. The radiative lifetime of this new excimer has been determined along with the quenching rate by F₂.

1. P.J.Hay & T.H.Dunning, J. Chem. Phys. 66, 1306 (1977)

AA-5

Photolysis of XeF₂ By ArCl* : Collisional Deactivation of XeF*(B). ‡ J.G. Eden and R.W. Waynant, Naval Research Laboratory, Washington, D.C. 20375 -- The radiative lifetime and deactivation rates of XeF*(B) by Ar and Xe have been measured by photolyzing XeF₂ with ArCl* excimer radiation at 175 nm. The short (~3 ns FWHM) ArCl spontaneous emission pulse was generated by exciting 99.5% Ar/0.5% Cl₂ (p_{total}=2050 Torr) gas mixtures with a Febetron 706 electron beam. Upon absorbing a 175 nm photon, the XeF₂ dissociates, forming XeF*(B) which subsequently radiates at 351 nm. By monitoring the exponential decay rate of the B→X emission as a function of the diluent pressure, the following radiative and collisional rates were determined:

- a) XeF*(B) → XeF(X) + 351 nm: τ = 14.25 ± 0.5 ns,
- b) XeF*(B) + Ar → products; k_b = 3.58 · 10⁻¹² cm³ · sec⁻¹,
- c) XeF*(B) + Xe → products; k_c = 3.27 · 10⁻¹¹ cm³ · sec⁻¹,
- d) XeF*(B) + 2Xe → products; k_d = 2.36 · 10⁻²⁹ cm⁶ · sec⁻¹,
- e) XeF*(B) + XeF₂ → products; k_e = 2.56 · 10⁻¹⁰ cm³ · sec⁻¹.

The significance of these results to XeF laser development will be discussed.

‡ Work supported in part by DARPA.

AA-6

Radiative Lifetime and Quenching Kinetics for the XeF (B 1/2) State, C.H. Fisher and R.E. Center, Mathematical Sciences Northwest, Inc. -- A state-selective laser-induced-fluorescence technique has been used to determine the radiative lifetime and quenching kinetics for the XeF (B 1/2) excited state. Fluorine atoms are formed by flash dissociating a mixture of UF₆ and Xe in He. After a suitable delay to allow recombination of Xe and F atoms, ground state XeF molecules are excited to the XeF (B 1/2) state by passing a 3511 Å XeF laser beam through the cell. The fluorescence decay at 3533 Å is monitored perpendicular to the exciting light using a spectrometer-photomultiplier combination. Quenching rate coefficients for the collision partners He, Ne, Xe, F₂, and NF₃ have been determined. Fluorescence emission at 460 nm due to collisional transfer from the XeF (B 1/2) to the XeF (C 1/2) state has also been observed.

*Supported by DARPA Order No. 1806, ONR Contract No. N00014-76-C-1066.

SESSION AB

9:00AM - 11:20 AM, Tuesday, October 18

Room B

LTE ARCS I

Chairman: J. UHLENBUSCH,
UNIVERSITÄT DUSSELDORF

AB-1

Transport Properties and Convection in Vertical High Pressure Mercury Arcs. R.J. ZOLLWEG, Westinghouse R&D Center--Free convection in wall-stabilized mercury arcs at several mercury pressures and power loadings has been studied. Because convection is sensitive to the difference between power input and radiative and conductive losses, emphasis has been placed on obtaining transport properties consistent with measured arc temperature profiles and the radiation escaping. The electrical conductivity obtained using the electron-Hg elastic scattering cross section deduced by Rockwood was found superior to that of McCutchen. The cylindrical arc convection model developed by Lowke¹ was used to obtain numerical results. These show in agreement with experiment: (1) constriction at the electrodes with increased axial arc temperature and electric fields, (2) the conical arc appearance at the lower electrode which increases in length with mercury pressure and with decreasing arc power, and (3) increased convection velocities with increase in mercury pressure and decrease in arc power. No evidence was found for an eddy diffusion increase in radial heat loss at high pressure which had been suggested earlier to account for reduced radiation escaping.

¹J.J. Lowke, Bull. of APS 21 (2), 134 (1976).

AB-2

Cataphoretic Segregation of Sodium in a High Pressure Sodium Discharge. R. S. BERGMAN and J. H. INGOLD, General Electric Co., Cleveland, Ohio 44112--The conservation of momentum equation, coupled with the continuity equation, is used to derive a theoretical model for steady-state cataphoretic segregation of sodium in a high pressure sodium discharge. The analysis assumes a convection free LTE plasma consisting of xenon, mercury and sodium atoms, sodium ions and electrons. The arc current, which is easily related to the electron flux, is chosen as the independent variable. The model gives the functional dependence of the sodium pressure gradient on the arc radius, arc gap, and various initial partial pressures, as well as the various binary diffusion coefficients involved. The role of the central-axis temperature is also made explicit. The theoretical predictions of the sodium pressure increase from anode to cathode show good agreement with measurements over a limited range of currents and initial partial pressures.

AB-3

Measurements of the electron density in a high-pressure Na-Xe discharge.

J.H.WASZINK and H.J.FLINSENBURG, Philips Research Labs., Eindhoven, The Netherlands. Measurements have been made in an ac discharge (50 Hz, 6A rms) at current maximum, p_{Na} is varied from 100 to 200 Torr, $p_{Xe} \approx 1200$ Torr, tube ϕ 7.5 mm. A small amount of K has been added (K/Na ratio 4×10^{-3}). The electron density n_e is derived from the profile of the Stark-broadened, optically thin K 6S-4P line at 6939 Å (FWHM $\lesssim 2$ Å in the present case). The side-on intensity distribution is recorded with a scanning Fabry-Perot interferometer (FSR 9.6 Å, finesse about 40). Fourier transformation and Abel inversion yields the local profile. Thus, n_e is found as a function of the radial coordinate. Temperatures are calculated from p_{Na} and n_e with the Saha equation. Axis values are $n_e = (1.0 \pm 0.2) \times 10^{22} \text{ m}^{-3}$, $T = 4100 \pm 120$ K for $p_{Na} = 100$ Torr, and $n_e = (2.1 \pm 0.4) \times 10^{22} \text{ m}^{-3}$, $T = 4350 \pm 120$ K for $p_{Na} = 200$ Torr.

AB-4

DETERMINATION OF THE Na AND Hg VAPOUR PRESSURE IN HIGH PRESSURE Na-Hg DISCHARGES. J.J. de Groot and J.A.J.M.van Vliet, Philips' Gloeilampenfabrieken, Lighting Division, Eindhoven, The Netherlands. In order to compare model calculations of high pressure Na-Hg discharges with experiments, it is necessary to measure the Na and Hg vapour pressures. For a pure sodium discharge the Na vapour pressure can be determined from the measured contour of the self-reversed D-lines¹⁾. The partial Na vapour pressure in a Na-Hg discharge can be determined in a similar way from the wavelength difference between line centre and the maximum in the undisturbed blue wing of the self-reversed D-lines. An analogous method has been developed for the measurement of the Hg vapour pressure from the wavelength difference between the line centre and the maximum in the red wing of the self-reversed Hg254nm line. This relationship is based on the assumption of van der Waals broadening due to Hg-Hg interaction. Using these spectroscopically determined values of partial vapour pressures in the numerical solution of the energy balance equation, good agreement is found between the measured and calculated electrical data for discharges with various mercury and sodium partial vapour pressures.

1) Teh-Sen-Jen et al. J.Q.S.R.T. 9 (1969) 487

"D" Line Radiation in Afterglow of High Pressure Sodium Arc. E. F. WYNER, GTE Sylvania, Danvers, Massachusetts -- Spectral data on the shape and magnitude of the sodium D line in the afterglow of a high pressure sodium arc is presented. In the early afterglow, the line shape changes from self reversed to a broad band as the arc temperature profile relaxes toward the wall temperature. In the late afterglow, the plasma temperature becomes isothermal with the wall and the intensity at 589 nm can be used to determine this temperature, (1500°K and above). Spectral diagnostics of this unique high temperature isothermal plasma will be discussed. The decay of wall temperature with time in the very late afterglow is consistent with reasonable values for the thermal emissivity of the wall material.

Spectroscopic Investigation of K and Rb Arc Plasmas.

R. Bleekrode, Philips Research Laboratories, Eindhoven, The Netherlands.

A study has been made of dimer emission from ac operated K and Rb noble gas(Kr,Xe)discharges between 250 and 900nm. In addition to earlier work¹ the following observations were made (vapour pressures between 100 and 1000 torr): (i) a symmetrical band around 421.5nm (half-width \approx 2nm) with a tail to longer wavelengths; (ii) bands having maxima at about 452 and 457 nm. The bands of (i) and (ii) do not depend on the type or pressure of the noble gas and seem to indicate the existence of electronic states of K₂ not identified before; (iii) bands with maxima at about 377, 379 and 381nm possibly associated with the E-X system; (iv) bandlike structure between 310 and 365nm. For Rb similar observations were made: (i) bands with maxima at about 453, 465 and 480nm together with strong emission of the "known" 475nm band; (ii) band structure between 390 and 400nm; (iii) strong emission features with superimposed absorption in the 540-610nm system². The spectral analysis of high-temperature K and Rb plasmas is much complicated by the presence of these bands.

¹ K. Schmidt, ICPIG, Paris, 1963.

² J.M. Brom and H.P. Broida, J. Chem. Phys. 61, 982 (1974).

AB-7

Spectroscopic Measurements on Dy/Cs/Hg/I-arcs.

W.J. van den HOEK and J.A. VISSER, Philips Gloeilampenfabrieken, Lighting Division, Eindhoven, Netherlands

The broadening of the temperature profile of constricted¹ Dy/I/Hg-arcs by the addition of CsI has been studied. The action of CsI may be reduced if excess iodine is present. The effect of increasing the iodine-cesium ratio was studied in a series of Cs/I/Hg-arcs. The arc constriction and the axis temperature increase with increasing amounts of iodine. This can be related to the reduction in the electrical conductivity at lower temperatures due to the formation of negative iodine ions, and to radiation from HgI². The 50 Hz AC arcs (400W) were operated horizontally and centered by means of a 50 Hz magnetic field ($H_{\text{eff}}=40-400 \text{ Am}^{-1}$). Under these conditions arc oscillations in the vertical plane with frequencies of 0.5-5 Hz are sometimes observed in Dy/Cs/Hg/I-arcs. A mechanism involving a time-varying constriction due to metal iodide evaporation is discussed in terms of the balance between the Lorentz force and the buoyant force.

1. J.F.Waymouth, *Electric Discharge Lamps*, MIT Press Cambridge Mass. (1971) p. 172, 216.
2. R.J. Zollweg et al., *J.Appl.Phys.* 46, 3828 (1975).

AB-8

The Collisional Broadening of Li 4603 A in Dense Plasmas. A. J. BARNARD and E. KALLNE, Univ. of British Columbia, Vancouver, Canada.*

--Electron and ion collisions with neutral lithium atoms in a plasma lead to a broadening of the 4603 A (2p-4d) line, and also to the appearance of an overlapping, forbidden (2p-4f) component. We have calculated the combined line shape for electron densities in the range 10^{15} to 10^{17} cm^{-3} , using the impact approximation for the electron collisions and the quasistatic approximation for the ion interactions. At densities above 10^{17} cm^{-3} the intensity of the forbidden component exceeds that of the allowed line. Measurements of the profile have been made with a carbon arc and a shock heated hydrogen plasma (both seeded with lithium) as sources, for electron densities in the range of 10^{16} to 10^{17} cm^{-3} . The measured and computed profiles are in reasonable agreement, indicating that at high densities the ions can be regarded as static, even for the forbidden component.

*Supported by the NRC of Canada.

Statistical Aspects of Partially Ionized Systems. G.H. ECKER, Ruhr-Universität, Germany

-- The statistics of the partially ionized system is even more complicated and involved than that of the fully ionized plasma. Therefore we characterize the state of the understanding reached by representative examples. In doing so, we consider first the equilibrium state with the problem of the "quasi-free contributions". Formalisms for systems with non-equilibrium radiation only are critically discussed and their applicability is demonstrated. Finally stationary general non-equilibrium states are considered and their present understanding is described. In closing we discuss where the frontiers of further investigations should be.

SESSION BA

10:45 AM - 12:15 PM, Tuesday, October 18

Room A

RARE GAS HALIDES AND DIMER ION SPECTROSCOPY

Chairman: R. P. SAXON, SRI INTERNATIONAL

BA-1

Electronic Structure and Spectral Properties of Rare-Gas Dimer Ions (Ne_2^+ , Ar_2^+ , Kr_2^+ , Xe_2^+) and Triatomic Rare-Gas Fluorides (Ar_2F , Kr_2F). W. R. WADT, D. C. CARTWRIGHT, P. J. HAY and J. S. COHEN, Los Alamos Scientific Laboratory. -- Near-ultraviolet absorption spectra for the $I(1/2) \rightarrow II(1/2)$ transition have been calculated for Ne_2^+ , Ar_2^+ , Kr_2^+ , and Xe_2^+ using ab initio configuration interaction methods. The spectra are similar except that the position of maximum absorption shifts to longer wavelengths for the heavier rare gases. The absorption cross-sections are tabulated at the wavelengths of the KrF, XeBr, XeCl and XeF lasers. Ab initio configuration interactions calculations were performed on Ar_2F and Kr_2F to determine their spectral properties, both emission and absorption wavelengths, lifetimes and oscillator strengths. The results also shed light on the stability and mechanisms of formation for these triatomic species in the ArF and KrF lasers.

BA-2

Photodissociation of Noble Gas Dimer Ions. H. H. MICHELS* and R. H. HOBBS, United Technologies Research Center. -- A systematic study of the photodissociation of noble gas dimer ions has been carried out to determine the relative importance of these species in analyzing loss mechanisms in the noble gas-halide excimer systems. This study included detailed quantum mechanical calculations of the pertinent potential energy curves for the ions Ne_2^+ , Ar_2^+ , Kr_2^+ and Xe_2^+ , and an analysis of photodissociation from the $A \ ^2\Sigma_u^+(1/2_u)$ state by absorption to the $B \ ^2\Pi_g(1/2_g, 3/2_g)$ or $D \ ^2\Sigma_g^+(1/2_g)$ states. For the heavier systems (Kr_2^+ and Xe_2^+) spin-orbit coupling is important, resulting in a significant mixing of the strong Σ - Σ oscillator strength into the Σ - Π transition. We find peak photodissociation cross-sections of $\sim 0.5 \text{ \AA}^2$ in the region 300-350 nm for all of these ions. A detailed analysis of calculated spectroscopic properties of the bound $A \ ^2\Sigma_u^+$ state of these ions has also been performed. We find a regular progression in these properties and show that Hartree-Fock results can be misleading for these systems owing to a more serious (HF) asymptotic error for Ne_2^+ than for the other dimer ions.

* Supported in part by AFOSR

BA-3

Photoelectron Spectrum of the Xe₂ Dimer. *P. M. DEHMER and J. L. DEHMER, Argonne Nat'l. Lab. --A concentration of 1% Xe₂ in atomic Xe was produced in a supersonic expansion using a 35μ diameter jet and a stagnation pressure of 460 torr. The HeI(584.334 Å) photoelectron spectrum was recorded at a resolution of 20 meV using a hemispherical photoelectron spectrometer. Transitions from Xe₂ X¹Σ_g⁺ to the Xe₂⁺ A²Σ_{1/2u}⁺, v=0 ground state were not observed due to the poor Franck-Condon overlap; however, transitions to excited states dissociating to Xe(1S₀) + Xe⁺(²P_{3/2} or ²P_{1/2}) were observed. These states have dissociation energies of up to 0.37 eV, which is significantly larger than those expected from consideration of weak polarization forces. This experiment determined the Xe₂⁺ potentials in the region of r_e of Xe₂ (4.37 Å). These results are combined with the repulsive potentials determined from differential elastic scattering measurements of Xe⁺ on Xe, ¹ in order to map out the potentials over the entire range of internuclear separation.

*Work performed under the auspices of the U.S. ERDA.

¹P. R. Jones, G. M. Conklin, D. C. Lorents, and R. E. Olsen, Phys. Rev. A**10**, 102 (1974).

BA-4

Photodissociation Cross Sections in Ar₂⁺ for the Σ - Σ Transition. * D. KATAYAMA, J.F. PAULSON and T.L. ROSE, ⁺Air Force Geophysics Laboratory. --Absolute cross sections have been measured for the photodissociation reaction Ar₂⁺ (X²Σ_u⁺) + hν → Ar₂⁺ (2²Σ_g⁺) → Ar⁺(²P_{1/2}) + Ar. A 500 eV, mass analyzed beam of Ar₂⁺ produced by the Hornbeck-Molnar reaction in an electron impact ionization source was crossed at right angles with a pulsed light beam from a tunable dye laser. The photofragment ion was detected with a 50 cm quadrupole mass spectrometer which permitted low resolution energy analysis by the time-of-flight technique. The shapes of the TOF Ar⁺ peaks for polarization of the laser beam parallel and perpendicular to the ion beam direction confirmed that the transition being observed was primarily Σ - Σ. Substantial cross sections (10⁻¹⁷ - 10⁻¹⁸ cm²) were measured over the wavelength range of 290 to 670 nm. The results will be discussed in terms of the theoretically calculated cross-section and the vibrational population of the Ar₂⁺ ground state.

* Supported in part by the Defense Nuclear Agency.

+ NRC-NAS Senior Post Doctoral Research Associate

BA-5

Photodissociation Cross Sections of Ar_2^+ , Kr_2^+ , and Xe_2^+ from 6950 to 8600 Å.* L. C. LEE, G. P. SMITH, T.M. MILLER, and P.C. COSBY, Molecular Physics Center, SRI International--The absolute total photodissociation cross sections of Ar_2^+ , Kr_2^+ , and Xe_2^+ , which are identical to the absorption cross sections at these wavelengths, have been measured from 6950 to 8600 Å. The noble-gas molecular ions were produced from a drift-tube mass spectrometer, and were irradiated by a dye laser. The photodissociation cross section of Ar_2^+ has a broad maximum of 0.19 Mb ($1 \text{ Mb} = 10^{-18} \text{ cm}^2$) at 7200 Å and decreases monotonically to .05 Mb at 8400 Å. The shape of the Ar_2^+ cross section agrees quite well with several theoretical calculations, although the presently measured values are systematically lower than those of the calculations. The cross section of Kr_2^+ decreases monotonously from 2.5 Mb at 7000 Å to 0.6 Mb at 8600 Å. The cross section of Xe_2^+ reaches a maximum of 12 Mb at 7300 Å and then decreases monotonically to 2 Mb at 8600 Å.

*This work supported by the National Science Foundation.

BA-6

UV Absorptions of Rare Gas Ions in E-Beam Pumped Rare Gases.* R. O. HUNTER, J. OLDENETTEL, C. HOWTON, Maxwell Laboratories Inc. and M. V. McCUSKER, SRI International--The transient absorption spectra of electron beam pumped argon and argon/krypton mixtures have been measured in the wavelength region between 240 and 400 nm. The e-beam parameters were: 200 cm x 20 cm, 1.5 A/cm² and 350 KV, 500 ns duration. The excited gas was probed with a frequency doubled N₂ pumped dye laser, 350 ns after initiation. In pure argon at 1470 torr, the peak absorption feature is at 292 nm, with a FWHM of ~ 90 nm, and an absorption coefficient of $1.7 \times 10^{-2} \text{ cm}^{-1}$. This feature is due to Ar_2^+ . In the argon/krypton mixture of 1470/50 torr the peak is at 325 nm, with a FWHM of ~ 100 nm, an absorption coefficient of $0.9 \times 10^{-2} \text{ cm}^{-1}$ and is due to Kr_2^+ . Comparison of these absorptions with several recent theoretical computations of the absorption spectra of Ar_2^+ and Kr_2^+ will be made. The presence of non-saturable absorbers in a laser medium, for example argon, krypton, fluorine, may severely limit the extraction efficiency.

*Supported by DARPA through U.S. Army BMDATC.

BA-7

Absorption Processes and Molecular Ion Kinetics in E-Beam Excited Rare Gas Plasmas, J. B. WEST and W. H. LONG, JR., Northrop Research & Technology Center, Hawthorne, Ca. -- Experiments to investigate absorption at 249 nm in electron beam excited rare gases have been carried out. In these experiments, the rare gas (either Ar, Kr, or Xe) was excited by a 20 ns pulse of 1 MeV electrons at 400 A/cm². Absorption was probed with a KrF laser at 249 nm. Data taken over a pressure range of 1 to 7 atms show a nonlinear behavior of absorption with total pressure. For Kr and Xe, the observed absorption saturates at about 6.5 and 5.5 atm, respectively. The probable identity of the absorber is the diatomic ion Ar₂⁺, Kr₂⁺, etc. A model will be presented to explain the pressure dependence of the absorption in terms of the diatomic ion concentrations. Implications for the performance of excimer lasers such as KrF*, Kr₂*, and Xe₂* will also be discussed.

BA-8

CF₂ Absorption in KrF Discharge Lasers.*
J. GOLDHAR and J. R. MURRAY, Lawrence Livermore Laboratory. Spectroscopic investigations suggest that the well-known hole in the KrF fluorescence spectrum at 248.8 nm, as well as several other absorptions across the peak of the KrF fluorescence band, are caused by absorption into the 060-000 band of the A-X transition of CF₂ radicals formed in the laser discharge. Elimination of these rather stable radicals will therefore be required if efficient KrF lasers are to be operated in closed cycle systems. Absorption by atomic carbon is also observed.

*Supported by US ERDA Contract W-7405-Eng-48.

SESSION BB

11:20 AM - 12:15 PM, Tuesday, October 18

Room B

LTE ARCS II

Chairman: R. J. ZOLLWEG, WESTINGHOUSE

BB-1

A Complex Impedance Model of an Electrodeless Discharge, Paul Haugsjaa, William McNeill, Robert Regan, GTE Laboratories, Inc., Waltham, Massachusetts

A simple channel model of an electrical discharge has been used to determine the microwave impedance of an electrodeless high-pressure mercury discharge. The dependence of discharge impedance on the electrical conductivity of the discharge, the attenuation factor, the propagation constant and the extent of the discharge will be described. The derivation of the TM mode propagation parameters for a cylindrical electrodeless discharge, which was used in these calculations, will be discussed. Knowledge of the complex discharge impedance has allowed the development of a new and efficient way of coupling microwave power into an electrodeless discharge.

BB-2

Interaction of Microwaves with High-Pressure Discharges, William McNeill, Paul Haugsjaa, Robert Regan, GTE Laboratories, Inc., Waltham, Massachusetts

Microwave power has been efficiently coupled into high-pressure discharges. Theoretical and experimental details of how this coupling has been accomplished will be discussed. In particular, the field configuration in a coaxial, highly overdense, collisional plasma and the arc physics of high frequency, electrodeless discharges will be analyzed. The discharge consists of mercury plus metal-halide molecules for tailoring the emission spectrum. Typical pressures are 1 - 4 atm. Means for achieving arc isolation from discharge vessels using field shaping will be presented. A model, based on the classical conductivity of a plasma, will be shown. Comparison to dc and low frequency ac discharges will be made.

BB-3

Spectrometric Gas Composition Measurements of UF₆ RF Plasmas*. WARD C. ROMAN, MARTIN F. ZABIELSKI, United Technologies Research Center -- Experiments and associated diagnostics are discussed in which an rf heated argon confined uranium plasma was investigated using both off- and on-line gas composition diagnostic techniques. Both infrared and mass spectrometric (Time-of-Flight) techniques were employed to quantitatively determine the concentration of UF₆ and other gaseous constituents. In all tests, pure UF₆ was used as the source of uranium atoms and the tests were conducted in the UTRC 1.2 MW rf induction heater facility. The plasma was a fluid-mechanically confined vortex type approximately 3-cm-dia and 10-cm-long contained within a water-cooled fused-silica cylindrical test chamber. Power levels of approximately 50 kW, chamber pressures 1-3 atm, and test times 1-6 min. were employed. Results indicated the feasibility of employing both on-line diagnostic techniques; however, the mass spectrometric system possessed several distinct advantages.

*Sponsored by NASA Langley Research Center,
Contract NAS1-14329.

BB-4

THERMODYNAMIC AND TRANSPORT PROPERTIES OF UF₆ AND UF₆ + H₂ MIXTURES. R. W. Liebermann and C. L. Chen, Westinghouse R&D Center, Pittsburgh, Pennsylvania, 15235, USA - Thermodynamic and transport properties of UF₆ and UF₆ + H₂ gas mixtures were calculated at atmospheric pressure and temperatures of 800 to 20000°K for atomic ratio U:F = 1:6 and U:H = 1:0 to 1:6. The results include molar fractions of the chemical species (i.e., molecules, atoms, positive ions, negative ions and electrons) as well as enthalpy, specific heat, viscosity, thermal conductivity and electrical conductivity. The present calculations include all known condensable species. The thermochemical properties and gas collision interaction parameters used for each chemical species considered are reported. Comparison of our results with limited experimental data and other calculations are also made.

BB-5

THERMODYNAMIC AND TRANSPORT PROPERTIES OF SF₆. R. W. Liebermann and C. L. Chen, Westinghouse R&D Center, Pittsburgh, Pennsylvania 15235 - The equilibrium compositions together with interaction integrals between chemical species were used to calculate the transport properties of SF₆. In particular the heats of formation of SF₄, SF₃ and SF₂ were adjusted until the computed thermal conductivity agrees with the Motschmann's experimental data in the temperature range of 2300 to 4500°K, the derived heats of formation are: $\Delta H_{f298}(\text{SF}_4) = -185.2$ Kcal/mole, $\Delta H_{f298}(\text{SF}_3) = -117$ Kcal/mole and $\Delta H_{f298}(\text{SF}_2) = -68$ Kcal/mole. The equilibrium compositions and transport properties were then used to calculate the temperature profiles of low current arc in SF₆. The predicted profiles are in good agreement with those observed experimentally.

SESSION CA

1:45 PM - 3:30 PM, Tuesday, October 18

Room A

KINETICS AND MODELING OF RARE GAS-HALIDE
LASERS

Chairman: D. W. SETSER,
KANSAS STATE UNIVERSITY

CA-1

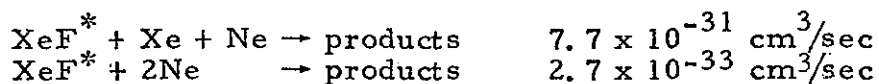
Kinetic Model of an XeF* Laser.* L.J.PALUMBO, T.F. FINN† and L.F.CHAMPAGNE; Naval Research Laboratory. -- A computer code has been developed to describe the operation of the NRL long pulse XeF* laser for both direct e-beam pumping and e-beam-controlled discharge pumping. The code takes into account e-beam and discharge energy deposition, XeF* formation and quenching channels, and laser light extraction and absorption. The XeF* spontaneous lifetime and quenching rates recently measured at NRL are used. Predicted absorption, gain, and laser output compare well with experiment. The details of the formation kinetics and processes which limit laser efficiency for both the e-beam pumped and the e-beam sustained cases will be discussed.

*Work supported in part by DARPA

† Science Applications, Inc., Arlington, VA

CA-2

Formation and Quenching Kinetics of XeF* in E-beam pumped Ne/Xe/F₂ Mixtures. M. ROKNI¹, J. H. JACOB and J. A. MANGANO, Avco Everett Res. Lab., Inc. †† -- The kinetics of the XeF* formation and quenching were investigated by irradiating mixtures of Ne/Xe/F₂ with high energy electrons. The fluorescence emanating from these mixtures was studied as a function of mixture ratio and pressure. In particular, the spectroscopic data indicates that the formation processes of XeF* in Ne rich mixtures is different from the formation process in Ar rich mixtures. The possible formation channels in Ne mixtures will be discussed. The dominant quenching processes of the upper laser level associated with Ne were identified¹ and the rate constants were measured to be²



† On leave from Hebrew University of Jerusalem, Israel.

†† Supported by Advanced Research Projects Agency and monitored by the Office of Naval Research.

¹M. Rokni, J. H. Jacob, J. A. Mangano and R. Brochu, Appl. Phys. Lett. **30**, 458 (1977).

²G. J. Eden and S. K. Searle, 3rd Summer Colloquium on Electronic Transition Lasers, Snowmass, CO (1976)

CA-3

Absorption in E-beam Pumped XeF* Laser Medium with Ne and Ar Diluents. M. ROKNI†, J. H. JACOB and J. A. MANGANO, Avco Everett Res. Lab., Inc. ††--The absorption in E-beam pumped Ar/Xe/F₂ and Ne/Xe/F₂ mixtures was measured using a flashlamp pumped dye laser at 340 nm. The photo-absorption of the active medium affects the extraction efficiency and the length scaling of the laser. The gas mixtures were excited by a 150 keV, 5A/cm² beam of fast electrons. The pumping conditions and gas mixtures used were typical of E-beam pumped XeF lasers. Our results confirm that the absorption in Ne diluted mixtures is appreciably smaller than in Ar diluted mixtures.¹ Data was obtained for a wide variety of mixture pressures and ratios. Using our kinetic model^{2, 3}, the results were analyzed and the dominant absorbing species were identified.

†On leave from Hebrew University of Jerusalem, Israel.

††Supported by Advanced Research Projects Agency and monitored by the Office of Naval Research.

¹L. F. Champagne, 7th Winter Colloquium on High Power visible Lasers, Utah (1977).

²M. Rokni, J. H. Jacob, J. A. Mangano and R. Brochu, Appl. Phys. Lett. 30, 458 (1977).

³M. Rokni, J. H. Jacob and J. A. Mangano, preceding paper.

CA-4

Investigations of XeF Laser Characteristics with Ne and Ar Diluents. J. HSIA, J. A. MANGANO, M. ROKNI*, A. HAWRYLUK and J. H. JACOB, Avco Everett Res. Lab., Inc. **--A comparison of laser results from E-beam pumped mixtures of Ne/Xe/NF₃ and Ar/Xe/NF₃ will be presented. The improved laser performance using Ne diluent is a result of two main reasons: (1) decreased absorption of active media and (2) Ne quenches XeF* more slowly than Ar. Factors that may affect the XeF laser extraction efficiency will be discussed in detail. These include: (a) the finite vibrational relaxation time of the upper laser level, (b) the finite lifetime of the lower laser level, and (c) the excited and ionic states absorption.

Experimental results indicating the relative importance of these factors will be discussed. Possible methods of improving the XeF* laser performance by minimizing the adverse effects will be presented.

*On leave from Hebrew University of Jerusalem, Israel.

**Supported by Advanced Research Projects Agency and monitored by the Office of Naval Research.

CA-5

Multiatmosphere Operation of the KrF Laser in Neon Diluent. L.F. CHAMPAGNE, Naval Research Laboratory.

-- The experimental results for the long pulse KrF laser in neon diluent will be presented. The threshold pumping current required to obtain stimulated emission is reduced by a factor of 2 when neon is used as the diluent in place of argon. For equal energy input to the gas 5.5 J/l is extracted in neon as compared to 43J/l in argon in a 0.5 μ s optical pulse. Small signal gain and absorption measurements will be discussed and compared for the two diluents.

CA-6

Theoretical Model for uv-Preionized Fast Transverse Discharge KrF Lasers.* A. E. GREENE, C. A. BRAU, Los Alamos Scientific Laboratory. - A theoretical model has

been developed to examine the behavior of small, uv-preionized, fast transverse discharge KrF lasers. This model integrates the time-dependent circuit equations for the discharge, the kinetic equations for the important atomic and molecular species and electrons, and the equations describing the growth of the spontaneous and stimulated radiation.

Earlier results for ArF lasers will be reviewed briefly to compare them with new results, theoretical and experimental, for KrF. The model has been used to examine the effects of medium self-absorption including photo-dissociation of F_2 and Kr_2^+ , photodetachment of F^- , and photoionization of Kr^* . The possible effects of electron impact equilibration of the KrF excited states will also be discussed.

* Work supported by USERDA.

CA-7

Parametric and Scaling Studies of Spark-Preionized Discharge-Excited Rare-Gas Halide Lasers

D. E. ROTHE, Northrop Research & Technology Center, Hawthorne, Ca. -- UV preionized discharge-excited XeF and KrF lasers have been operated with a number of fluorine donors, including F₂, NF₃, N₂F₄ and SF₆. Results of a parametric study of experimental laser performance as a function of gas composition, total pressure, electrode voltage and energy loading are presented. The effects of easily ionizable seed gases and pulse delay times were also studied. Lasing pulses obtained from a 0.3ℓ and a 1.0ℓ discharge volume gave specific pulse energies of approximately 1 J/ℓ from KrF and 0.5 J/ℓ from XeF with pulse durations as long as 100 ns. Results indicate that ion recombination reactions are at least as important as metastable reactions for XeF* and KrF* excimer formation. An analytic scaling study, based on experimentally determined discharge parameters, shows that multikilowatt high-PRF XeF and KrF lasers may be possible with present technology.

CA-8

Electron Kinetics of Rare Gas Halogen Lasers.*

W. L. MORGAN, JILA, Univ. of Colorado and NBS, and R. A. HAAS and R. D. FRANKLIN, Lawrence Livermore Laboratory. An electron Boltzmann analysis has been developed which includes the production and loss of electrons due to ionization and attachment in a self-consistent manner. In addition, a source term for secondary electrons has been provided which includes the effect of electron beam excitation. The source term is calculated using a discrete slowing down approximation. This composite method allows accurate partitioning of electron beam energy into various collisional excitation channels. This electron kinetics analysis has been combined with a heavy particle kinetic code to study the electron kinetics of electron beam and/or electric discharge excited rare gas halogen laser media. The results of this analysis will be presented and discussed in the context of laser fusion applications.
*Supported by US ERDA Contract W-7405-Eng-48.

SESSION CB

1:45 PM - 3:30 PM, Tuesday, October 18

Room B

ELECTRODE EFFECTS AND VACUUM ARCS

Chairman: G. ECKHARDT, HUGHES
RESEARCH LABORATORIES

CB-1

Initiation Processes of Cathode Spots in Vacuum Arcs. J. MITTERAUER, University of Technology, Vienna.---

Notwithstanding the different methods to initiate a vacuum-discharge, the general feature of cathode spot initiation is assumed to be a very localized evaporation at the cathode microstructure at high current densities. The most typical example is the explosionlike evaporation of a cathode microprotrusion due to the thermal effects of high current density field emission in cathode induced vacuum-breakdown. In order to analyse the dynamics of this initiation process in detail, computer simulation of the non-stationary electrical and thermal response of a typical field emitting microprotrusion was performed using computational methods of control theory.

Based on experimental investigations of non-stationary cathode spot characteristics, the results of this computer simulation were generalized to a 'dynamic model' of cathode spot, considering a substructure of the macroscopic spot consisting of consecutive individual breakdown events at the cathode microstructure.

CB-2

Calculated Characteristics of Isolated, Stationary Cathode Spots on Copper Electrodes. L.P. HARRIS, General Electric Corporate R&D.---An earlier theory of cathode spot operation that models the flows of ions, atoms and electrons associated with a single cathode spot by use of the usual plasma constitutive relations and conservation laws for charge, mass, momentum and energy has been improved through the inclusion of plasma thermal ionization of evaporated atoms as well as beam ionization. For copper, this change gives higher voltage requirements at low spot currents, lower preferred current densities ($\approx 10^7$ A/cm²) and correspondingly larger preferred currents (≈ 100 A). The calculated average ion multiplicities (≈ 1.7) and fractional ion currents (≈ 0.11) of the preferred spots agree better with experimental measurements. The calculations are being extended to include electron-ion recombination in the expanding flow of plasma from the spot and to other electrode metals.

Cathode Spot Properties of a DC Mercury Vacuum Arc. GISELA ECKHARDT, Hughes Research Labs--Ensembles of anchored cathode spots of a dc mercury vacuum arc have been studied as a function of several parameters by fast framing and streak photography. From these photographs, some statistical properties of the cathode spots have been determined: distribution functions for their diameters, velocities, and displacements, as well as average values for the current they carry and its density. For the parameter variations used in this investigation, a most probable value of 14.7 μm was obtained for the spot diameter, the average current per spot varied between 0.7 and 2.5 A, and the cathode spot current density was computed to span a range from $4 \times 10^5 \text{ A/cm}^2$ to $1.5 \times 10^6 \text{ A/cm}^2$. The spots appear to execute two principal types of movements: rather rapid minute displacements about their position and a slower drift motion. No evidence for the existence of a microstructure within the individual cathode spot was found at an optical resolution of 0.37 μm .

Erosion Products from the Cathode Spot Region of a Copper Vacuum Arc. D. T. TUMA*, C. L. CHEN and D. K. DAVIES, Westinghouse R&D Center--Combined electrical, optical, and spectroscopic measurements have been used to determine the total flux, ion flux, particle flux, and neutral atom flux emitted from the cathode spot region of a copper vacuum arc of 80 A total current and 2 sec duration. It is found that the cathode erosion products consist predominantly of ions and particles, the contribution of neutral atomic flux being less than 1% of the total flux. The total and particle flux distributions are peaked in the direction of the cathode plane whereas the ion flux distribution is forward peaked. However, both ions and particles are detected in the cathode shadow, a result which is contrary to the hypothesis of purely collisionless transport of cathode erosion products. The neutral atom density measurements are consistent with a model assuming the source of the vapor to be evaporation in flight from the hot particles emitted from the cathode spot region. The size distribution of the particles has a maximum for particles of diameter in the range 0-1 μm .

*Carnegie-Mellon University

CB-5

Measurement of the Angular Distribution of the Ion Current From a Vacuum Arc. J.V.R. HEBERLEIN, Westinghouse Electric Corp., R&D Center.--A dc vacuum discharge was surrounded by four concentric cylinders at different heights above the cathode plane. The ion currents to these cylinders were recorded, and their values per unit solid angle were determined as a function of the angle θ from the surface normal of the electrode. Arcing currents ranged from 80A-1600A, and the gap-anode diameter ratio varied from 0.4 to 1.7. For values of θ between 40° and 90° , the results show that the cathode ion currents per unit solid angle decrease with increasing angle θ . This decrease becomes less pronounced as the current is increased. The total ion current from the cathode increases very little if the gap-anode diameter ratio is increased. This indicated that the ion current per unit solid angle which is intercepted by the anode is less than the corresponding value measured by the adjacent probe. One explanation for this observation would be peaking of the ion current per unit solid angle for an angle $\theta_m < 40^\circ$. The ion currents emitted from the anode spot seem to have a more uniform angular distribution for $\theta > 50^\circ$.

CB-6

Anode Heat Fluxes During the Initial Phase of Pulsed High Intensity Arcs*. D. Johnson and E. Pfender, Department of Mechanical Engineering, University of Minnesota. A previously developed method⁽¹⁾ for measuring quasi-steady local anode heat fluxes in high intensity pulsed arcs has been extended to investigate the initial transient period of such arcs. This extension requires a suitable model which is derived from high speed streak photographs of the arc and the measured temperature-time history of the rear face of a thin anode. The input heat flux model consists of linked segments of linearly time-varying heat fluxes. Results for 5 kA arcs in atmospheric pressure argon indicate initial transient heat fluxes up to 4×10^9 W/m² followed by quasi-steady heat fluxes of approximately 1×10^8 W/m². At reduced pressures the heat fluxes are also somewhat reduced.

- (1) J.L. Smith and E. Pfender, "New Technique for Measuring Extremely High Heat Transfer Rates to Surfaces," Rev. Sci. Instrum., Vol. 47, No. 9, 1056-1058, 1976.

*Supported by NSF Grant ENG 71-02478 A01.

CB-7

Ion and Neutral Excited State Densities of
Multi-Cathode-Spot Vacuum Arc

R. Boxman and S. Goldsmith, Tel Aviv University

Excited state densities in the interelectrode plasma produced by a 1.1 kA peak current 0.65 ms HAFW discharge between Al butt electrodes, 10 mm diam spaced 4.4 mm apart and located in a vacuum ambient, were determined by measurement of the absolute line intensities. Densities at mid-plane near peak current for the Al I $3s^2 4s^2 S$, Al II $3p^2 D$, and Al III $4p^2 P$ states were 8×10^{14} , 2×10^{16} , and 3×10^{16} respectively. Densities in Al II and Al III states studied could be described by distribution temperatures of 1.1 and 1.3 eV respectively. As a function of distance from the cathode, Al I and Al II densities declined from their maximum near the cathode, with the Al I density rising slightly near the anode, while Al III states generally rose from minimum values near the cathode, reaching maximums after mid-plane. As a function of time, Al III densities reached a maximum near current maximum, and then decayed rapidly, while Al II densities reached their maximum about 0.2 ms after peak current, and Al I reached its maximum only at the tail end of the current pulse, and continued to be present a considerable time after current zero.

CB-8

Temperature of the Cathode Region of the
Surge Discharge in Vacuum. L. M. Burrage,
Thomas A. Edison Technical Center, McGraw-
Edison Co. -- Emission spectroscopy in the
2100-4300 Å span 1st order and 2000-2150 Å
2nd order has been used to determine the near
cathode arc temperatures for 400 thru 11000
ampere unidirectional surge discharges between
vacuum melted, recrystallized, copper elec-
trodes in a 3×10^{-6} torr ambient. LTE was
assumed to exist. The derived temperatures,
somewhat dependent upon the current magnitude,
range from 5000°K to 6600°K. The temperatures
in the 400-5500 ampere surge discharges,
5000°K to 5260°K, are surprisingly close to the
Corliss' value for the 10 ampere dc arc in
air at atmospheric pressure.

CB-9

The Effect of Alumina Inclusions on the Breakdown and Emission Properties of Copper Surfaces in Vacuum. G.A. FARRALL, F.G. HUDDA AND R.H. JOHNSTON, General Electric Corporate R&D. --We

have studied electrical breakdown in vacuum for copper electrodes which have been intentionally contaminated by adding $\frac{1}{2}\%$ by weight of alumina powder having a size of 500 μ , 50 μ or 5 μ . Electron emission, pulse breakdown and scanning electron microscopy have been used to evaluate the dielectric characteristics of the surfaces. Comparison of these results with those obtained using a zone refined copper surface indicate an initial degradation of about 30% for the surface containing 50 μ particles and little effect for the surface containing 500 μ particles. All surfaces conditioned to about the same voltage. Breakdown to all samples containing particles was clearly associated with metal-insulator boundaries.

SESSION DA

3:45 PM - 4:35 PM, Tuesday, October 18

Room A

RARE GAS-HALIDE DISCHARGES

Chairman: J. G. EDEN, NRL

DA-1

Plasma Kinetics in KrF* Laser Discharges.*

W. L. Nighan, United Technologies Research Center, -- Plasma processes in KrF* lasers have been analyzed for conditions typical of electron-beam sustained discharges. Particular emphasis has been placed on evaluating the influence of: electron-electron collisions, electron collisions with F₂, and electron collisions with metastable atoms. It has been determined that for values of fractional ionization above approximately 10⁻⁶, e-e collisions exert a significant influence on ground state atom ionization rates and on plasma stability by way of their effect on the high energy portion of the electron distribution function. For values of fractional ionization above about 3x10⁻⁶ electron excitation of metastables to higher excited states has been found to be an important loss process for rare gas metastable atoms. In addition, it has been found that direct electron impact dissociation of F₂ may represent a major loss process for electron energy and for F₂ molecules. Specific details of these and other processes of importance will be discussed. * Work performed in part through the sponsorship of the Office of Naval Research.

DA-2

Discharge Stability and Scaling of the KrF Laser,

W.H. LONG, JR., Northrop Research & Technology Center, Hawthorne, Ca. -- The discharge power density in e-beam sustained KrF lasers is limited by ionization runaway leading to arcing. This instability occurs at well-defined values of E/N depending on gas mixture, pressure, and e-beam current density. A model is presented which describes the ion and metastable kinetics in electronegative gases. A criterion for the existence of a steady state is derived. The predicted stability limit in Ar-Kr-F₂ mixtures is in excellent agreement with experimental observations for e-beam power densities between 0.1 MW/cm³ and 1 MW/cm³. Nonuniform e-beam deposition also leads to instability by creating regions of high electric field strength where ionization runaway begins. Even slight nonuniformities can severely limit the discharge power loading. The most effective means of achieving uniform deposition over large volumes is through the use of opposed e-beams. With this technique, it is expected that 40 J// can be extracted from KrF with an enhancement factor of four at low e-beam current densities.

DA-3

Quasi-Steady Operation of Self-Sustained Rare Gas-Halide Discharges. G.L. ROGOFF, L.E. KLINE, J.L. PACK, and W.H. KASNER, Westinghouse R&D Center*--Quasi-steady, self-sustained glow discharges have been established in 0.5% SF₆/5-15% Kr/He mixtures at 100-800 Torr. With uv preionization through a planar screen anode, diffuse discharges have been maintained for up to 1 μsec, the limit of the pulse-forming network used. Measured electric fields in the positive column agree well with fields calculated from a steady-state model based on electron production by one- and two-step electron impact ionization of Kr and loss by attachment to SF₆. The discharge duration is limited above some values of pressure, Kr concentration, and/or current density by the glow-to-arc transition, i.e., by filament formation within the diffuse glow. The observed quasi-steady discharges violate a predicted stability criterion¹ generalized to include the effects of single-step ionization. That criterion apparently describes the onset of a bulk instability corresponding to a negative V-I characteristic. This effect is stabilized with appropriate circuit ballasting. *Supported in part by US ERDA Contract EY-76-C-02-4030
1J.D. Daugherty, J.A. Mangano, and J.H. Jacob, Appl. Phys. Lett. 28, 581 (1976).

DA-4

TIME-RESOLVED DISCHARGE DEVELOPMENT IN HIGH PRESSURE, GLOW-DISCHARGE EXCIMER LASERS, W.J. Sarjeant, A.J. Alcock and K.E. Leopold, National Research Council of Canada, Ottawa, Canada K1A 0R6 Preliminary results are reported on the time-evolution of the discharge plasma in a 6 atm, glow-discharge excimer laser system. Streak photographs of the discharge are correlated with the evolution of breakdown in a surface spark gap used to transfer the stored electrical energy into the discharge. The data obtained are used to investigate the effects of gas composition (Kr, Xe, Ar, F₂, NF₃, and He), type of excitation circuitry and surface spark gap operating pressures and gas mixtures. The significant parameter for obtaining glow-discharges was determined to be the number of simultaneous channels in the surface spark gap. Detailed results covering discharge development in both the surface spark gap and the laser discharge will be presented. The significance of the latter from a scaling point of view in both excimer and other fast-discharge laser systems will be discussed.

DA-5

Hollow Cathode Discharges in Electronegative Gases. * S. GRIFFIN, M. SIMMONS, J.T. VERDEYEN, B.E. CHERRINGTON, Gaseous Electronics Laboratory, University of Illinois, Urbana, IL 61801.--Experiments will be described involving the excitation of mixtures of rare gases with NF_3 and SF_6 in a hollow cathode geometry. Whereas a positive column discharge is striated and unstable with these gases, the hollow cathode discharge is stable even with large percentages (> 50%) of the attaching gas. Preliminary studies of a 1 cm OD x 10 cm long hollow cathode discharges have been performed for mixtures of Xe and NF_3 . Power loading greater than 1 kW/cm^3 has been achieved and the spontaneous fluorescence shows an intense well developed XeF excimer band even at the low pressures used.

*Work supported by the Army Research Office, Durham, NC.

SESSION DB

3:45 PM - 4:55 PM, Tuesday, October 18

Room B

ARCS AND FLOWS

Chairman: H. T. NAGAMATSU,
GENERAL ELECTRIC

DB-1

Temperature Profiles and Fluctuation Levels Measured in an Arc in an Axial Gas Flow, J. F. Driscoll, R. W. Anderson, K. P. Zondervan, K. L. Zondervan, Univ. of Michigan--Interaction between an electric arc discharge and a coaxial supersonic nitrogen flow was investigated by measuring radial temperature profiles and fluctuations in arc temperature, diameter, and voltage. A 200 ampere D.C. arc was stabilized axially in a supersonic nozzle at 4 atm reservoir pressure. A polychromator and rotating mirror were synchronized with gated digital recorders capable of 10 nsec sampling of arc emission intensity. Temperature determination using the emission line ratio technique proved most straightforward in this case, using NII multiplets at 5679A and 4793A, if background radiation is carefully subtracted. Two mechanisms resulting in large plasma fluctuations were observed. At the throat, fluctuations in arc voltage and diameter were <10%; however, light intensity fluctuations were large (40%) indicating convection of nonuniform regions of plasma. Downstream fluctuations in arc voltage, diameter, and light intensity were considerably larger, believed due to turbulence promoted by large gradients of plasma velocity.

DB-2

Experimental and Theoretical Study of a D.C. Arc in a Constant Diameter Nozzle Flow. H. T. Nagamatsu, General Electric Co., Corporate Research & Development -- The cold flow field for a 1.27 cm constant diameter nozzle was determined for subsonic and transonic flow velocities. In addition, d.c. arc voltage, current and diameter measurements were made for an arc gap of 5.52 cm and a current of approximately 100A. Arc voltage increased rapidly as the flow velocity increased from zero to sonic velocity. Using a channel flow model with constant arc temperature and the energy integral for the convective cooling, analytical expressions were derived for the arc radius, electric field strength, arc voltage, resistance, and power as functions of the cold flow properties, current, and axial distance. Calculated arc voltages, resistances, and powers compare favorably with measured values.

DB-3

Dielectric Recovery Rate of Repetitive Discharges in a Transverse Gas Flow, J.F. DRISCOLL, Univ. of Michigan--Numerical predictions of dielectric recovery rates are described for repetitive (100 pulses/sec) kiloampere discharges in a transverse air flow of 6000 cm/sec. Numerical solutions of the simplified conservation equations predict the time history of spacially averaged arc temperature, arc radius, and arc length. Results show an initial peak in arc radius and temperature corresponding to the peak in the 32 microsecond current pulse, followed by the effects of radiative cooling, convective cooling and length variations of the travelling arc. Predicted dielectric recovery rate of the plasma column increases by increasing flow velocity, and in fact, by decreasing electrode spacing to optimize the gasdynamic effects. In a parallel experimental effort, high speed photographs (10^6 frames/sec) of the discharge reveal a slanted arc with an attached anode root and cathode root convected downstream. Reasonable agreement is obtained between calculated and measured time variations of arc diameter.

DB-4

INVESTIGATIONS OF THE DIELECTRIC BREAKDOWN OF SF-6 AT HIGH TEMPERATURES. B.Eliasson and E.Schade, Brown Boveri Research Center, CH-5405 Baden, Switzerland.

In the wake of a SF-6 cross flow arc measurements have been made of the break-down voltage and the pre-breakdown currents as a function of temperature ($T < 2300K$, $p = 2$ bar, v -flow = 80 m/s). The electrical field was homogenous. The currents were in the range of mA. A theoretical model which takes the space charge due to the high temperatures into account has been solved. The ionization and attachment coefficients (α, η) were calculated as a function of field and temperature. It is shown how the breakdown voltage drops with increasing space charge.

DB-5

Transport Mechanisms in the Anode Region of High Intensity Arcs*. C.H. Liu**, E. Pfender. Department of Mechanical Engineering, University of Minnesota. -- Arc behavior and anode erosion at high current levels are determined by the interaction of thermal, electric, magnetic and fluiddynamic effects in the anode region. In order to assess the relative importance of these effects, the highly non-linear conservation equations for the anode region of rotationally symmetric arcs have been solved numerically for currents between 100 and 500 A with argon and nitrogen at atmospheric pressure as working fluids. The results indicate that enthalpy transport by the electron current and convective cooling due to the development of an anode jet are the dominating transport mechanisms in axial direction. The individual contributions to the energy balance reflect the characteristic behavior of the transport coefficients and their temperature dependence.

* Supported by NSF grants ENG 71- 02478 A 01 and ENG 77 - 04108.

** Now with Owens-Corning Fiberglass, Granville, Ohio.

DB-6

Calculation and Experimental Procedures in Turbulent Arcs*, Y-K CHIEN and D.M. BENENSON, State University of New York at Buffalo--Determination of spatial (r) distribution of time-averaged temperature ($\langle T \rangle$), particle densities ($\langle n_o \rangle$ and $\langle n_e \rangle$) and of fluctuations ($\langle \delta^2 T \rangle$), ($\langle \delta^2 n_e \rangle$), etc. in a turbulent DC plasma involves development of appropriate analytical models and related experiments. Three models (extensions of Schreiber and Hunter) are discussed. All models (1) use relations for line and continuum emission coefficients and (2) introduce the turbulent aspect by expressing the variables of interest as sum of time-averaged and fluctuating components. Model I uses only equations cited in (1) above. In addition to (1), Model II employs the Saha equation. Model III uses (1), the Saha equation, equation of state and an assumed relation between pressure and temperature fluctuations. The assumptions, restrictions, and associated requirements upon experiments (number of independent measurements involving line, continuum, and correlations) will be described.

* Research supported by National Science Foundation grant ENG76-17009, General Electric Foundation, and Electric Power Research Institute Contract RP246-2.

DB-7

Acoustical Resonances in Cylindrical Cesium Arcs. Harald L. Witting, General Electric Corporate Research & Development, Schenectady, NY--Cesium and cesium-xenon arc discharges were operated in cylindrical arc tubes at 20 to 200Torr and at 1 to 3A rms. The frequency of the AC current was varied between 1 and 50 kHz at constant input power. It was found that at certain "resonance frequencies" the arc becomes unstable and assumes characteristic stationary or oscillating shapes. The arc deflection and the frequency interval of the resonances increases with pressure. The resonance frequencies are compared with previous data on sodium discharges and with a refined theoretical model.

1. H.L. Witting, Bull. Am. Phys. Soc. 20, 245, 1975.

SESSION FA

8:30 AM - 10:30 AM, Wednesday, October 19

Room A

ELECTRON ATTACHMENT AND TRANSPORT, AND
NEGATIVE IONS

Chairman: S. F. WONG, YALE UNIVERSITY

FA-1

Isotopically Selective Photo-enhanced Dissociative Attachment in SF₆. C. L. CHEN and P. J. CHANTRY, Westinghouse R&D Center--Production of SF₅⁻ by dissociative attachment of very low energy electrons to SF₆ is known¹ to be strongly enhanced by increasing the SF₆ gas temperature. The expectation² that this effect can be produced by direct optical excitation of the ν_3 vibrational mode has been confirmed by using a tunable CW CO₂ laser focussed colinearly with the electron beam inside a room temperature collision chamber. The product ions are monitored using a quadrupole mass filter. The observed enhancement of the SF₅⁻ signal by the radiation is strongly wavelength dependent and is linearly dependent on the laser intensity, implying single photon absorption. The peak enhancements of the ³²SF₅⁻ and ³⁴SF₅⁻ signals are well resolved in wavelength and are separated by the known isotope shift of the ν_3 SF₆ absorption. Both peaks, however, are red-shifted from their respective room temperature absorption peaks. This suggests that efficient promotion of the (SF₆⁻)* dissociative decay channel requires a total of two or more vibrational quanta to be present in the SF₆.

1.C.L.Chen & P.J.Chantry, Bull.Am.Phys.Soc.15, 418 (1970).
1.C.L.Chen & P.J.Chantry, Bull.Am.Phys.Soc.21, 172 (1976).

FA-2

Calculation of Dissociative Attachment and Vibrational Excitation in F₂^{*}. R. J. Hall and W. L. Nighan, United Technologies Research Center, -- Self-consistent dissociative attachment and vibrational excitation cross-sections for F₂ have been calculated using Herzenberg's theory of resonance electron scattering. Potential parameters for the 2 Σ_u^+ negative ion have been varied to fit the predicted attachment cross-sections to available experimental rate constant data. The best fit was obtained for a negative ion potential curve which crosses that of the ground state in the vicinity of the equilibrium internuclear separation, and which has a width of 0.3-0.4 eV. The associated total vibrational cross-section has a peak of about 2.5 x 10⁻¹⁶ cm² at an incident electron energy of 0.5 eV, and decreases to a value of about 10⁻¹⁷ cm² in the 2.0 to 3.0 eV range. A strong dependence of the attachment rate on F₂ vibrational level is predicted.

*Work performed in part through the sponsorship of the Office of Naval Research.

FA-3

Attachment of Slow Electrons to Br₂ and HBr, Daniel W. Trainor and M.J.W. Boness, Avco Everett Research Laboratory, Inc.-- Electron attachment to Br₂ and HBr has been studied over a range of E/P values using a high-pressure electron beam sustained gas discharge apparatus. Experiments were performed in gas mixtures containing the attaching specie and a large excess ($\geq 99\%$) of N₂ which was included to control the electron temperature. Total gas pressure employed was in the range 1/2-1 atm. Attachment coefficients were obtained from an analysis of the steady-state discharge current which for strongly attaching species is determined by the balance between attachment and ionization. Values of the dissociative attachment rate constants at an average electron energy of 1.0 eV for Br₂ and HBr were found to be 1.0×10^{-10} cm³/sec and 8×10^{-10} cm³/sec respectively. Using the known electron energy dependencies of the dissociative attachment cross sections, a Boltzmann computer program has been exercised in order to estimate the magnitudes of the dissociative attachment cross sections for Br₂ and HBr.

*Work supported by Avco Everett Research Lab., Inc.

FA-4

Electron Attachment to Polymers of Nitrous Oxide and Carbon Dioxide.* CORNELIUS E. KLOTS and R. N. COMPTON, Health & Safety Research Division, Oak Ridge National Laboratory, Oak Ridge, TN 37830 -- We have studied electron attachment to polymeric species formed in the adiabatic expansion of nitrous oxide and of carbon dioxide through a sonic nozzle. We note: (1) The absence of O⁻ formation via attachment to vibrationally - excited monomers; (2) Formation, by evaporative electron attachment, of species such as (CO₂)_n⁻, with $n \geq 2$, and CCl₄⁻ (from CCl₄ impurity in the carbon dioxide); (3) A clarification of the mechanism of three-body attachment of electrons to nitrous oxide.

*Research sponsored by the Energy Research and Development Administration under contract with Union Carbide Corporation.

FA-5

Electron Affinities of Strongly Polar Molecules.* W. R. GARRETT, Health & Safety Research Division, Oak Ridge National Laboratory, Oak Ridge, TN 37830 -- Through a number of theoretical studies the critical electron binding properties of polar molecules have been rather thoroughly elucidated. However, for practical purposes the experimental observation of certain stable negative ion species may prove to be very difficult or impossible even though such states can be shown, mathematically, to exist (with very low binding energies). In the present study a molecular pseudopotential method has been used in conjunction with the close coupling technique to establish general guidelines on the magnitudes of dipole moments which are required in order to assure a molecular electron affinity which is equal to or greater than thermal collisional energies.

*Research sponsored by the Energy Research and Development Administration under contract with Union Carbide Corporation.

FA-6

The Drift Velocity of Low Energy Electrons in Oxygen. I.D. REID and R.W. CROMPTON, Electron and Ion Diffusion Unit, Australian National University, Canberra. A drift tube using a pulsed RF electron detection technique has been constructed to measure electron drift velocities in attaching gases. The detection system discriminates between electrons and negative ions and thus permits the detection of electron swarms in the presence of a high concentration of negative ions produced by attachment. Measurements of electron drift velocities have been made in oxygen in the range 0.14 - 1.4 Td at pressures of 0.20, 0.33, 0.41 and 0.53 kPa using a differencing technique. These are the first measurements below 1.0 Td in which a systematic investigation has been made of the pressure dependence of the measured drift velocity. The effects of diffusion and attachment on the results have been taken into account and the data are considered to be in error by less than 5% at 0.14 Td, and 2% at 1.4 Td.

FA-7

Electron Drift Velocities in Fluorine-Helium Mixtures.* S. R. HUNTER, J. FLETCHER†, S. R. FOLTYN, and K. J. NYGAARD, University of Missouri-Rolla.-- We have produced a burst of photoelectrons by means of light from a pulsed Xenon ion laser (2315 Å; 150 nsec) and measured the drift velocity of the electrons as a function of E/p from 0.1 to 10 volts/(Torr. cm). The apparent drift velocity increases as the F₂ concentration increases from 0.2 to 1%. This effect is due to a loss of low-energy electrons in dissociative attachment processes and a subsequent redistribution in the helium buffer gas.

*Supported in part by ERDA.

†Permanent address: The Flinders University of South Australia.

FA-8

Electron Attachment in Fluorine-Rare Gas Mixtures.* K.J.NYGAARD, S.R. HUNTER, and S.R. FOLTYN, University of Missouri-Rolla, and J. FLETCHER†, The Flinders University of South Australia.--We have studied the reaction rate for electron dissociative attachment in fluorine under experimental conditions prevailing in rare gas-halide lasers. Measurements have been made in gas mixtures consisting of 0.1% F₂ in He, 1% F₂ in He, and 0.2% F₂ + 4.8% Kr + 95% He. The principle of the experiment is to produce a burst of photoelectrons (by means of a light pulse from a Xe ion laser at 2315 Å) and subsequently observe the motion of all charged carriers in a well-defined drift region. Typically, we find a value of $K = 7 \times 10^{-10} \text{ cm}^3/\text{sec}$ at an average electron energy of 5eV.

*Supported in part by ARPA/ONR

†Visiting Professor

FA-9

Drift Velocities of Negative Fluorine Ions in Helium.* J. FLETCHER†, S. R. HUNTER, S. R. FOLTYN, and K. J. NYGAARD, University of Missouri-Rolla.--We have produced negative ions in fluorine (by electron dissociative attachment in F₂) and studied their motion in a constant electric field drift region. The negative ion drift velocity has been determined for $22 \text{ Td} \geq E/N \geq 1 \text{ Td}$ for total He pressures between 1 and 250 Torr and relative F₂ concentrations between 0.2 and 1%. Our results fall considerably below those of Dotan et al.†

*Supported in part by ARPA/ONR

†Permanent address: The Flinders University of South Australia.

†I. Dotan, D. L. Albritton, and F. C. Fehsenfeld, J. Chem. Phys. 66, 2232 (1977).

FA-10

Transport Parameters of a Pulsed Townsend Discharge in Hydrogen at Elevated Swarm Energies* S.R. Hunter**, J. Fletcher, and H.A. Blevin, Flinders University of South Australia--A new technique has been developed to study the drift velocity, the lateral and longitudinal diffusion coefficients and Townsend ionization coefficient for electron swarms over the E/N range $50 < E/N < 200 \text{ Td}$. The technique involves observing the ultra violet photon flux produced in inelastic collisions between the electrons and gas molecules, enabling the transport parameters to be obtained free from any boundary effects. The present lateral and longitudinal diffusion coefficient measurements are in considerable disagreement with the results obtained by other methods. The results of a theoretical Monte Carlo study will also be given which confirms the validity of the present experimental technique.

*Submitted by K.J. NYGAARD

**Present address, University of Missouri-Rolla.

FA-11

Production and Confinement of Negative Hydrogen Ions in Low Pressure Hydrogen Plasma.

M. BACAL, E. NICOLOPOULOU and H.J. DOUCET, Ecole

Polytechnique---It was found that usual methods for plasma confinement are unefficient for negative ions. Hydrogen plasmas with a negative ion density of $\sim 10^{10} \text{ cm}^{-3}$ have been produced in a hybrid magnetic multipole device. The equilibrium density of H^- ions in this plasma is calculated taking into account the known production and destruction processes ; the calculated densities are ~ 100 times lower than the experimental values. The observed dependence of H^- density on plasma density indicates that a non-linear H^- formation process is dominating. Dissociative attachment to an excited hydrogen molecule is suggested as a possible H^- formation process.

SESSION FB

8:30 AM - 10:30 AM, Wednesday, October 19

Room B

METAL-HALIDE, METAL-RARE GAS, AND OTHER
DIATOMICS

Chairman: J. J. EWING, LAWRENCE LIVERMORE
LABORATORIES

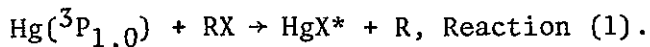
FB-1

HgCl*(B-X) Emissions at 560 nm From E-Beam Pumped Ar/Hg/Cl₂ Mixtures.* J.A. MARGEVICIUS, M.V. McCUSKER, D.L. HUESTIS, and D.C. LORENTS, Molecular Physics Center, SRI International--We have used a 180 keV electron accelerator to excite mixtures of argon, mercury and chlorine additives. We observe a banded emission sharply peaked at 570 nm that extends blueward to 430 nm. From this profile we compute a reduced stimulated emission cross section $\sigma_{\text{peak}}^{\text{rad}}$ of $1.8 \times 10^{-24} \text{ cm}^2 \text{ sec}$. Absolute fluorescence yields have been determined by comparison with previously calibrated second positive emissions in argon/N₂ mixtures. We observe that for 1000 torr total pressure, the optimum yield of the band is 75% for Ar/Hg/Cl₂, 45% for Ar/Xe/Hg/CCl₄, and 15% for Ar/Hg/CCl₄. Under these extremely low current (few μamps) conditions in our source, the kinetic mechanism that populates the upper state is via the Hg(³P) and Hg(³S) states. This mechanism will be discussed, as well as the implications for HgCl* laser operating conditions.

*Supported by DARPA through the U.S. Army BMDATC.

FB-2

Reactive quenching of Hg(³P_{1,0}) by halogens and halogenated molecules, T. SHAY, J. E. VELAZCO, and G. J. COLLINS, Dept. of Electrical Engineering, CSU--We have measured the rate constants for the reactive quenching of Hg(³P₁) and Hg(³P₀) by a variety of halogen and halogen-containing molecules in reaction of the type,



In addition, we have also determined the rate constants for the Hg(³P₁) \rightarrow Hg(³P₀) intramultiplet quenching collisions by RX and will report on preliminary results for the radiative lifetimes of HgX*.

The rate constants were obtained from a series of experiments involving steady-state and pulsed photolysis of Hg-RX mixtures at 253.7 nm, while the lifetime measurements were performed using Phase Shift Spectroscopy.

FB-3

Effect of Dissociative Recombination on Steady State Excited Atom and Electron Densities in High Pressure Discharges.* A. V. PHELPS,† DAVID LEEP and ALAN GALLAGHER,† JILA, U of Colo. & NBS/Boulder.--The theory of collisional-radiative recombination¹ is modified to include the effects of dissociative recombination. At electron and gas densities of interest² radiative transitions can be neglected, but the importance of collision induced quenching of intermediate excited states by ground state atoms is not yet clear. Excited state and electron densities calculated using hydrogenic models will be used to illustrate the effects of these processes. By balancing the energy loss by dissociative recombination against the power input, one obtains a moderately accurate expression for the discharge volt-ampere characteristic.² The result of combining this energy balance with the hydrogenic excitation model will be compared with results calculated using Sahia ionization and with experiment to show the need for more accurate models.

*This work was supported in part by ARPA/ONR and by AFWL.

†Staff Member, Quantum Physics Division, NBS.

¹L. M. Biberman, V. S. Vorob'ev and I. T. Yakubov, Usp. Fiz. Nauk 107, 353 (1972) [translation: Sov. Phys.-Uspekhi 15, 375 (1973)].

²H. Rothwell, D. Leep and A. Gallagher, this meeting.

FB-4

High-Power Discharges in Na- and Tl-doped Xe.* H. ROTHWELL, DAVID LEEP and ALAN GALLAGHER,† JILA, U. of Colo. & NBS/Boulder.--Self-initiated, pulsed discharges of 10-200 MW/l have been operated for periods of several μ s in 10^{19} - 10^{20} cm⁻³ of Xe doped with 10^{15} - 10^{16} cm⁻³ of Na or Tl. A steady-state volume discharge of typically 100 V/cm is obtained, fed by bright cathode spots of ~20 V cathode fall. A positive resistance characteristic is observed at the electron densities (10^{14} - 10^{16} cm⁻³) investigated. The emission spectrum is dominated by the NaXe or TlXe excimer bands associated with the metal resonance lines. Intensities of these bands and of lines from higher excited states are analyzed to obtain excited-state densities. The Na excited-state densities nearly fit a thermal relationship with an excitation temperature of typically ~0.4 eV. The Tl excited-state densities do not have a thermal relationship. At the higher powers the first excited (7S) state has an excitation temperature of ~1 eV, but the densities of higher states represent a much lower temperature. Possible causes of this disparate behavior will be discussed. The implications of these results to potential efficient, high-power, visible, tunable excimer lasers based on these vapors will be discussed.

*Work supported by AFWL and ARPA.

†Staff Member, Quantum Physics Division, NBS.

FB-5

Models of High-Power Discharges in Na-doped Xe.*

R. SHUKER, W. L. MORGAN, ALAN GALLAGHER[†] and A. V. PHELPS,[†] JILA, U. of Colo. & NBS/Boulder.--Electric discharge excited metal-noble gas excimers could provide efficient, high-power, tunable, visible lasers. We have modeled a homogeneous discharge in a characteristic mixture of $3.5 \times 10^{16} \text{ cm}^{-3}$ of Na in $2.7 \times 10^{20} \text{ cm}^{-3}$ of Xe. The non-linear rate equations for the various excited-state, ion, and electron densities are solved self-consistently with the electron energy distribution $f(E)$, for E/N of 10^{-17} - 10^{-16} V cm^2 and mean electron energies of 0.8-1.6 eV. Inelastic, superelastic, momentum transfer, ionization, recombination, and electron-electron collisions are included in the Boltzmann equation to obtain $f(E)$. At steady state, most of the discharge energy goes into Na excited-state (Na^*) ionization, followed by association of Na^+ to NaXe^+ then dissociative recombination of NaXe^+ to $\text{Na}^* + \text{Xe}$. A positive resistance characteristic is obtained, in agreement with observations. When only the lowest few Na^* states are included in the model, the results are not in quantitative agreement with measurements. Increasing the number of Na^* states improves the agreement, and more are being investigated to test convergence.

*Supported by ARPA.

[†]Staff Member, Quantum Physics Division, NBS.

FB-6

E-Beam Excitation of Mixtures of TlI and Xe.

L. A. SCHLIE and D. L. DRUMMOND, AFWL, Kirtland AFB, NM. The spectral and kinetic behavior of TlI/Xe mixtures produced via excitation from an electron beam are presented. The use of this salt enables the gas temperature to be lowered from 800°C to 400°C. Mixtures of approximately 1 torr of TlI metal vapor at 400°C and 10-100 psi of xenon buffer gas produce five very strong continuum bands. Each of these bands correspond to excimer transition to the red side of the excited Tl atomic lines at 5350, 3776, 3519/29, 3230, and 2919/21 Å. The TlXe bands peak at 5800, 4400, 3650, 3400, and 3050 Å. The time history of these bands/Tl atomic lines indicates that the 1470/1700 Å Xe and Xe_2 radiation photodissociate the TlI into free excited Tl which subsequently forms TlXe excimer states that radiate as the continuum bands. The importance of volume on the "optical trapping" of the free atomic Tl produced via photodissociation of the TlI will be described. The photoabsorptive effect of the TlI on the 4400 Å band of TlXe emission is discussed along with using the other salts of Tl. The possible applications of these TlXe continuum bands for high power lasers are discussed.

FB-7

Analytical Model of Thallium-Mercury Kinetics.

R. P. BENEDICT, L. A. SCHLIE, and D. L. DRUMMOND, AFWL, Kirtland AFB, NM.--An analytical model has been constructed to follow the time-dependent kinetics of a Tl-Hg inert gas mixture. This model includes the primary electron processes (momentum-transfer, inelastics, ionization and superelastics), excitation transfer between the Hg metastables and Tl, and molecular formation into the $B^2\Sigma_{1/2}$ state of TlHg. The electron rate constants are determined from a numerical solution of the electron Boltzmann transport equation, whereas all others are taken from values given in the literature. The solutions to the kinetics model indicate that initially most of the electron energy goes to pumping the $3P$ states of Hg. Subsequently, a significant fraction of that energy is transferred to the Tl atoms, mostly the 7^2S state. Formation of Tl $7S$ atoms into TlHg ($B^2\Sigma$) molecules gives relative population ratios of greater than 10%. The results of these calculations will be used to assess the potential of TlHg as a high efficiency laser at both 4590 and 6560 angstroms.

FB-8

Fluorescence Yields of Metal Halide Vapors

Excited by Photodissociation. J. MAYA, GTE Sylvania, Danvers, MA. - - Many metal halides are known to yield atomic and/or molecular fluorescence owing to excitation by photodissociation. We have measured the absolute quantum efficiency of this fluorescence for TlI, InI, HgI_2 and $HgBr_2$ at an excitation of 205 ± 10 nm. The TlI and InI fluorescence is due to ($7S - 6^2P$) and ($6S - 5^2P$) transitions of Tl and In respectively. The HgI_2 and $HgBr_2$ fluorescence results from (B-X) transitions of HgI and HgBr. The fluorescence spectra were corrected for spectral response, integrated and compared under the same optical conditions to the spectra of fluorescein whose quantum efficiency is well known. The absolute quantum efficiencies of TlI, InI, HgI_2 and $HgBr_2$ are 0.42, 0.20, 0.09 and 0.26 respectively. We estimate the accuracy of the relative results to be about 25%.

FB-9

The Electronic States of Alkali-Rare Gas Diatomics. B. Laskowski*, S. Langhoff* and J. Stallcop, NASA-Ames Research Center, Moffett Field, CA 94035--The report¹ that alkali-rare gas atom pairs are possible candidates for excimer lasers has stimulated the study of the electronic surfaces of these diatomics. In this paper we present the results of a self-consistent field plus configuration interaction calculation on the low lying Σ , Π and Δ electronic states of LiAr, NaAr, NaXe and CsXe. The core of each atom was described by a pseudo-potential². The calculated states agree better with experiment and are less steep in the repulsive region than the previously published semiempirical calculations of Pascale and Vandeplanque³. Spin orbit coupling is included in a semiempirical manner. Transition moments and lifetimes are given.

1. A. V. Phelps, Joint Institute for Laboratory Astrophysics, University of Colorado, Report No. 110, 1972 (unpublished).
2. L. Kahn, P. Baybutt and D. Truhler, J. Chem. Phys. 65, 3826 (1976).
3. J. Pascale and J. Vandeplanque, J. Chem. Phys. 60, 2278 (1974).

*National Research Council Postdoctoral Associates

FB-10

Laser Candidate Molecules in Excited States of Ionic Character.* D. L. HUESTIS, Molecular Physics Center, SRI International--The successful rare gas halide, mercury halide, and molecular halogen lasers share the common feature that the laser transition is from a strongly bound excited state of ionic character to a weakly bound or repulsive lower covalent state. The selectivity of production in harpooning reactions or ion-ion recombination clearly favors such ionic excited states. In an attempt to identify other candidate molecules of this class, semiquantitative rules have been derived with the requirements that the ionic state must not be the ground state of the molecule and must not be easily quenched or predissociated. Several new candidates of this class have been identified. The ionic states of all other diatomic molecules are expected to be less promising as laser candidates.

*Supported by DARPA through U.S. Army BMDATC.

A Periodic Table for Diatomic Molecules.* RAY HEFFERLIN,† Dept. of Phys., Southern Missionary College.- The need for laser-related data on free diatomics led to studies of dissociation and ionization potentials, spring constants (data 1); μ , r_e , $R_e[A-X(0,0)]$, etc. (data 2). When plotted against A, each data set for molecules AB or A₂ shows periodicity as for atoms (similar profiles between atomic "magic numbers" N and similar inserted profiles for transition metals). Configurations for A₂ close at A=N. The periodic table can be made thus: given a 2-dim. atomic chart, replace each symbol (=B) with a small chart, each of whose symbols A is replaced by AB. Data 1 for A=B show maxima at $A \approx N+3$, ignoring transition metals. For A≠B, these maxima tend to be arranged isoelectronically. This agrees with the invariance of orbitals for parts of isoelectronic sequences. A more elegant table is made by stacking portions of the A,B plane so that isovalent molecules are above each other.

*Research sponsored by the Energy Research and Development Adm. under contract with Union Carbide Corp.

†Consultant to the Oak Ridge National Laboratory, Health and Safety Research Division, where this work was performed.

SESSION GA

10:45 AM - 12:15 PM, Wednesday, October 19

Room A

ELECTRON-MOLECULE SCATTERING

Chairman: R. N. CROMPTON,
AUSTRALIAN NATIONAL UNIVERSITY

GA-1

Excitation of Molecular Nitrogen by Low-Energy Electron Impact in the Region of the Dissociation Threshold.*

D. SPENCE, R. H. HUEBNER, Argonne National Laboratory and P. D. BURROW, University of Nebraska.--Many previous measurements of threshold electron spectra in N_2 at low incident energy (<15 eV) have indicated a sharp rise in signal at approximately the dissociation limit, followed by a slow decrease in signal over the next 1.5 eV. All previous measurements of this prominent feature have been limited to essentially zero scattered electron energy (eg the SF_6 scavenger technology and the trapped electron method). Using a modified AC trapped electron technique we are able to measure slow scattered electrons at other than zero energy as a function of incident energy. Our measurements show that the triangular-shaped structure above has an essentially vertical onset at the dissociation limit (within 0.05 eV), and that this structure essentially disappears for scattered energies other than zero (within the beam resolution, about 0.08 eV). The effect of this resonance phenomenon on the dissociation of molecular nitrogen and its atmospheric implication will be discussed.

*Work performed under the auspices of the U.S. ERDA.

GA-2

Excitation of Rydberg States in the Energy Region of the Schuman-Runge Continuum of O_2 by Low-energy Electron Impact.* D. SPENCE, R. H. HUEBNER, ANL.

--Using a modification of the trapped electron technique, we have studied discrete excitation in the energy region of the Schuman-Runge continuum of O_2 , a region of intense solar atmospheric absorption. Our technique detects electrons of constant residual energy as a function of incident electron energy, and structures in the spectra are proportional to the total (i.e., integrated w.r.t. angle) cross sections for electron impact. This technique is analogous to that used by Trajmar et al.¹ who measured a signal proportional to the differential cross section using hemispherical analyzers. However, using a much closer mesh of different residual energies, (0.05 eV as opposed to 0.5→1.0 eV), our measurements indicate very rapid variation in cross sections within 1.0 eV of thresholds and lead to band assignments somewhat different from previously published data.

*Work performed under the auspices of the U.S. ERDA.

¹S. Trajmar, D. C. Cartwright, and R. I. Hall, J. Chem. Phys. 65, 5275 (1977).

GA-3

Excitation of $(2p\sigma)(np\sigma)^1\Sigma_g^+$ by Electron-H₂ Impact.* F. A. Sharpton, Northwest Nazarene College, R. L. Day and R. J. Anderson, University of Arkansas.-- The optical method and delayed coincidence techniques are used to examine twelve rotational lines of the H₂ spectrum corresponding to the electronic transitions $(2p\sigma)(np\sigma)^1\Sigma_g^+ \rightarrow (1s\sigma)(2p\sigma)^1\Sigma_u^+$, (n=3,4). The emission lines are spectrally isolated at $\Delta\lambda < 2$ Å FWHM and are identified with the following vibrational transitions: n=3 ($v'=0,1 \rightarrow v''=0$), n=3 ($v'=2 \rightarrow v''=1$) and n=4 ($v'=1 \rightarrow v''=0$). Optical excitation functions are obtained for the electron energy range 0-500 eV at H₂ target gas pressures of < 50 mtorr. Intensity measurements of the rotational lines are placed on an absolute scale by direct comparison with the H γ and H δ spectral lines produced by electron-impact dissociation-excitation of H₂. Radiative-lifetime measurements for the rotational transitions yield values in the range 38 to 70 nanoseconds.

*Research supported by the Atmospheric Sciences Section of the National Science Foundation.

GA-4

Resonances in Electron Scattering from Substituted Benzene Molecules. P. D. BURROW, Univ. of Nebraska, J. A. MICHEJDA and K. D. JORDAN, Yale U.-- The electron transmission technique of Sanche and Schulz¹ is used to study temporary negative ion formation in several mono-substituted benzene compounds. The substituents, -CN, -CHO, and -C₂H₃, each possess one or more low-lying unfilled molecular orbitals which cause additional shape resonances to appear in the transmission spectrum. The negative ion energies may be understood from simple perturbation theory arguments and effects such as inductive charge transfer. The resonance lifetimes will be discussed qualitatively in terms of the angular momentum barrier seen by the detaching electron.

¹L. Sanche and G. J. Schulz, Phys. Rev. A₅, 1672 (1972).

GA-5

Application of Semiclassical Perturbation Scattering Theory to $e^- + CO$.* F.T. SMITH and A.P. HICKMAN, Molecular Physics Center, SRI International--The interaction of an electron with CO is characterized at long range by the dipole potential (in a.u.) $\mu(R)\cos\theta/r^2$, where r and θ are the radial and angular coordinates of the electron with respect to the molecule, and R is the internuclear separation. An important feature of the interaction is that the dipole moment μ depends strongly on R .¹ We will discuss the treatment of electron scattering by this potential using the recently developed semiclassical perturbation theory. The analysis, coupled with the known resonance at 1.7 eV due to a CO^- state, may lead to a qualitative understanding of the energy dependence of the momentum transfer observed by Land² in swarm experiments.

1. K. Kirby-Docken and B. Liu, J. Chem. Phys. 66, 4309 (1977).
2. J.E. Land, Conference on MHD Systems, Argonne National Laboratory, April, 1977.

*Research supported by Air Force Office of Scientific Research.

GA-6

Momentum Transfer and Vibrational Excitation Cross Sections for Electron-Carbon Monoxide Collisions in the Range 1-4 eV. H.B. MILLOY, Electron and Ion Diffusion Unit, Australian National University, Canberra. The scattering of electrons from CO molecules has been studied by analysing new drift velocity data for pure CO and CO-inert gas mixtures at 294 K. The drift data for pure CO were taken in the E/N range from 10 to 100 Td while data for CO-Ar and CO-He mixtures were taken in the E/N range from 1.7 to 20 Td. The pure CO and the mixture data are thought to be in error by $< \pm 1.5$ and $< \pm 3\%$ respectively. The momentum transfer cross section for CO has been determined with errors of $< \pm 10\%$ from 1 to 2 eV and $< \pm 15\%$ from 2 to 4 eV. The relative vibrational cross section measurements of Schulz and Ehrhardt et al at energies > 1 eV have been normalized to an absolute scale. This involved increasing Ehrhardt et al's cross sections systematically by 22%, while Schulz' cross sections were reduced by 5% together with a reduction of the first vibrational cross section in the range from 1.0 to 1.75 eV. It was unnecessary to modify Hake and Phelps' vibrational cross sections at energies < 1 eV.

GA-7

Rate Coefficients and Inelastic Momentum Transfer Cross Sections for Electronic Excitation of N₂ by Electrons.* D. C. CARTWRIGHT, Los Alamos Scientific Laboratory.

--Differential and integral cross sections for excitation of nineteen singlet and triplet electronic states of N₂, within 14.2 eV of the ground state, have recently been determined.¹ Rate coefficients for excitation of these states have been calculated from the integral cross sections and compared to that for ionization and to the limited results previously reported. Momentum transfer cross sections for electronic excitation were determined from the differential cross sections and combined with that recently determined for elastic scattering to obtain the total momentum transfer cross section from 6 to 60 eV. These results are compared to that determined from swarm measurements. The implication of these and related results for understanding the mechanisms for various N₂ laser transitions will be presented.

*Supported by the US ERDA to Los Alamos.

1. D. C. Cartwright, A. Chutjian, S. Trajmar and W. Williams, papers I, II and III, to be published, Phys. Rev. A (Sept. 1977).

GA-8

Absolute Oscillator Strengths (10-60 eV) for Photoabsorption, Photoionisation and Breakdown of H₂O.

C. E. BRION and K. H. TAN, Department of Chemistry, University of B.C., Vancouver, Canada, V6T 1W5 and PH. E. VAN DER LEEUW and M. J. VAN DER WIEL, FOM-Institute, Amsterdam, The Netherlands.--Dipole oscillator strengths (cross sections) for the photoabsorption, partial and total photoionisation and photofragmentation of H₂O have been obtained over a range up to an equivalent photon energy of 60 eV, using electron-impact coincidence simulation techniques. The results are quantitatively equivalent to those that would be obtainable by photoelectron spectroscopy (Vancouver) and photoionisation mass spectrometry (Amsterdam) with continuously tuneable light sources. The photoionisation efficiency is also reported. The results of the two experiments are combined to provide a quantitative picture of the dipole induced breakdown of H₂O in the region up to 60 eV. Work supported by NRC (Canada) and NATO.

SESSION GB

10:45 AM - 12:15 PM, Wednesday, October 19

Room B

GLOW DISCHARGES

Chairman: A. GARSCADDEN, AIR FORCE
AEROPROPULSION LABORATORY

GB-1

Measurement of Townsend Ionization Coefficient and Breakdown Potentials for the Penning Mixtures of Ne and Kr. A. K. BHATTACHARYA, General Electric Co., Cleveland, Ohio 44112—The Townsend primary (α), secondary (γ) coefficient and breakdown potentials for Ne, Kr and their mixtures are reported. The primary coefficient was determined by measuring the variation in the luminous flux in a self-sustained Townsend discharge between two parallel plate nickel electrodes spaced 21.5 mm apart. Ne-Kr mixtures behave similar to Ne-A. The ionization efficiency function η , ($= \alpha/E$, where E is the electric field), has a maximum value for Ne + 0.1% Kr; and also the value of η for this gas mixture is larger than that for Ne + 0.1% A, especially at small values for E/p_0 (1 to 10 $\text{V cm}^{-1} \text{ Torr}^{-1}$).

GB-2

Calculation of Townsend's α at High E/p. J. H. INGOLD and R. S. BERGMAN, General Electric Co., Cleveland, Ohio 44112—A new theoretical method for calculating Townsend's α at high values of E/p is described. The method consists in assuming a displaced spherical shell for the electron velocity distribution, and using moment equations to determine the variation of electron drift velocity and average energy with E/p. Values of α/p calculated for argon show very good agreement with measurements in the E/p range of 100 to 1500 $\text{V cm}^{-1} \text{ Torr}^{-1}$. Possible reasons for disagreement at low E/p will be discussed.

GB-3

The Negative Glow Efficiency with Recombination.

W.P. ALLIS, ONERA--The ambipolar diffusion equation with a source function s and a recombination coefficient α is reduced to a dimensionless form by the two scales factors $n_0 = \sqrt{s/\alpha}$ and $l_d^2 = 2D_a(\alpha s)^{-1/2}$. The equation is then soluble in terms of elliptic functions, but if the penetration of the fast electrons from the cathode $l_p \gg l_d$, the solution takes a simpler form in terms of a hyperbolic secant, or is very close to this. The negative glow efficiency, ratio of ions diffusing from to fast electron current J_- incident on, the negative glow, is then

$$\delta = (pD_a/3)^{1/2} (P_i(V_c))^{3/4} (\alpha J_-/pe)^{-1/4}$$

where $P_i(V_c)$ is the probability of ionizations by electrons with the full cathode energy. As the cathode fall potential V_c is beyond the maximum of P_i , δ is a decreasing function of V_c . It is also a decreasing function of the current density J . The ions not diffusing toward the cathode recombine and if the recombination is dissociative, the ionization energy goes entirely into heating the gas. This is destabilizing and produces cathode streamers.

GB-4

Pre-breakdown Discharges, W. D. Partlow and

L. E. Kline, Westinghouse R&D Center--We have examined the properties of mercury-rare gas discharges operated at low fields where volume ionization is negligible. The discharge current is due to thermionically produced electrons and is limited by the electron mobility. The mixtures consisted of mercury and either Ar, Kr, or Xe at 30 to 760 torr. Temperatures were varied from 50 to 250°C. UV and visible radiation production, as well as electrical properties, were measured and compared to theoretical calculations. The measured positive volt-ampere characteristics agree well with theory. The calculated efficiency for excitation of $Hg^3P_{0,1,2}$ in these discharges is greater than 50% over a wide range of conditions. The low measured radiation production efficiency (less than 5%) is consistent with model calculations which include quenching of the 3P by Hg and the rare gas. Observation of Hg_2 emission bands suggests that $Hg+Hg^* \rightarrow Hg_2^*$ is a quenching mechanism.

GB-5

Ionization processes in the low-pressure Hg-Ar discharge. R.A.J. Keijser, L. Vriens, F.A.S. Ligthart, Philips Research Labs, Eindhoven, The Netherlands.

In model calculations on the positive column of Hg-noble gas discharges only direct and two-step ionization by electron impact have been taken into account thus far. The stepwise ionization via the 6^3P_0 , 6^3P_1 and 6^3P_2 levels was considered to be the most important process. Recent experiments and calculations have indicated that mutual collisions between 6^3P -atoms may also be important for the ion formation. We present a more detailed analysis of this problem for a range of conditions relevant for the Hg-Ar fluorescent lamp ($p_{Ar}=3$ torr; $R=1.8$ cm; $T_{wall}=20-80^\circ C$; $I=.2-.8$ A). In the analysis we have made use of experimentally determined values for particle densities and electron temperature. In the evaluation of the electron impact rates the two electron group model has been used. We find that at the higher Hg vapor pressures 6^3P collisions become even more important for the ion formation than electron impact. Both Hg^+ and Hg_2^+ will be formed. The additional ionization contributions are shown to be responsible for the well-known decrease in UV-efficiency of the Hg-noble gas discharge at temperatures above $40^\circ C$.

GB-6

The Influence of AC Current Waveform on Ultraviolet Output of Low-Pressure Mercury-Neon Gas Discharge.

S. G. Johnson, GTE-Sylvania, Danvers, Mass. The intensity variations of atomic resonance lines in a modulated low pressure Hg-Ne discharge were studied as a function of the current wave shape. The current wave shape was varied using an eight step function per half wave, while the voltage oscillated in phase as a square wave. The experimental data were obtained for a tube diameter of 2.2cm, an arc length of 50cm, and a Ne gas fill of 1.0, 3.0 and 8.0 torr. The two frequencies studied were 60 and 120 Hz for a discharge current varying from 0.4 to 1.2 Amps, and a mercury density varying from 2.5×10^{17} to 5.0×10^{17} cm^{-3} . Differences in the efficiency of the various waveforms to produce ultraviolet radiation became more pronounced as power to the lamp was increased. The intensity of the ultraviolet lines increased at a given power as the wave shape approached a square waveform.

GB-7

Multivalued V-I characteristic of Low pressure Na-Ne discharges. M.J.C. VAN GEMERT and T.G. VERBEEK, Philips Research Laboratories, Eindhoven-Netherlands.

Dynamical voltage-current measurements are reported for Na-Ne discharges (radius 1 cm; 5.5 torr Ne; 1 mtorr Na). When radial depletion of Na characterizes discharge behaviour the characteristics are found to be multivalued in V. Experimentally, such curves are found only when the rate of change in I is between 60 A/s and 4000 A/s. Below 60 A/s changes in discharge power dissipation lead to uncontrolled changes in Na-wall density. This explains why dc-experiments have failed so far to show multivalued curves, despite previous predictions¹. Above 4000 A/s the multivalued character also disappears because the loss rate of the electrons, by ambipolar diffusion and wall recombination becomes too slow to compensate the production rate. The multivalued curve is associated with discharge instability. A discontinuity in the positive column propagates in the direction cathode to anode. The velocities observed are between 10^3 and 5×10^3 m/s, depending on the discharge conditions used.

1. J.H. Waszink and J. Polman, J. Appl. Phys., 40, 2403, (1969).

GB-8

A New Theory for Striations with Experimental Verifications, E.E. KEMPE, NRL-A new general theory for striated positive columns containing atomic/molecular fill gases is elaborated that gives a unified explanation of both cathode/anode directed moving striations and standing striations along with the physical significance of the Novak potential. The p, r, and s striation varieties in neon are explained according to this new theory including the ionization mechanisms associated with their generation, and the results are experimentally verified via measurements in neon discharges and penning discharges of neon with argon admixtures. The mathematical model of the positive column derived for this theory identifies an open-loop instability that is an inherent feature of the process maintaining the charged particle density along the column. This new theory, therefore, contrasts with the widely accepted viewpoint of Pekarek that steady state striations are caused by closed-loop feedback paths consisting of propagating "ionization waves" which couple disturbances back to their point of origin with sufficient amplitudes to excite successive ionization waves. To illustrate the basic nature of the open-loop instability leading to steady state striations a simple analog of the positive column is presented.

An Exact Theory of Ionization Waves in Nitrogen,
W.H. LONG, JR., Northrop Research & Technology
Center, Hawthorne, Ca. -- The dispersion relation for
ionization waves in a low-current nitrogen discharge is
derived from a direct solution of the Boltzmann equation
and the ion continuity equation. The sharp space reso-
nances which lead to amplification of selected wave-
lengths in neon[‡] are not apparent in nitrogen because of
the many inelastic cross sections. Instead, a series of
broad resonances are found which stem from enhanced
ionization as electrons move through a periodic electric
field. The dispersion relation clearly shows the transi-
tion from spontaneously existing standing striations at
low pressure to damped, anode-directed, forward waves
at higher pressure. The mechanism for propagation of
the F⁻ wave is the fluctuation in ion drift velocity result-
ing from the electric field variation. The group velocity
at large wavenumbers is nearly constant and proportion-
al to the ion drift velocity.

[‡]K. Rohlena, T. Ruzicka, and L. Pekarek, Phys. Lett.
40A, 239 (1972).

SESSION HA

1:45 PM - 3:45 PM, Wednesday, October 19

Room A

ELECTRON-ATOM EXCITATION AND
IONIZATION

Chairman: P. BURROW,
UNIVERSITY OF NEBRASKA

HA-1

Electron Impact Excitation of SiIII. W.D. ROBB, Theoretical Division, Los Alamos Scientific Lab.*-- Recent absolute experiments on electron-impact excitation of the resonance lines of Li-like ions¹ show excellent agreement with close-coupling calculations. However, these ions have a simple structure and the calculations show relatively little sensitivity to details of the target states. Much more physically instructive experiments could be performed on ions which are isoelectronic with second-row atoms, such as Magnesium. In the present work, close-coupling calculations have been made to obtain preliminary estimates of the cross sections for $3s^2 1s - 3s3p^1 p^0$, $3p^0$ excitations in Si^{+2} . The intercombination line ($3s^2 1s - 3s3p^3 p^0$, 1894 Å) excitation cross section shows significant resonance structure at energies below the $3^1 p^0$ threshold. This structure increases the average cross section near threshold by a considerable factor (~10), and should provide an observable feature. The resonance line ($3s^2 1s - 3s3p^1 p^0$, 1207 Å) excitation cross section shows a broad (~1.5 eV) f-wave shape resonance about 1 eV above threshold which should also be amenable to observation.

*Work performed under the auspices of the U.S. Energy Research and Development Administration.

¹P.O. Taylor, R.A. Phaneuf, D. Gregory and D.H. Grandall, Abstracts of the Xth ICPEAC Conference, Paris, July (1977).

HA-2

Electron Excitation of the Alkali Resonance Lines.* S. T. CHEN and ALAN GALLAGHER,[†] JILA, U. of Colo. & NBS/Boulder.--The excitation cross sections and polarization of the K, Rb, and Cs resonance lines have been measured from threshold to 1500 eV with ~0.25 eV resolution using crossed beams. Relative intensity measurements are normalized to the Born Approximation in the high energy limit. Comparisons to previous measurements and theories are made. Combining these results with earlier data for Li and Na from this laboratory and H from others, we can see the extent of the systematic behavior for this entire series of group I elements.

*Work supported by NSF Grant PHY76-04761.

[†]Staff Member, Quantum Physics Division, National Bureau of Standards.

HA-3

Electron Impact Excitation of Metastable Argon and Krypton Atoms. * H. A. HYMAN, Avco Everett Research Laboratory, Inc., Everett, Mass. -- Calculations have been carried out in the Born approximation for electron impact excitation of metastable argon and krypton. Specifically, cross sections have been determined in the intermediate coupling scheme for the transition arrays $\text{Ar}^* (4s; J \rightarrow 4p; J')$ and $\text{Kr}^* (5s; J \rightarrow 5p; J')$, and effective cross sections have been obtained between the configurations $\text{Ar}^* (4s \rightarrow 3d, 5s, 5p, 4d)$ and $\text{Kr}^* (5s \rightarrow 4d, 6s, 6p, 5d)$. The principal conclusions of the calculations are that the cross sections for the $4s \rightarrow 4p$ and $5s \rightarrow 5p$ arrays are large and are much more important than transitions to the higher-lying states. The validity and range of application of the Born approximation for this type of electron-excited atom scattering problem will be discussed.

* Work supported by the Advanced Research Projects Agency.

HA-4

Absolute Differential Cross Sections for Elastic and Inelastic ($^1P, ^1D$) Excitation of Atomic Barium by Electron Impact. ‡ S. JENSEN†, D. REGISTER*, S. TRAJMAR* (*Jet Propulsion Laboratory; †University of California, Riverside)--As part of a continuing study on electron-photon-atom collision processes, absolute Ba elastic and inelastic ($^1P(6s,6p)$ and $^1D(6s,5d)$) differential cross sections (DCS) have been obtained in our laboratory. Utilizing a crossed beam geometry, measurements have been made at 5, 10, 20, 30, 40, 60, 80, and 100 eV throughout the angular range of 0 to 135 degrees. Data was obtained using both a high resolution gun (0.030 eV) and a low resolution gun (0.35 eV) with a collimated Ba beam which required no correction for scattering geometry. Both DCS and momentum transfer cross sections have been put on an absolute scale by normalization to the optical excitation function measurements of Chen and Gallagher.¹

¹S. T. Chen and A. Gallagher, Phys. Rev. A14, 593 (1976).

‡Work supported in part by NASA Contract No. NAS7-100 to JPL and by the Caltech President's Fund.

HA-5

Electron Impact Spectroscopy of Laser Excited Barium.[‡]

D. F. REGISTER^{*}, S. W. JENSEN[†], S. TRAJMAR^{*}, and R. T. POE[†] (^{*}Jet Propulsion Laboratory; [†]University of California, Riverside)--Utilizing a crossed electron-photon-atom beam geometry, the electron impact energy-loss spectrum of laser excited Ba ¹P(6s,6p) atoms has been studied. Laser pumping at 5535Å using Rh 110 dye in a scanning dye laser (Coherent Radiation CR-599-20) results in a ¹P population of greater than 5% of the atomic beam. Cascade from the ¹P level populates lower lying levels sufficiently so that eight superelastic and more than thirty excited state to excited state processes are observed. Some of the latter transitions exhibit cross sections comparable to ground state to excited state processes. Low angle differential cross sections for the superelastic transition ¹P(6s,6p) → ¹S(6s²) have been measured using both high resolution (.030 eV) and low resolution (.35 eV) electron optics. Variation of the superelastic scattering intensity as a function of laser light polarization with respect to the scattering plane has been measured and is found to be in agreement with theoretical predictions.

[‡]Work supported in part by NASA Contract No. NAS7-100 to JPL and by the Caltech President's Fund.

HA-6

Electronic Collisional Transfer between High

Rydberg Levels of Helium, J.-F. DELPECH, J. BOULMER and F. DEVOS, Paris U., 91405 - ORSAY, France.-- Electronic transfer rates from levels with principal quantum number n from 8 to 14 have been measured by the technique of laser-induced fluorescence spectroscopy in an afterglow plasmas at electron temperatures from 300 to 2000°K. The binary encounter theory overestimates considerably total transfers, while impact-parameter and classical Monte-Carlo theories ^{1,2} are in fair agreement with experiment. Our evidence indicates also that transitions with $\Delta n > 1$ have a substantial probability; this favors a classical treatment in this energy range.

¹ Johnson and Hinnov, Phys. Rev. 187 p.143 (1969)

² Boulmer et al., Phys. Rev. 15 p.1502 (1977).

HA-7

A New Technique to Differentiate between Resonance (Negative Ion) and Doubly-Excited Autoionizing States in the Ionization Continuum of the Rare Gases. * D. SPENCE, Argonne National Laboratory. --Doubly-excited autoionizing states in the rare gases have been studied by observations of scattered electrons, ejected electrons, photons, and positive ions, following excitation by electron impact. However, structures in the spectra obtained by the above techniques may often be attributed to energetically interspersed negative ion states (resonances), and it is not usually possible to differentiate a priori between the two above problems. We have developed a technique dependent upon scattered electron spectra whereby the two "ladders" of resonances and doubly-excited states appear to move, as a whole, relative to one another, as a function of scattered energy. Our technique provides simple differentiation between negative ion states (resonances) and doubly-excited autoionizing states. We point out that many features previously identified as autoionizing states are, in fact, resonances.

* Work performed under the auspices of the U.S. ERDA

HA-8

Measurement of Doubly-Excited States in Ne from Scattered Electron Spectra. * D. SPENCE, Argonne National Laboratory. --Using a modification of the trapped-electron method, we have located doubly-excited autoionizing states in Ne from studies of the scattered-electron spectra, obtained as a function of fixed scattered energy. Energy locations and probable configurations of the states located will be given, and a comparison with previous, more limited measurements and theoretical values will be given. The effect of "post-collision interactions" on the present and previous spectra obtained by other techniques in which such effects are expected to be relevant, will be discussed.

* Work performed under the auspices of the U.S. ERDA.

HA-9

Studies of Post-Collision Interactions in Ne from Scattered Electron Spectra. * D. SPENCE, Argonne National Laboratory. -- Recent studies of the effect of "post-collision interactions" between the scattered and ejected electrons following autoionization of a doubly-excited state, excited by electron impact, have indicated that the exchange of energy δE between the two electrons is given by $\delta E = A e^{-1.2 E_1}$, where A is a constant and E_1 is the energy the scattered electron would have had in the absence of PCI. It has been suggested¹ that the exponent 1.2 may be a "universal" constant applicable to all transitions in which PCI plays a role. With more accurate measurement of δE and E_1 , and by extending measurements closer to lower values of E_1 , we show that the energy exchange is not given by the simple exponential relationship given above. Special emphasis will be made with regard to the low-lying autoionizing states of Ne.

* Work performed under the auspices of the U.S. ERDA.

¹ D. G. Wilden, P. J. Hicks, and J. Comer, J. Phys. B 10, 1477 (1977).

HA-10

Electron Photon Angular Correlation Measurement for the 2^1P_1 State of Helium, V. C. SUTCLIFFE, N. STEPH, G.N. HADDAD and D. E. GOLDEN, U. of Oklahoma-- Electron-photon angular correlation measurements for an incident electron energy of 80 eV and scattering angles between 5° and 155° have been made in which photons from the $2^1P_1 \rightarrow 1^1S_0$ transition and electrons which have excited the 2^1P_1 state of helium are detected in coincidence. These measurements which yielding the ratio λ of the excitation cross section for the $M_J=0$ magnetic substate to the total differential cross section represent a significant extension of the previous measurements and provide extensive experimental data for comparison with theoretical calculations. Evaluation of the absolute magnetic substate excitation cross sections have been evaluated from measured total differential cross sections.

HA-11

Triple-Differential Cross Section for Low-Energy Electron Impact Ionization of Argon. S. P. HONG and E. C. BEATY,* JILA, U. of Colo. & NBS/Boulder.--Measurements have been made of the triple differential cross section for ionization of argon by electron impact. The three-dimensional shape of the cross section was investigated for the primary electron energies near 100 eV and scattering angle 15°. As observed by Ehrhardt et al., we found that in the scattering plane the "forward" lobe has a minimum for certain cases. Data taken away from the scattering plane indicate that the minimum is indeed a minimum in a full three-dimensional sense. Some approximate rotational symmetry is observed in a few cases. However no common simple symmetry has been found for all the cases.

*Staff Member, Quantum Physics Division, National Bureau of Standards.

HA-12

Electron Impact Double Ionization Cross Sections of K⁺ Ions.* R. K. FEENEY and W. E. SAYLE, II, Georgia Institute of Technology.--Absolute cross sections for the electron impact double ionization of K⁺ ions have been measured as a function of incident electron energy from below threshold to approximately 1000 eV. The peak cross section was found to be approximately $2.9 \times 10^{-18} \text{cm}^2$ at approximately 150 eV electron energy. The measurements were accomplished with a crossed beam facility operating in the pulsed beam mode. The electron source utilized an oxide cathode and operated with typical currents of 1 mA. A thermionic-type ion source produced a collimated ion beam of approximately 100 nA. After undergoing collisions with the electron beam, the ion beam charge state components were separated in a two-stage parallel plate electrostatic analyzer. Two stages of analysis were used to improve the signal-to-noise ratio. The two beam current distributions were determined by means of a movable slit scanner. Numerous consistency checks were performed to evaluate possible sources of error.

*Work partially supported by USERDA.

SESSION HB

1:45 PM - 3:45 PM, Wednesday, October 19

Room B

DISCHARGES AND AFTERGLOWS

Chairman: L. CHANIN, UNIVERSITY OF
MINNESOTA

HB-1

Stabilization of Glow Discharges by Supersonic Flows*. E. WASSERSTROM, Y. CRISPIN and O. BIBLARZ, Technion, Haifa, Israel. -- It is known that there is a strong coupling between electrical discharges and gas flows. In our work, this interaction is studied for supersonic flow¹, where the gas temperature is strongly coupled to the kinetic energy of the flow. Experimental results of supersonic flow discharges in cylindrical and conical tubes are described. It is found that the flow stabilizes the discharge and reduces the gas temperature. The results of some numerical calculations of a simplified model indicate that the computed exit temperature agrees rather well with our experiments. Our work is relevant to the stabilization of electric discharges in lasers.

-
1. E. Wasserstrom, Y. Crispin, J. Rom, and J. Shwartz: "The Interaction between Electrical Discharges and Gas Flow," to be published in the Journal of Applied Physics.

*Submitted by Oscar Biblarz

HB-2

The Maximum Constriction Phase of a Weakly Ionized Discharge in Helium. L. OSTER, JILA, U. of Colo. & NBS/Boulder.--Expanding the computer-based analysis of Jaeger, Oster and Phelps¹ we have studied in detail the behavior of weakly ionized discharges in helium during the period of maximum constriction of the radial electron density profile. At this time, the final values of electron and neutral density, and the width of the radial profile of the electron density are essentially established, whereas the final neutral density profile is reached subsequently by means of slow diffusion and conduction processes. Making use of simple analytic approximations, we present qualitative scaling relations for electron and neutral density, and for the width of the electron density profile as functions of gas pressure, external voltage, and circuit resistance.

¹Phys. Fluids 19, 819 (1976).

HB-3

Pressure and Voltage Dependence of the Electron Density in a Pulsed Helium Discharge.* M. STOCKTON, M.J. CLEARY†, and S.A. TAYLOR‡, Dartmouth College.--The experimental system consists of an externally triggered pulsed helium discharge in which the helium pressure can be varied from 0.5 to 3.5 atmospheres and the breakdown electric field from 10kV/cm to 40kV/cm. Electron densities have been determined for these conditions at various points in the discharge by observing the forbidden component of the 4471 Å line of atomic helium. These densities are then related to the spectral output of the system from these points at other wavelengths. Most electron densities observed were on the order of $n_e = 10^{16}/\text{cm}^3$.

*Supported in part by NSF and Research Corporation.

†Present address: Middlebury College, Middlebury, VT

‡Present address: Wake Forest U., Winston-Salem, NC

HB-4

Analysis of the Glow Discharge in Oxygen. J.W. DETTMER*, W.F. BAILEY, M.R. STAMM and A. GARSCADDEN, AFAPL, Wright-Patterson AFB.--Glow discharges in O₂ exist in a low field form, which has moving striations, and a relatively stable high field form. The low field form is at low current densities and high pressures. The transition between the forms is sudden and exhibits hysteresis. In the range of 1 to 10 torr and 1 to 100 ma, impedance characteristics, striation electric fields, optical outputs, wave velocity and dispersion, electron densities, neutral species mass spectra and the effects of inert and electron-detaching gas diluents were measured. The results are compared with an analysis using a Boltzmann code to determine transport properties, electron energy distribution function (EEDF), generation rates and a chemistry code to determine the species concentrations. The transition is directly related to a sudden decrease in the electron to negative ion ratio. The suggestion is made that the sudden transition is caused by dissociation reducing the vibrational cross-section influence on the EEDF permitting increased dissociation, and the atomic species changing the relative negative ion concentrations. *Now with 4950th Test Wing.

HB-5

Ozone balance in an electron beam controlled discharge in oxygen* - G. Fournier, R. Lucas, D. Pigache, Office National d'Etudes et de Recherches Aérospatiales 92320 Châtillon, France and M. Lécuyer, CNRS-ESE 91190 Gif-sur-Yvette, France - - An unusual model for ozone balance in a discharge is (1) $e + O_2 \rightarrow O + O^-$, (2) $O + 2O_2 \rightarrow O_3 + O_2$, (3) $O + O_3 \rightarrow 2O_2$. The ozone production rate predicted by processes (1-3) as well as the loss rate are more than an order of magnitude lower than those measured. It is demonstrated that the additional processes (4) $e + O_2 \rightarrow O_2^*$, (5) $2O_2^* + O_2 \rightarrow 2O_3$ along with the quenching reaction (6) $O_2^* + O_3 \rightarrow 2O_2 + O$ make up a satisfactory model. The suggested rate for reaction (5) is of the order of $10^{-31} \text{ cm}^6 \text{ s}^{-1}$. The relative importance of impurities and wall effects is also considered. The efficiency for ozone production at 800 mbar reaches 50 g/kWh.

* Submitted by J. Taillet

HB-6

Opto-Galvanic Spectroscopy of Glow Discharges: Ionization Processes. K.C. SMYTH and P.K. SCHENCK, National Bureau of Standards, Washington, D.C. --When an atomic species in a discharge is irradiated with light whose wavelength corresponds to that of an electronic transition, an easily measured voltage change is often produced. These voltage signals are due to absorption by the discharge species, and most of the results are readily interpreted in terms of photon-induced processes which either enhance or decrease ionization. Thus, opto-galvanic spectroscopy is a convenient new method for probing the many radiative and collision processes in a discharge. Detailed measurements have been made on neon in the 572-654 nm region, where transitions originating in the 1s and 2p levels are detected. The resulting voltage signals are both positive and negative, and some transitions exhibit sign changes as a function of discharge current. In addition, absorption by Ba^+ has recently been observed. In this case the second ionization potential is low (10.0 eV), so that irradiation of Ba^+ may also affect ionization processes under discharge conditions.

HB-7

Solar Radiation Maintained Optical Discharge in Cesium

A. JAY PALMER, Hughes Research Laboratories, Malibu, CA
We disclose a new concept for solar electric conversion based on the maintenance of an optical discharge in cesium vapor by concentrated solar radiation. The radiation is absorbed primarily on excited state photoionization transitions and electric power is coupled out of the plasma via MHD. General thermodynamic arguments are used to motivate the concept as an optimal approach to efficient solar electric generators. The results of a computer model of the radiatively maintained discharge will be presented. The model predicts that an optical discharge can be initiated and stably maintained at a plasma temperature of 3000-3500°K by solar radiation concentrated by a factor of a few thousand incident on cesium vapor at a vapor pressure of one atmosphere. The conductivity of the plasma is $\sim 10^3$ mho/m which is comparable to the plasma conductivity in existing MHD generators.

HB-8

The Effect of Electron Temperature Relaxation on Plasma Afterglow Processes, G.L. OGRAM, JEN-SHIH CHANG, J.G. LAFRAMBOISE and R.M. HOBSON, Dept. of Physics & CRESS, York University, Canada -- An improved theory of electron temperature relaxation effects in monatomic and molecular gas afterglow plasmas has been developed. For many gases the electron-neutral collision frequency and fractional energy transferred per inelastic collision, have dependences on electron temperature T_e which may be well approximated at low energies by simple power-law relations. Using such relations, T_e relaxation and plasma density n decay profiles have been derived for a variety of afterglow conditions. The analytical results show that: (1) For a diffusion controlled afterglow, the effects of T_e relaxation produce a rapid density decay in the early afterglow, and a slower exponential decay in the late afterglow; (2) For a volume-recombination controlled afterglow, the effects of T_e relaxation produce a slow density decay in the early afterglow, and a decay linear in $(1/n)$ in the late afterglow. Thus, the measurement of volume recombination coefficient will be underestimated under conditions when the T_e relaxation cannot be neglected; (3) These effects also lead to underestimates of the power-law exponent of the T_e dependence of the volume recombination coefficient.

HB-9

The Production of Excited Cesium Ions in Helium-Cesium Afterglows.* C.P. DE VRIES, and H.J. OSKAM, University of Minnesota--Time resolved emission and absorption spectroscopy was used to study the production of excited cesium ions in helium-cesium afterglows. The cesium pressure ranged from 10^{-6} to 10^{-5} Torr and the helium pressure was varied from 1 to 20 Torr at a gas temperature of 87°C . Strong emission was observed from the lowest six levels in the $5p^56p$ configuration of Cs^+ . Only the lowest energy level is produced by the reaction: $\text{He}^m(3\text{S}) + \text{Cs} \rightarrow (\text{Cs}^+)^* + e + \text{He}$, even though the next lowest level is more nearly in resonance with $\text{He}^m(3\text{S})$. All six states are produced by the reaction $\text{He}_2^+ + \text{Cs} \rightarrow (\text{Cs}^+)^* + 2\text{He}$, where the energy defect is from 1.9 to 2.7 eV. A dissociative charge exchange reaction mechanism is proposed to explain the occurrence of the process in spite of the large energy defect.

*Work supported by the National Science Foundation
(Grant # ENG-76-10905)

HB-10

Relaxation of Neodymium in a Weakly Ionized Expanding Plasma.* Hao-Lin Chen, Ray Bedford, C. Borzileri, W. Brunner and M. Hayes, University of California, Lawrence Livermore Laboratory.--The laser resonance absorption technique has been used to determine the relaxation rate of electronically excited neodymium vapor during its expansion into a vacuum. Significant increases of population into ground and 1128 cm^{-1} levels were found. Analysis shows that interaction between excited metastable atoms and electrons are much more important for relaxation than atom-atom collisions. The final population of neodymium appears to be frozen at a temperature lower than the surface temperature of melt.

*This work was performed under the auspices of the U.S. Energy Research and Development Administration under contract No. W-7405-Eng-48.

SESSION JA

8:30 AM - 10:30 AM, Thursday, October 20

Room A

RARE GAS, METAL, AND GROUP VI KINETICS
AND SPECTROSCOPY

Chairman: J. MANGANO, AVCO

JA-1

Radiative Lifetimes and Reaction Rates of the Lowest Bound Molecular States in Krypton and Krypton-Xenon Mixtures.* F.H.K. RAMBOW, T.D. BONIFIELD, and G.K. WALTERS, Rice University--Time dependences of the VUV emissions near 1450 Å from pure krypton and from xenon-doped krypton were measured following pulsed excitation by a low intensity e-beam. The radiative lifetimes of the lowest O_u^+ and 1_u molecular states of krypton are 4.1 ± 0.6 nsec and 370 ± 10 nsec respectively. $Kr_2^*(O_u^+)$ is produced in three body reactions with rate $(1.6 \pm 0.3) \times 10^{-32}$ cm⁶/sec. Rates for the collisional mixing reactions $Kr_2^*(O_u^+) + Kr \rightleftharpoons Kr_2^*(1_u) + Kr$ are $< 10^{-13}$ cm³/sec (forward) and $< 10^{-14}$ cm³/sec (reverse), based on preliminary analysis of density dependences of the O_u^+ and 1_u destruction frequencies. In xenon-doped krypton, the $Kr_2^*(1_u)$ state is quenched by energy transfer to $Xe(^3P_1)$ with rate coefficient $(3.0 \pm 0.2) \times 10^{-10}$ cm³/sec.

*Supported by Division of Physical Research USERDA.

JA-2

Spectroscopic Studies on Recombination Fed Line Emissions in High Pressure Rare Gases.* A. SZOKE and E. V. GEORGE, Lawrence Livermore Laboratory. Xenon (and Argon) gas were excited by a short pulse (25 nsec) 80 keV electron gun at pressures up to 4 atmospheres. The intensity and time dependence of 6p-6s Xenon emission lines (and 4p-4s Argon emission lines) were monitored at various pressures. These lines are emitted following dissociative recombination of Xe_2^+ (Ar_2^+). Our observations will be presented and compared to computer model calculations.

*Supported by US ERDA Contract W-7405-Eng-48.

JA-3

Kinetics and Spectra of E-Beam Excited Ar/Xe Mixtures.* H. T. POWELL and A. SZOKE, Lawrence Livermore Laboratory. The time dependence and spectra of emission bands at 1260, 1290, 1470, 1720, and 3300 Å have been studied as a function of Ar and Xe pressures using either a 20 ns, 1 A/cm² or a 50 ns, 100 A/cm² e-beam pulse. Typical mixtures studied are a few Torr of Xe in several atmospheres of Ar. The 1260 and 1720 Å bands arise from Ar₂^{*} and Xe₂ excimers while the 1290 and 1470 Å bands are believed to result from excited Xe (6s 1P₁ and 3P₁) in collision with Ar, i.e., ArXe*. Collision induced ArXe absorption is also observed within the Ar₂^{*} emission band. The 3300 Å band is identified as XeAr⁺ emission. Kinetic channels for formation of the various species will be discussed and attempts to produce laser action on the ArXe* bands will be described. *Supported by US ERDA Contract W-7405-Eng-48.

JA-4

Performance of Rare Gas Excimer Laser and Fluorescence Sources.* H. T. POWELL, J. J. EWING, R. D. FRANKLIN, and R. A. HAAS, Lawrence Livermore Laboratory. Experimental and analytical studies of large volume e-beam pumped rare gas excimer laser and fluorescence sources is reported. The efficiency of converting e-beam pump energy into vuv excimer radiation coupled into a photolytic laser medium has been modeled and measured for both coherent and incoherent modes of extraction. Large area (>20 cm²) superfluorescent Kr₂^{*} and Xe₂^{*} sources routinely produce fluences of 0.1 and 1 J/cm² respectively in 50 ns pulses. Unlike the fluorescence time dependence, the superfluorescent emission is strongly peaked toward the leading edge of the excitation pulse. The instantaneous extraction efficiency in this leading edge spike is considerably greater than the 50 ns average. Modeling interpretations including the effects of excited state loss processes are reported. Comparisons are made between experimental measurements of fluorescence coupling into a 50 cm long cell and theoretical calculations which include nonuniform electron beam excitation and geometric fluorescence coupling. *Supported by US ERDA Contract W-7405-Eng-48.

JA-5

Rare Gas Excimer Radiation Pumping for Photolytic Laser Media.* R. A. HAAS, R. D. FRANKLIN, J. J. EWING, C. W. WERNER, Lawrence Livermore Laboratory, and W. L. MORGAN, JILA, University of Colorado and NBS. An Analysis of incoherent and coherent pumping of photolytic laser media with electron beam excited rare gas excimer radiation has been developed. Conditions suitable for driving photodissociation waves during Group VI laser excitation have been investigated. The incoherent pumping calculations include nonuniform electron beam excitation in the rare gas fluorescing medium, geometric radiation coupling to the absorber and bleaching wave propagation. Fluorescer to absorber coupling efficiencies of $\leq 25\%$ are calculated for single side pumping. An improvement in efficiency can be achieved if vuv reflecting optics and other coupling geometries are employed. Analysis of rare gas excimer laser pumping was carried out using a kinetics code modified to self-consistently calculate amplifier performance. For the Xe_2^* laser the calculations indicate that the effective laser saturation flux is $\sim 10 \text{ MW/cm}^2$ and that laser efficiency is limited, primarily by photoionization of $\text{Xe}_2(^3\Sigma)$ molecules, to values $\leq 5\text{-}10\%$. Improvements in laser efficiency may be achieved if rare gas mixtures are employed.
*Supported by US ERDA Contract W-7405-Eng-48.

JA-6

Collision-Induced Predissociation of Sr_2 Molecules. R. R. FREEMAN and P. F. LIAO, Bell Labs--We have observed strong collisionally induced predissociation of laser excited $A\Sigma_g$ Sr_2 molecules to an excited 3P_1 ground 1S_0 atom and have made the first quantitative measurements of the dissociation. Cross section for dissociation in the range of 100Å^2 for Sr_2 collisions with Ar have been measured. The dissociation rate is a sensitive function of excitation level in the excited molecular potential and is a maximum near the potential minimum. The rapid dissociation rate prevents significant vibrational relaxation within the radiative lifetime and appears to reduce the prospects of Sr_2 singlet systems (and by implication, other alkaline earth dimers) being effectively employed as an excimer laser system.

JA-7

Multiphoton Ionization of Cs₂ Dimers Through Dissociative Molecular States*. J.A. ANDERSON and C.B. COLLINS, Univ. of Texas at Dallas, D. POPESCU, Institute of Physics of Bucharest, IOVITZU POPESCU, Univ. of Bucharest, Romania--Hybrid resonances observed in the multiphoton absorption spectrum of cesium and rubidium dimers have recently contributed to an improved understanding of the interatomic potentials of the heavy alkalis.^{1,2} Such hybrid multiphoton resonances generally occur through dimer or excimer states of a collision complex and those reported here have been excited by superimposed beams from two separately tunable dye lasers. The wavelength of one laser was fixed on an atomic transition resonance while the other was scanned through the visible wavelength range. The resulting spectrum showed new transitions to molecular states dissociating to give the atoms excited by photons of the other wavelength.

*Conducted as part of the U.S.-Romanian Cooperative Program in Science and Technology, supported in part by the U.S. N.S.F. Grants GF443 and INT76-18982.

1. C.B. Collins, B.W. Johnson, M.Y. Mirza, D. Popescu, and Iovitzu Popescu, Phys. Rev. A10, 813 (1974).

2. C.B. Collins, S.M. Curry, B.W. Johnson, M.Y. Mirza, M.A. Chellehmalzadeh, J.A. Anderson, D. Popescu and Iovitzu Popescu, Phys. Rev. 14, 1662 (1976).

JA-8

Sequential Two-Photon Ionization of Li₂ and Na₂*. GENE P. RECK, B. P. MATHUR and ERHARD W. ROTHE, Wayne State University -- The two-photon sequential ionization of Li₂ and Na₂ is observed. In each case the dimers constitute about 1% of an effusive alkali beam. A cw multimode argon-ion laser intersects the alkali beam and the resulting ions are mass analyzed. Similar experiments have been reported¹ with Cs₂, CsRb, and Rb₂, in which both atomic and molecular ions were produced. In contrast, only dimeric ions are obtained here. The intermediate species are the B¹Π_u states. Large isotopic effects are observed at each of the laser wavelengths for the production of ⁷Li₂⁺, ⁶Li₂⁺ and ⁶Li⁷Li⁺. The relative two-photon ionization probability for various wavelengths [\equiv ion production rate/(photon flux)²] are also presented for Li₂ and Na₂.

*Research supported by the Air Force Office of Scientific Research, the Army Research Office and the National Science Foundation.

¹E.H.A. Granneman, M. Klemer, K. J. Nygaard and M. J. Vander Wiel, J. Phys. B. 9, 865 (1976).

JA-9

Photolytic Production of S(¹S) in Liquid Ar.[†]

L. ABOUAF, J. MARGEVICIUS, M.V. McCUSKER, and D.C. LORENTS, Molecular Physics Center, SRI International-- OCS at a few ppm in liquid Ar at 83°K has been photolyzed using an H₂ laser at 161 nm [where OCS has a large quantum yield for dissociation to S(¹S)]. We observed a narrow emission (FWHM < 65 Å) peaked at 456 nm and a broad, weaker emission from 376-470 nm. The 456 nm peak is identified as the S(¹S-³P) emission blue shifted relative to its atomic wavelength. The decay time of this emission is exponential with a lifetime of 35 ± 10 μs independent of OCS density in the low ppm range. This lifetime is believed to be the collision induced radiative lifetime of S(¹S) in Ar at 83°K. The broad spectral feature is probably unresolved S₂(B-X) emission and shows a similar 35 μs decay consistent with production by the reaction S(¹S) + OCS → S₂^{*} + CO. Intensities were found to be dependent on total pumping time because of photodestruction of OCS.

[†]Supported in part by USERDA.

JA-10

Optical Emissions from Doped Condensed Rare Gases Excited by Electrons.^{*}

J. MARGEVICIUS, L. ABOUAF, M.V. McCUSKER, D. L. HUESTIS, and D.C. LORENTS, SRI International--We have observed the optical emissions from e-beam excited liquid phase Ar at 85°K doped with OCS or O₂ at the level of a few ppm. Undoped Ar is characterized by broadband emissions peaking at 203 nm and 275 nm as well as a broadened O(¹S-¹D) emission peaked at 558 nm. Addition of O₂ to the 10 ppm level enhances the O(¹S) and 203 nm emissions. Doping with OCS leads to a prominent S₂^{*}(³Σ_u⁻ - ³Σ_g⁻) band progression (v' = 0 to v'') similar to those observed in matrices but with a lesser red shift. The time decay of these bands exhibits a fast component (< 5 μs) and a long non-exponential component extending to ~ 1 ms that appears to be due to recombination of S(³P) atoms. Spectral study of the slow decay component shows a peak at 455 nm identified as a blue shifted S(¹S-³P) transition. The decay of this emission has a ~ 35 μs component but in addition a longer component related to the S₂^{*} decay. The possible mechanisms for this behavior will be discussed.

^{*}Supported in part by USERDA.

SESSION JB

8:30 AM - 10:55 AM, Thursday, October 20

Room B

CHARGE TRANSFER AND FAST BEAMS

Chairman: N. ADAMS, UNIVERSITY OF
BIRMINGHAM

JB-1

Spin Dependent Charge Transfer in Low-Energy Collisions Between Helium Ions and Cesium Atoms.* H. A. Schuessler, Texas A&M University. -- The experiment demonstrated that total spin angular momentum is conserved in the near resonant charge transfer collisions between oriented helium ions and oriented cesium atoms. The resulting spin dependence of the total charge transfer cross sections is described using singlet and triplet channels based on the molecular potential energy curves of the collision pair. The experiment was performed with helium ions stored in a rf-quadrupole trap in interaction with an optically pumped beam of cesium atoms. Total spin dependent charge transfer cross sections were measured¹ in the energy range of a few eV and are, for example, for a well depth of 3eV for the singlet cross section $Q_1 = 1.0(2) \times 10^{-14} \text{cm}^2$ and for the triplet cross section $Q_3 = 0.5(1) \times 10^{-14} \text{cm}^2$.

* Supported by the National Bureau of Standards, the Robert A. Welch Foundation, and the Center for Energy and Mineral Resources of Texas A&M University.

¹H. A. Schuessler, Metrologia 13, May (1977)

JB-2

Spin-Conservation in Double Charge Transfer Collisions.* G.D. MYERS, J.G. AMBROSE, P.B. JAMES, and J.J. LEVENTHAL, Univ. of MO-St. Louis.--The restrictions imposed by spin conservation on HeI states formed by two electron transfer in He⁺⁺-He, H₂, Ne and O₂ collisions have been investigated by measuring the relative $(3d^3D \rightarrow 2p^3P^0)/(3d^1D \rightarrow 2p^1P^0)$ emission intensity from these collisions. The experiments were performed by directing a magnetically selected He⁺⁺ beam, at the desired kinetic energy (4-500 eV), into a collision cell containing neutral gas at 1 mtorr pressure and spectroscopically analyzing the collision-produced radiation; thus unambiguous comparison of intersystem data is possible. The H₂, Ne and O₂ results are consistent with the Wigner spin-conservation rule, but He yields an anomalously high triplet/singlet ratio. This result and the extremely low measured emission cross section ($\sim 10^{-3} \text{Å}^2$) for production of these states in He⁺⁺-He collisions are correlated by attributing the spin-flip interactions to short range He⁺⁺-e encounters in which strong coupling between spin and collisional angular momenta is possible.

*Work supported by the Office of Naval Research under Contract No. N00014-76-C-0760.

JB-3

Fine Structure in Low Energy Charge Transfer in Argon. K. B. MC AFEE, W. E. FALCONER, R. S. HOZACK and D. J. MC CLURE, Bell Laboratories--Mobility experiments of atomic ions in argon at room temperature have uniquely defined a single value for Ar^+ mobility despite attempts to resolve the expected fine structure of the arrival ion currents. To understand the momentum exchange which accompanies charge transfer during collisions of the two electronic states ($^2P_{1/2}$, $^2P_{3/2}$) of the argon ion with the parent atom, a crossed atom-ion beam apparatus was designed to measure the kinetic energy of the target atoms after charge transfer. The interaction region of the particles was maintained at essentially zero intensity of electric and magnetic fields. After a drift space the kinetic energy of the charged target species was measured using a spherical energy analyzer. Ion identity was determined by a tandem mass analyzer. The ion source consists of a low pressure electron-emission sustained ionization region followed by magnetic Ar^+ ion selection. For laboratory-frame collision energies of about 123 eV two principal scattering peaks are observed. They correspond to exothermic and endothermic processes requiring about 0.17 eV energy separation. The argon ion fine structure separation is about 0.178 eV. Without energy analysis the two peaks are unresolved.

JB-4

Atomic Ion-Metal Atom Charge Transfer.* J. A. RUTHERFORD and D. A. VROOM, IRT Corp.--Charge transfer cross sections for atomic ions in collision with metal atoms have been measured in the energy range from 1 to 5000 eV. Specifically, the ions Hg^+ , Xe^+ and Cs^+ and the neutrals Mo, Fe, Al, Ta, Ti, and C were considered. In general, cross sections for charge transfer were found to be less than 10^{-15} cm² for most processes over the total energy range. Exceptions are Hg^+ in collision with Ti and Ta. In some cases, simple models are given to explain the results obtained.

*Work supported by NASA under Contract No. NAS3-17759.

JB-5

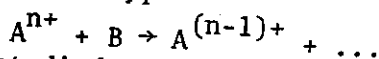
Excited Hydrogen Atom and Argon Atom Production by Charge Transfer of $(Ar^+)^*$ in H_2 . H. L. ROTHWELL, Joint Institute for Laboratory Astrophysics, R. C. AMME and B. VAN ZYL, Univ. of Denver. -- An atomic beam apparatus equipped with a vacuum ultraviolet monochromator and channel electron multiplier detector has been used to study production of excited H and Ar atoms from the low energy charge transfer of metastable argon ions $(Ar^+)^*$ in H_2 . The observed emissions of Lyman-alpha (121.6 nm) and argon resonance line (106.7 and 104.8 nm) radiations confirm the formation of these excited neutral atoms in the charge transfer process. Metastable argon atoms are also produced in significant quantities. Measurements performed as a function of ion source electron energy show that the ultraviolet radiation and metastable argon atom formation exhibit an apparent threshold at about 32 eV electron energy, or 16.4 eV above the threshold for ground state Ar^+ formation. This energy is close to the threshold for population of the $3s^2 3p^4 ({}^3P) 3d^4 D_{7/2}$ level of the argon ion, the lowest of several excited states of the ion expected to be metastable. For electron energies in the 50 eV range, it is estimated that of order 1 % of the argon beam ions are in such metastable states and that their charge transfer cross section in H_2 is of order 10^{-15} cm^2 .

JB-6

Charge Transfer Reactions of Excited $O^+({}^2D)$ and $C^+({}^4P)$ State Ions with Neutral Molecules. T.F. MORAN and J.B. WILCOX, Chemistry Department, Georgia Institute of Technology -- Charge transfer cross sections have been measured for reactions of excited $O^+({}^2D)$ and $C^+({}^4P)$ atomic ions with Ar, H_2 , N_2 , O_2 , CO, NO, and CO_2 in the 0.7 to 2.5 keV ion kinetic energy range. Reactant O^+ and C^+ ion beams have been produced by controlled electron impact ionization of neutral oxygen and carbon monoxide respectively. Fast neutral products resulting from the charge transfer reactions have been measured using time-of-flight techniques. Cross sections determined for reactions involving excited state reactants range from 6 to 30 \AA^2 depending on the neutral reactant species. Charge transfer cross sections measured for ground state $O^+({}^4S)$ and $C^+({}^2P)$ ions are uniformly smaller than the corresponding excited state reactions throughout the kinetic energy range. Differences between the cross sections for excited and ground state reactions in particular systems are consistent with the smaller energy defects and favorable vibrational overlaps for the reactions involving excited states.

JB-7

Electron Transfer in Collisions of Doubly Charged Atomic Ions with Rarer Gas Atoms for Primary-Ion Energies Below 100 eV. WILLIAM B. MAIER II, Los Alamos Scientific Laboratory. *--Twelve electron-transfer processes of the type



have been studied, and cross sections have been measured for nine of them, where A is He, N, O, Ne, or Ar, B is He, Ne, Ar, or Kr, and n=2 or 3. Most of the cross sections studied are moderately large ($>0.5 \text{ \AA}^2$) somewhere in the energy range studied. For $\text{He}^{++} + \text{He}$, $\text{Ne}^{++} + \text{He}$, $\text{Ne}^{++} + \text{Ne}$, and $\text{Ar}^{++} + \text{Ar}$, the cross sections are $<0.2 \text{ \AA}^2$. For $\text{Ar}^{++} + \text{He}$, $\text{He}^{++} + \text{Ne}$, $\text{Ne}^{++} + \text{Ar}$, and $\text{Ar}^{++} + \text{Kr}$, the cross sections are $\geq 1 \text{ \AA}^2$ at the lowest (0.1-0.4 eV) center-of-mass energies reached. The observations can be qualitatively understood by examining the pseudocrossings of the potential-energy curves of the reactants and products.

*Supported by U.S. Energy Research And Development Administration

JB-8

Energy Transfer in Collisions of He and H Atoms with N_2 , CO , and O_2 .* G.H. BEARMAN and J.J. LEVENTHAL, Univ. of MO-St. Louis.--Spectroscopic analysis of optical emissions resulting from collisions between neutral hydrogen or helium atoms and diatomic molecules (N_2 , CO , O_2) has been performed at energies down to 140 eV. Processes observed include collision induced excitation, impact ionization, Penning ionization and excitation transfer. Optical spectroscopy yields electronic and vibrational state distributions of the reaction products. For most of the processes observed, the Wigner spin rule is obeyed. Vibrational state distributions of excited molecular ions differ markedly from those predicted by a simple vertical transition model. This is particularly true for low energy impact ionization. On the other hand, impact excitation to electronic states of the neutral molecules [such as $\text{N}_2(\text{C}^3\pi_u)$] produced nearly Franck-Condon vibrational distributions at all energies.

* Work supported by U.S. ERDA under Contract No. EY 76-S-02-2718.*000.

JB-9 Collisional Dissociation of NO_3^- and of Some Solvated Hydroxyl Ions.* JOHN F. PAULSON, Air Force Geophysics Lab.--A double mass spectrometer system has been used to study the dissociation of NO_3^- , $\text{OH}^- \cdot \text{HNO}_3$, $\text{OH}^- \cdot \text{H}_2\text{O}$, and $\text{OH}^- \cdot 2\text{H}_2\text{O}$ in collisions with Ar, N_2 , and O_2 . For NO_3^- formed in a mixture of NO and O_2 , the products are O^- , O_2^- , and NO_2^- . The ions at a mass-to-charge ratio of 80, formed in a mixture of NO, O_2 , and H_2O , dissociate to produce OH^- rather than NO_3^- . This species is therefore believed to be $\text{OH}^- \cdot \text{HNO}_3$ rather than $\text{NO}_3^- \cdot \text{H}_2\text{O}$, consistent also with the expected greater stability of the former structure. Cross sections for dissociation of the hydrated hydroxyl ions reach values of 10 to 20×10^{-16} cm^2 and show onsets which are in fair agreement with the more accurate enthalpy changes measured by Payzant et al¹ for loss of the water of hydration.

* Supported in part by the Defense Nuclear Agency

1. J.D. Payzant, R. Yamdagni, and P. Kebarle, Can. J. Chem. 49, 3309 (1971).

JB-10 Ionizing Collisions Between Molecules in the Near-Threshold Energy Region. NYLE G. UTTERBACK, TRW, Inc., and BERT VAN ZYL, Univ. of Denver. -- Absolute total ionization cross sections for N_2 and CO beam molecule collisions with N_2 , CO, NO, and O_2 targets have been measured to within about 1 eV of their respective ionization thresholds. Mass spectrometric identification of the product ions scattered in the forward direction has been used to investigate specific reaction channels and explain characteristic structures in the total ionization cross sections near threshold. Such structures, the most dramatic of which results from the $\text{N}_2 + \text{CO} \rightarrow \text{NO}^+ + \text{CN}^-$ ion pair formation reaction, often tend to dominate the cross section shapes in the threshold regions. Dissociative ionization reactions are also major contributors to the total ionization processes when their somewhat larger threshold energies are reached. In fact, "simple" ionization, where one of the initial molecules simply gives up an electron, is not even an important process for some reactions in this low energy regime. A crude model to explain these observations is presented along with the results of the cross section measurements and the mass spectrometric investigations.

JB-11

Formation of UF_6^- by Impact of Cs Atoms.*

R. J. WARMACK, J.A.D. STOCKDALE, and R. N. COMPTON
Health & Safety Research Division, Oak Ridge
National Laboratory, Oak Ridge, TN 37830 -- The
formation of UF_6^- has been studied using crossed
cesium and UF_6 beams for Cs laboratory energies
ranging from 6.5 to 100 eV and laboratory scattering
angles from zero to five degrees. Both positive
(Cs^+) and negative ions were examined by a quadru-
pole mass spectrometer and their energy spectra
recorded by electrostatic energy analysis. The
resulting distributions of reaction Q against Cs^+
ion intensity were negative, peaking at -4.8 eV for
a laboratory energy of 8.7 eV and scattering angle
of 0° and at -5.3 eV for 37.9 eV and 0° . (Q =
excess kinetic energy of products over reactants).
These results suggest that for this energy range
the reaction in which UF_6^- is formed proceeds via an
excited electronic state of UF_6^- .

*Research sponsored by the Energy Research and
Development Administration under contract with
Union Carbide Corporation.

SESSION KA

10:45 AM - 12:15 PM, Thursday, October 20

Room A

BREAKDOWN, CORONA, AND BOUNDARY
EFFECTS

Chairman: L. E. KLINE, WESTINGHOUSE

KA-1

Continuous Current in the Positive Point-to-Plane Corona:

M. HIRSH and M. GOLDMAN, Labo. Physique des Décharges (CNRS), Gif-sur-Yvette, FRANCE. Separate measurements have been made of the continuous (I_C) and impulsive (I_P) components of corona current in a diffuse stressed-anode point-plane discharge in laboratory air under continuous applied voltage. The diffuse discharge, which is normally avoided in fundamental studies, shows a much longer range of continuous current, free from streamer pulses, than does the "well-aligned" discharge; this permits some new insights into the origins of both I_C and I_P (see also next abstract). It also closely resembles some situations of practical interest. For currents below $17 \pm 1 \mu\text{A}$, I_C is the total corona current, and satisfies a Townsend-like law $I_C = 0.1 L^{-3/2} V(V - V_S)$ as a function of applied voltage V , for gap lengths L from 3 to 40 mm, and point radius r between 6 and 32 μm ; we find $V_S = A(r) + B(r) \cdot L$. This is compatible with positive space charge control of current in the pulseless regime. For higher currents, between the onset of streamer pulses but below spark breakdown, I_C is somewhat larger than the law predicts, as measured between pulses. This explains the persistence of the Hermstein glow in the streamer regime; reasons for deviations from the law in terms of space-charge depletion, etc., are given.

§ Permanent address: Univ. of Minnesota, Morris

KA-2

Streamer Pulses and the Spark Transition in Positive-

Point-to-Plane Corona. M. HIRSH and G. HARTMANN, Labo. Phys. des Décharges (CNRS), Gif-sur-Yvette, FRANCE. In positive point-plane discharges in laboratory air for sufficiently high current and for gap lengths $L > 3$ mm, streamer pulses are seen whose waveform shows the streamer transit, followed by a fast-rising spike of electron current with a slowly falling "tail" having a well-marked transition back to continuous current I_C at a time T after the streamer. We interpret this tail as the transit time of negative ions from the plane to a detachment zone several mm from the point. Measurements of T vs gap voltage V give a consistent value of mobility of the negative ions. In a well-aligned discharge, the pulses start at low currents; from their repetition frequency f one can calculate a positive-ion mobility, suggesting that f is controlled by sweeping times of the positive ions. Also, T is smaller than, but nearly equal to, $1/f$, except at small gaps, where it is noticeably smaller. In the diffuse discharge (see preceding abstract), pulses occur at $I_C > 17 \mu\text{A}$; T again yields good mobilities, but the pulse frequency no longer does. There is a marked delay between T and the next pulse which decreases as V is increased, until it vanishes at breakdown, which occurs for $I_C \approx 12 L^{1/3} \mu\text{A}$.

§ Perm. Address: Univ. of Minnesota, Morris

KA-3

The role of neutral density variations in the formation of streamer induced spark. E. MARODE, F. BASTIEN Lab. Phys. Dech. (CNRS) ESE 91190 Gif/S/Yvette, France, M. BAKKER, Math. Centrum, Amsterdam, Holland. - The breakdown of a point-plane gap in electronegative mixtures near atmospheric pressure begins with the formation of a low conductivity filament. At this stage, the $(\alpha - \eta)$ coefficient is negative (α ionisation, η attachment) within the filament so that the current decreases. This decrease is however followed by a sudden increase leading to the transient spark. Till now only qualitative explanations of the increase involving detachment or ionization by new space charge waves have been given. In this paper a different model is proposed. The rather small current is enough to increase the neutral temperature within the filament. The resulting increase in pressure has the tendency to relax to the normal external pressure inducing a decrease in density within the filament. As a result E/N rises until $(\alpha - \eta)$ becomes positive, leading to the final current increase. The model leads to hydrodynamics equations (similar to¹) and electrical equations which are solved numerically to compare theory with experiment.

1 G.L. Rogoff, Phys. of fluids, 15, 11, 1931 (1972).

KA-4

Prevention of Spark Development in Intense Corona Discharges. M. J. KOFOID, Seattle, Wash. -- A practical means has been developed which allows greatly increased corona currents to flow between a field-concentrating cathode and a plane unclean anode without sparking. Basic operation is not that of a current limiting resistor. In the case discussed the anode is covered with dust of high enough resistivity ρ to produce back corona; voltage due to electron deposition on the dust causes breakdowns in the dust. With a simple metal anode ionization from a breakdown would trigger a spark. The improved "resistive" anode has the metal surface covered with high dielectric strength material of specific high ρ . Before a discharge precipitated by a breakdown can contract enough at the anode spot to convert from a low- to a high-current-density form, i.e. into a spark, the voltage drops in the resistance material immediately beneath the anode spot produce counter-acting expansion forces sufficient to prevent spark formation. From a study of anode spot development photographs of J.M. Sommerville and C. Granger it was estimated that the anode spot radius may contract to perhaps 0.03 mm without forming a spark. The resistive coating thickness should need to be only a few times greater; a 0.25 mm thick coating with $\rho = 10^{10}$ ohm-cm has been found to be sufficient.

KA-5

Surface Arcs. G.H. ECKER, Ruhr-Universität, Germany -- We investigate under what conditions in the absence of an external electromotive force an arc can operate on the surface of a wall in contact with a plasma. We call such an arc a "plasma induced arc". In addition to the crucial cathodic processes, we study the anodic current flow and here we consider especially the example of the so-called "unipolar arc".¹ Conditions are formulated for the existence of such an arcing phenomenon operating in a restricted area on the surface of a wall in contact with a plasma. Phenomena affecting the operation of this mode are discussed.

¹A.E. Robson and P.C. Thonemann, Proc. Phys. Soc. 73, 508 (1959)

KA-6

A Cold Cathode Glow Discharge Electron Gun, D.L. JORDAN, RSRE, MOD(PE), Baldock, Herts., G. G. ISAACS, GEC, Hirst Research Centre, Wembley, Middx, England-- Measurements have been performed on a cold cathode glow discharge electron beam gun at voltages up to 160 kV, current densities of 1-2000 A/m² and pulse lengths of 10-100 μ s, with the aim of understanding the discharge physics of this low pressure (\sim 30 mTorr) device. Scaling of the electron beam aperture from 25 mm x 150 mm to 100 mm x 1000 mm has been successfully demonstrated. Tailoring of the electron beam profile can be achieved by modifying the electric field distribution near the ion sheath-plasma boundary, the length of the ion sheath adjacent to the cathode being a function of both gun current and voltage for a given gas. The advantages of incorporating an auxiliary discharge (both dc and pulsed) into the plasma region of the main gun are described. Modulation of this auxiliary discharge to provide short ($<$ 1 μ s) electron beam pulses has been carried out; to achieve this it is necessary to enhance the recovery processes in the device. Finally, the application of the gun to both 1 kJ single shot and high pulse repetition frequency (\sim 200 Hz) electron beam CO₂ lasers is described.

Copyright © Controller, HMSO London 1977

KA-7

SOLUTION OF THE COLLISIONLESS PLASMA - SHEATH EQUATION FOR ION EXTRACTION THROUGH AN APERTURE*

J. H. Whealton and J. C. Whitson, Oak Ridge National Laboratory--Solution to the Poisson-Vlasov equations for ions extracted from a plasma is found in two dimensional axially symmetric geometry assuming a Boltzmann density of equilibrium electrons. The region of consideration is 1) where the ion-neutral mean-free-path is much larger than a debye length and aperture size, and 2) debye length on the order of aperture size or smaller. The variation of sheath position, shape and thickness as a function of aperture radius, source plasma density, potential (relative to extraction boundary), and electron temperature will be described explicitly. Also considered are the effect of these parameters on the ion flow with particular emphasis on causes of nonlaminar flow, sensitivity of ion flow on slow plasma density fluctuations, and ion transmission through the aperture.

*Research sponsored by the Energy Research and Development Administration under contract with Union Carbide Corporation.

KA-8

Investigation of the Velocity Distribution of Neutrals in the Wall Region of Low Pressure He-Discharges,

J. HACKMANN and J. UHLENBUSCH, Physics Institute II, University of Dusseldorf, 4000 Dusseldorf, FRG.--The velocity distribution of neutrals in the wall region of low pressure He-discharges ($n \approx 10^{15} \text{ cm}^{-3}$) was calculated from Boltzmann's equation. Charge transfer and ionisation processes as well as particle-wall interaction were taken into account. The results are compared to experimentally determined velocity distributions derived from Doppler broadened line profiles. Experiments and calculations show strong deviations from a Maxwellian distribution.

SESSION KB

10:55 AM - 12:15 PM, Thursday, October 20

Room B

ION-ION AND ION-ELECTRON RECOMBINATION

Chairman: T. M. MILLER, SRI INTERNATIONAL

KB-1

Binary Mutual Neutralisation Rate Coefficients Determined in a Flowing Afterglow. D.SMITH and M.J.CHURCH U of Birmingham, England-- A survey of the measurements of binary ion-ion mutual neutralisation rate coefficients determined in an ion-ion flowing afterglow plasma¹ will be presented. Several reactions of 'simple' ions have been studied² such as $\text{NO}^+/\text{NO}_2^-$, $\text{NO}^+/\text{NO}_3^-$ and $\text{NH}_4^+/\text{Cl}^-$ as well as several 'cluster ion' reactions³ such as $\text{H}_3\text{O}^+(\text{H}_2\text{O})_3/\text{NO}_3^-$ and $\text{NO}^+(\text{NO}_2)_2/\text{NO}_3^-(\text{HNO}_3)_3$, all ions being mass identified. Much of the data is, as yet, unpublished. The variation of the $\text{NO}^+/\text{NO}_2^-$ reaction has also been obtained over the temperature range 185-530K⁴ and is consistent with theoretical predictions. The binary rate coefficients for all the reactions studied to date lie within the limited range $3.5-9.5(-8)\text{cm}^3\text{s}^{-1}$, significantly lower than those deduced from merged beam experiments. The significance of the data to ionospheric de-ionisation will be briefly considered.

¹D.Smith and M.J.Church, Int.J.Mass Spectrom.Ion Phys. 19, 185 (1976)

²M.J.Church and D.Smith, Int.J.Mass Spectrom.Ion Phys. 23, 137 (1977)

³D.Smith, N.G.Adams and M.J.Church, Planet.Space Sci. 24, 697 (1976)

⁴D.Smith and M.J.Church, Planet.Space Sci. 25,433(1977)

KB-2

Mutual Neutralization of $\text{NH}_4^+(\text{NH}_3)_n$ Ions with NO_2^- and Cl^- . M.J.CHURCH, D.SMITH, and T.M.MILLER, U. of Birmingham--Measurements will be described of the rate coefficients α for the two-body mutual neutralization of positive ions of the type $\text{NH}_4^+(\text{NH}_3)_n$ with some negative ions including NO_2^- , Cl^- , and $\text{NO}_3^-(\text{HNO}_3)_{0,1,2}$. These were obtained using an ion-ion flowing afterglow plasma.¹ The magnitude of α for the "simple" ion reaction $\text{NH}_4^+ + \text{Cl}^-$ ($7.0 \times 10^{-8} \text{cm}^3\text{s}^{-1}$ at 300 K) is typical of those previously reported for simple ions,² and over a limited temperature range is again consistent with the $T^{-\frac{1}{2}}$ dependence predicted theoretically. The clustering of NH_3 molecules to NH_4^+ does not change α significantly (e.g., $\text{NH}_4^+(\text{NH}_3)_2 + \text{Cl}^-$, $\alpha = 7.9 \times 10^{-8} \text{cm}^3\text{s}^{-1}$). The same conclusion is also apparent even for the neutralization of $\text{NH}_4^+(\text{NH}_3)_n$ cluster ions with large negative ion clusters, e.g., $\text{NO}_3^-(\text{HNO}_3)_n$. However, the derived cross sections for the cluster ions are somewhat higher than those for the simple ions. The significance of these data will be discussed in relation to current theoretical models and to atmospheric de-ionization.

1. D. Smith and M.J. Church, Int. J. Mass Spectrom. Ion Phys. 19, 185 (1976).

2. D. Smith, N.G. Adams, and M.J. Church, Planet. Space Sci. 24, 697 (1976).

KB-3

Theory of Three Body Ionic Recombination for Different Ionic and Neutral Particle Masses.* J. M. WADEHRA and J. N. BARDSLEY, Univ. of Pittsburgh. --

The theory of Natanson for the three body ionic recombination is modified to include the case when the neutral particles and the positive and negative ions have different masses. The three body ionic recombination coefficient, an important parameter in the study of laser plasma, is calculated for various systems using this modified theory. No experimental data are available for comparison with the present results.

*This research was supported, in part, by the Advanced Research Projects Agency of the Department of Defense and was monitored by ONR under Contract No. N00014-76-C-0098.

KB-4

Three-body Recombination Rate for K^+e in Argon. L. D. SCHEARER, University of Missouri-Rolla.*--An unique technique has been developed to measure the loss rate of alkali metal ions due to 3-body recombination processes. The new method appears to have a number of distinct advantages over current experimental methods. Approximately 35 kw from an N_2 pumped tunable dye laser (bandwidth, 0.2 \AA - pulse width 4 ns) at 4046 \AA is focussed into a cell containing potassium metal vapor at 200°C and 0.9 atmospheres of argon. The 4046 \AA photons saturate the 4^2S-5^2P transition; a second photon ionizes the 5^2P atom. Both processes are saturated; consequently, the initial ion density is a known parameter depending only on the potassium vapor pressure. A 3-body radiative recombination process populates excited levels of the potassium system in the afterglow of the pulsed excitation. The time dependent decay of the radiative emission from the 6^2S and 7^2S levels at 6939 and 5802 \AA is observed. We obtain a preliminary recombination rate constant, $K = 6.3 \times 10^{-28} \text{ cm}^3 \text{ sec}^{-1}$ for the potassium-argon system.

*Supported by the Office of Naval Research

KB-5

Merged Beam Studies of the Dissociative Recombination of CH^+ .* J.B.A. MITCHELL, J.W.M. MCGOWAN and H.R. FROELICH, Dept. of Physics and Centre for Chemical Physics, The University of Western Ontario, London, Canada.--Theoretical models for molecule formation in interstellar space have been singularly unsuccessful in explaining the observed abundances of CH and CH^+ in diffuse interstellar clouds. Agreement between theory and observation has only been reached by artificially assuming a very low rate coefficient for the dissociative recombination of CH^+ . Recent measurements of this process have been made in the energy range $<10^{-2}$ eV to 0.45 eV using a merged beam apparatus. It has been found that in fact electrons recombine rapidly with CH^+ ions and that at 10^{-2} eV (116⁰K) the cross section is $(4.0 \pm 0.5) \times 10^{-14}$ cm² corresponding to a rate coefficient of approximately $(2.4 \pm 0.3) \times 10^{-7}$ cm³ sec⁻¹. As the electron energy is increased, the cross section decreases exhibiting an $E^{-0.9 \pm 0.1}$ dependence. A systematic investigation of the effects of varying the ion source conditions is continuing and will be discussed at the conference.

* Supported by National Research Council of Canada.

KB-6

Dissociative Recombination in Krypton: Dependence of the Total Rate Coefficient and Excited-State Production on Electron Temperature.* YUEH-JAW SHIU and MANFRED A. BIONDI, Univ. of Pittsburgh. -- Microwave afterglow and grating spectrometric apparatus are used to study dissociative recombination in krypton. Over the electron temperature range $300 \text{ K} \leq T_e \leq 8400 \text{ K}$ and with $T_+ = T_{\text{gas}} = 300 \text{ K}$, the total rate coefficient may be represented by $\alpha[\text{Kr}_2^+] (\text{cm}^3/\text{sec}) = 1.6 \times 10^{-6} [300/T_e(\text{K})]^{0.55}$, with an uncertainty of $\pm 10\%$. At thermal energy (300 K) excited states of Kr^* having energies up to that of the Kr_2^+ ion in its ground electronic and vibrational state are observed to result from the dissociative recombination. With microwave heating to $T_e \sim 7000 \text{ K}$ additional, higher-lying Kr^* states (up to ~ 0.5 eV above the Kr_2^+ ion ground state) are observed. In both cases the excited states most strongly populated by dissociative recombination appear to be the 5p states.

*This research was supported, in part, by the Advanced Research Projects Agency of the Department of Defense and was monitored by ONR under Contract No. N00014-76-C-0098.

KB-7

Electron Temperature Dependence of Recombination of Hydronium Cluster-Ions and Electrons. * C. M. HUANG,

M. WHITAKER, M. A. BIONDI and R. JOHNSEN, Univ. of Pittsburgh. -- The very weak dependence of the recombination coefficient α on electron temperature T_e for electron capture by ions to which polar molecules are clustered has been investigated further in studies of the hydronium series ions, $H_3O^+(H_2O)_n$, with $n = 0$ to 5. As was found for the ammonium series ions, $NH_4^+(NH_3)_n$, the variation of α with T_e over the range, $320K \leq T_e \leq 6000K$, is much closer to T_e^0 than to the usual T_e^{-2} dependence for dissociative recombination of simple, unclustered ions. For the $n = 2$ and 3 clusters, we find $\alpha[55^+](cm^3/sec) = (3.0 \pm 0.3) \times 10^{-6} [300/T_e(K)]^{.08 \pm 0.04}$ and $\alpha[73^+](cm^3/sec) = (3.6 \pm 0.4) \times 10^{-6} [300/T_e(K)]^{.00 \pm 0.04}$. The dependence of α on T_e for the higher clusters, $n=4$ and 5, also appears to be close to T_e^0 .

*This work was supported, in part, by the U.S. Army Research Office (DAAG-29-76-G-0343).

SESSION LA

2:15 PM - 4:15 PM, Thursday, October 20

Room A

PROCESSES IN VARIOUS LASERS

Chairman: W. H. LONG, JR., NORTHROP

LA-1

Parameter Studies on a CO Reactor-Excited Laser at Room Temperature.* David A. McArthur, Sandia Labs, Albuquerque, NM 87115. Measurements of laser pulse energy and of laser pulse shape within three wavelength bands near 5 μm have been made, for a room-temperature CO laser excited by fission fragments. Total gas pressure, CO diluent (He or Ar), peak excitation rate, and output mirror reflectivity were varied. Following a partial optimization of these parameters a peak laser power ~ 8 watts was obtained, in pure CO at ~ 50 Torr pressure. This is believed to be the highest power yet obtained from a room-temperature reactor-excited laser. Measurements of this type at 77K and 300K should help shed light on the amount of vibrational excitation produced by fission fragments and on the poorly-understood excitation mechanisms, because many potentially important excitation mechanisms (electronic recombination, V-V collisions, quenching) are functions of gas temperature.

*Work supported by U.S. E.R.D.A.

LA-2

A Nuclear Pumped Laser Using Ne-CO and Ne-CO₂ Mixtures*, M. A. PRELAS, J. H. ANDERSON, F. P. BOODY, S.J.S. NACALINGAM and G. H. MILEY, University of Ill., Urbana--Nuclear pumped lasing has been achieved using the Illinois TRIGA reactor at 1.45 μ in Ne-CO and Ne-CO₂ mixtures. The laser transition occurs in neutral carbon, and as is the case with He-CO₂¹, is delayed several milliseconds past the peak of the neutron pulse. This is in contrast to the He-CO laser where no delay was observed.¹ The delay phenomenon has important implications when possible excitation mechanisms are considered and for applications involving energy storage. In both Ne and He, the excitation mechanism must involve two or more collisions between metastable species and CO or CO₂. Similarities and differences between the He-CO and Ne-CO systems will be discussed, and pressure-mixture data for the Ne laser will be presented.

¹M. A. Prelas, M. A. Akerman, F. P. Boody, and G. H. Miley, Applied Physics Letters, to be published (October 1977).

*Work sponsored by ERDA Division of Physical Research

LA-3.

Optically Pumped Atomic Iron Laser *

Daniel W. Trainor and Siva A. Mani, Avco Everett Research Laboratory, Inc. -- A technique for producing stimulated emission in an optically pumped atomic iron system at room temperature will be described. The required iron density ($\sim 10^{14}$ atoms/cm³) for single pass amplified spontaneous emission was produced at room temperature in a low pressure (50 torr) discharge of iron pentacarbonyl and neon. A commercial KrF laser producing output powers of up to 1 Mw was modified to improve the beam quality, and the beam was focused into the discharge cell. Resonant processes involving the $3d^6 4s 4p$ ($^5F^o$) intermediate state of iron and the KrF laser field ($\lambda \approx 248$ nm) produced stimulated emission near 300 and 304 nm in agreement with theoretical predictions.

* Work supported by the Defense Advanced Research Projects Agency under Contract No. N0014-76-C-1162.

LA-4

Population Inversion for the Resonance Transitions of Atoms in Recombining Plasmas.

W.L. BOHN, DFVLR-Institut für Technische Physik, Stuttgart, FR Germany.--

Rapid cooling of a highly ionized plasma produces population inversions among various excited levels of the recombining ions or atoms. At high densities inversions with respect to even the ground level of hydrogenlike ions have been considered as well.-- In this paper we analyze the time history of such ground level inversions for realistic initial conditions. It is shown that recombination of the ground level of an ion is not the absolutely predominant inversion mechanism, as has been reported elsewhere. Consequently, laser action in the resonance transitions of atoms is to be expected. Inversion density and gain calculations are presented for the Lyman lines in hydrogen. Considerably lower cooling rate requirements let appear this potentially efficient short wavelength atomic laser more feasible than previously proposed schemes in multiply charged ions.

LA-5

A Technique for Determining Gas Temperature and Atomic Density from Absorption Measurements*. L.H. TAYLOR, R. B. FELDMAN, D. W. FELDMAN and C. S. LIU, Westinghouse R&D Center--We have developed a general technique for determining simultaneously both gas temperature and atomic number density of glow discharge constituents. A theoretical line profile is fitted, by minimizing the least squares, to the measured profile. The ground state or excited state density is accurately determined for a wide range of discharge operating conditions but the temperature can only be determined within a restricted range of discharge operating conditions. The technique is most accurate in the same region where absorption is most easily measured, i.e., 30-60% absorption. As an example of its usefulness we have applied this technique to the measured absorption of tunable dye laser radiation in CuBr laser discharges. The radial and temporal variation of both the ground state Cu density and the gas temperature were determined. In this case the temperature cannot be easily measured by other methods.

*Partially supported by ONR Contract N00014-74-C-0445.

LA-6

Temporally Resolved Cu Density Measurements in Continuously-Pulsed CuBr Laser Discharges.* C. S. Liu, D. W. Feldman and L. A. Weaver, Westinghouse R&D Center--Copper ground state and metastable densities have been measured in the afterglow of continuously pulsed CuBr laser discharges using the absorption of tunable dye laser radiation. Dissociated copper densities as high as 10^{16} cm^{-3} were measured at 550°C corresponding to $\sim 6\%$ dissociation. The copper density decays at 550°C with a rapid time constant of $\sim 35 \text{ } \mu\text{sec}$ followed by a $\sim 160 \text{ } \mu\text{sec}$ decay attributed to copper diffusion to the walls. Near laser threshold at 400°C dissociation fractions approach 30% with corresponding decay times of $52 \text{ } \mu\text{sec}$ and $210 \text{ } \mu\text{sec}$. Copper metastable densities of $\sim 10^{13} \text{ cm}^{-3}$ were measured at 550°C , with observed lifetimes of $\sim 8 \text{ } \mu\text{sec}$. These measurements were performed on a multipulse basis across the discharge tube diameter. Axial depletion of the copper density was observed as the discharge burst developed, and has been correlated with corresponding decreases in the laser output energy. The effects of gas heating and radial cataphoresis on axial depletion of the copper species will be discussed.

*Partially supported by ONR Contract No. N00014-74-C-0445

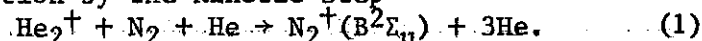
LA-7

Diffusion Processes and Quenching Mechanisms in Metal Vapor Lasers.* B.G. BRICKS, T.W. KARRAS, R.S. ANDERSON and R.J. HOMSEY, GE Space Sciences Lab.-- The output power of several efficient pulsed metal vapor lasers (Cu,Pb,Ba) shows a roll-off as the temperature of the active zone is increased beyond the optimum value for each particular metal. Thus the continued increase in metal atom density does not result in a corresponding increase in laser pulse energy. The dependence of the roll-off and the intensity distribution in the laser spot on temperature, diameter of the discharge tube, repetition rate and buffer gas pressure implies that this phenomena is caused by a reduction in metastable lower laser state quenching at the wall of the discharge tube with a resulting build up of metastable atoms in the volume of the discharge. Furthermore, the data suggest that the reduction in quenching is controlled by the diffusion of the metastable metal atoms in their own atomic vapor as opposed to the discharge buffer gas. Estimates can be made for the relative momentum-transfer cross section for the two processes for one case. Some experiments also indicate possible volume deactivation of the lower laser state.

*Supported in part by AF contracts F33615-76-C-1137 and F33615-77-C-1078, and Navy contract N00014-76-C-0975.

LA-8

Charge Transfer Pumping of the Helium-Nitrogen Laser in an Electrical Avalanche Discharge at Atmospheric Pressures.* C.B. COLLINS, K.N. TAYLOR, and J.M. CARROLL, Univ. of Texas at Dallas--An Atmospheric Electrical Avalanche (AEA) laser, stabilized by displacement current preionization, has been developed to support the study of the collisional pumping of the N_2^+ , B \rightarrow X, electronic transition by the kinetic step



With proper preionization, the AEA laser has been operated at a PRF of 10 to 20 Hz in an avalanche mode at 100 to 200 A/cm² and E/p of 10 v/cm/torr. At pressures from 1 to 8 atm an essentially uniform, 30 cm³ volume containing a high concentration of He₂⁺ has been produced. Resulting laser output pumped by reaction (1) has exceeded 800KW peak power at 4278 Å in a 4 nsec pulse. Efficiency with respect to the electrical power flowing through the laser tube has exceeded 0.5%.

*Research supported by ONR Contract No. N00014-77-C-0168.

LA-9

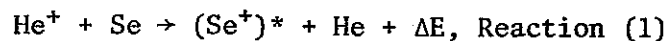
The Modelling of $\text{He}_2^+ + \text{N}_2$ Laser. W. W. Jones and A. W. Ali, Naval Research Laboratory. -- A kinetic model for the $\text{He}_2^+ + \text{N}_2$ charge exchange laser, excited by electron beams in a high pressure He, N_2 gaseous mixture have been developed. The charge exchange process excites the upper laser level, N_2^+ ($\text{B}^2\Sigma$) with lasing action occurring in the (0,0), (0,1) and (0,2) transitions of the N_2^+ first negative bands. The power output and the inversion density in these bands depend on N_2 partial pressure which affects them in two ways. One is the quenching of the upper laser level directly by N_2 and the other is the $\text{He}^+ + \text{N}_2$ charge exchange leading to N_2^+ ($\text{C}\Sigma$, $v=3$) state which decays partially to lower N_2^+ ground state vibrational levels. These and the dependence of the power output on total pressure and electron beam energy will be presented.

LA-10

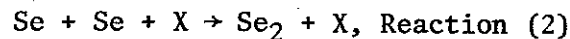
EXCITATION MECHANISM OF THE He-Se LASER,

W. L. Little, J. K. Boyer and G. J. Collins, CSU -- We have investigated the behavior of spontaneous emission in the afterglow of a He-Se discharge in order to determine the major excitation mechanisms operative in the selenium ion laser.

A charge-transfer reaction of the form,



is found to be the dominant excitation mechanism of the selenium ion laser. The total velocity average destruction cross section $\sigma(\text{He}^+-\text{Se})$ has been measured. In addition the three body recombination rate for the reaction,



(where X is a third body) has been estimated from our afterglow measurements.

LA-11

Experimental Determination of the Collisional Excitation and De-excitation Coefficients of the Upper Laser States of Ar⁺. J. JOLLY and J.L. DELCROIX, Lab. Physique Plasmas, 91405 ORSAY-FRANCE.--The absolute concentrations of the argon ion states (3d, 4s, 4p, 4d, 5s) have been measured for a pulsed laser discharge (25 μ s) whose plasma parameters have been previously determined⁽¹⁾. For the resonant levels, measurements were made by self-absorption⁽²⁾ and for all other levels by absolute spectroscopic observations. The variation of the population of these levels as a function of discharge current and pressure, i.e. electron temperature and density, allowed the calculation of the total excitation and the total de-excitation coefficients due to electrons as a function of temperature for each laser-level. For excitation, collisions with the fundamental (3p⁵) and long-lived states (3d, 4s) were taken into account, while for de-excitation electronic superelastic, excitation and ionization collisions had to be considered.

(1) J. JOLLY, J. Phys. (Paris) 38, 659 (1977).
(2) J. JOLLY and M. TOUZEAU, J.Q.S.R.T. 15, 863 (1975).

SESSION LB

2:15 PM - 4:15 PM, Thursday, October 20

Room B

REACTIONS OF EXCITED SPECIES

Chairman: B. VAN ZYL, DENVER UNIVERSITY

LB-1

Collisional Relaxation of Ionic $^2P_{3/2}$ Excited States in Rare Gases. E.W. WEBER⁺ and W. BUTTLER, Phys. Inst., Univ. of Heidelberg.-- Optical pumping with the D_2 line is used to study the depolarization of the first excited $^2P_{3/2}$ states of alkaline earth ions and Yb^+ ions in collisions with rare gas atoms. The $6p$ $^2P_{3/2}$ deorientation cross sections for the even isotopes of Ba^+ and Yb^+ ions are obtained (in units of 10^{-16} cm²):

rare gas	He	Ne	Ar	Kr	Xe
σ_1 (Ba^+)	79(11)	89(13)	123(18)	152(22)	204(30)
σ_1 (Yb^+)	60(10)	62(9)	107(18)	133(17)	167(37)

The cross sections are discussed in comparison with theoretical calculations and those of iso-electronic atoms. The comparison of the $^2P_{3/2}$ relaxation of even and odd ($I=3/2$) isotopes of Ba^+ allows to draw conclusions on the nature of the depolarization interaction.

⁺ Present address: Dep. of Physics, Stanford Univ., Stanford, CA 94305

LB-2

$O(^1S)$ Production Through Collisional Electronic Energy Transfer From Two-Photon Excited Xe Atoms.* D. KLIGLER, D. PRITCHARD, W. K. BISCHEL and C. K. RHODES, Molecular Physics Center, S.R.I. International--The observation of electronic energy transfer to $XeO(^1\Sigma^+)$ from xenon atoms excited by two-photon absorption is reported. Electronically excited xenon atoms in the $5p^56p$ configuration are produced through two-photon excitation at 248.4 nm (KrF^*). Subsequent energy transfer from excited rare gas atoms and dimers to N_2O in dissociative processes leads to the appearance of $O(^1S)$ which is observed through the detection of the characteristic green emission of XeO . These measurements are in agreement with estimates of the relevant two-photon amplitudes for Xe and N_2O . Kinetic studies utilizing these techniques provide a flexible method for the study of selective excitation and energy transfer in a wide class of atomic and molecular materials.

*Supported by the USERDA.

LB-3

Quenching of $N_2(A^3\Sigma_u^+)$ By I_2 . * A. MANDL and J. J. EWING, ** Avco Everett. -- Production and decay of $N_2 A^3\Sigma_u^+$ ($v = 0, 1, 2$) states were monitored photoelectrically from the sensitized fluorescence of NO γ -bands. These states were produced by collisional transfer from excited Xe ($1S_4$) which in turn was produced by radiative energy transfer via resonance radiation (147 nm) from a closely coupled Xe flash lamp. The rate coefficient for the deactivation of $N_2(A^3\Sigma_u^+)$ by I_2 was measured as $k_{I_2} = 6.9 \pm 1.9 \times 10^{-12} \text{ cm}^3/\text{sec}$. The deactivation by NO itself was measured as $k_{NO} = 4.5 \pm 0.5 \times 10^{-11} \text{ cm}^3/\text{sec}$.

*Work supported by ERDA, Contract # EY-76-C-02-2811

**Present address, Lawrence Livermore Laboratory, Livermore, California 94550.

LB-4

Chemiluminescence Studies of Alkaline Earth Collision with Metastable Argon. J.H. GOBLE, D.C. HARTMAN and J.S. WINN Univ. of California, Berkeley. -- Electronic energy transfer from metastable Ar to the alkaline earths Mg - Ba were studied in a high temperature flowing after-flow apparatus. Light emission from atomic excitations, excitive Penning ionization processes and associative ionization processes were considered. Comparison of these emissions to Kr emissions of known excitation cross-sections allowed rate constants to be evaluated in favorable cases. The atomic triplet manifold was strongly excited in these metals, and excitive Penning ionization was found to be a major chemiluminescent channel. The bonding and potential energy curves for the associative ionization products have been explored in detail and a simple (exponential, 4) model potential which includes the effective charge of the metal as a variable was found to give an excellent description of the true potential.

LB-5

Excitation Reactions of He(2^3S) and Ar($3P_{0,2}$) Metastable Atoms with CH₄, C₂H₄, C₂H₂, Cyclo-C₃H₆, C₆H₆, C₆F₆ and C₆F₅H. G.W. TAYLOR, Los Alamos National Laboratory; R.S.F. CHANG and D.W. SETSER, Kansas State U.--The excitation reactions of He(2^3S) and Ar($3P_{0,2}$) atoms with hydrocarbons, C₆F₆, and C₆F₅H have been examined via spectroscopic observation of emission from the product fragments using the flowing afterglow technique. Rate constants for excitation channels were assigned by comparison to reference reactions. The only significant emission with Ar($3P_{0,2}$) was from the reaction with C₂H₂ which gave C₂(A-X) and a visible continuum which may originate from C₂H. Reaction of He(2^3S) with hydrocarbons gave primary emission from CH, C₂ and H. With C₆H₆ the C₆H₆($1^1B_2-1^1A_1$) molecular emission, which probably arises via a secondary process, was found. Excitation channels account for ~8% of the total quenching reaction with C₂H₂; and is much less important for the other hydrocarbons. The only observed ionic emission observed from hydrocarbons was the very weak CH⁺ transition from C₂H₂. In contrast He(2^3S) with C₆F₆ and C₆F₅H gave relatively strong emission from the parent ion.

LB-6

Reaction Rate Measurements of Helium Metastable Species at Atmospheric Pressures.* A.J. Cunningham and G.D. Myers, Univ. of Texas-Dallas.--Quenching reaction studies of He(2^3S) and He₂($2^3\Sigma$) metastable species have been extended to include reactions with additives, N₂ and O₂. The work was accomplished employing resonance absorption spectroscopy in the afterglow period of electron beam discharge excited plasmas of helium at .5-5 atms, with admixtures of 1 to 100 mTorr. Destruction rates were determined by simple extension of a model developed for pure afterglows. For the atomic metastable species both bimolecular and termolecular processes were measured, while for the molecular metastables only bimolecular destruction was observed. Additionally, the product state for the termolecular destruction of He(2^3S) was identified as the molecular metastable.

*Work supported in part by Univ. of Texas-Dallas Organized Research Fund.

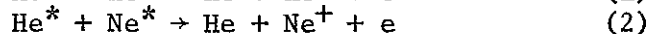
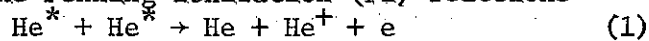
LB-7

Energy Transfer Between Helium Metastable Particles and Neon.* D.W. FERNIE and H.J. OSKAM, University of Minnesota.--Light emission and absorption spectroscopy was used to study the energy transfer mechanisms of $\text{He}(2^3\text{S})$ and $\text{He}_2(2^3\Sigma)$ with Ne. The time dependencies of the densities of $\text{He}(2^3\text{S})$ and $\text{He}_2(2^3\Sigma)$ were compared with those of the neon excited states during the afterglow of helium-neon discharges. The neon concentration was varied from $10^{-4}\%$ to $10^{-3}\%$ at helium pressures from 1.5 to 35 torr. The energy transfer mechanism and its cross section for $\text{He}(2^3\text{S})$ with Ne was found to be in agreement with published data. The time dependencies of the densities of neon excited states above 17 eV is different from that of $\text{He}_2(2^3\Sigma)$. The density of the neon metastable state, $\text{Ne}(^3\text{P}_2)$, was found to have the same time dependence as that of the density of $\text{He}_2(2^3\Sigma)$, although there is at least 1.4 eV energy difference between these states. Therefore, these studies show that the energy transfer mechanism between $\text{He}_2(2^3\Sigma)$ and Ne is a dissociative excitation transfer mechanism producing $\text{Ne}(^3\text{P}_2)$.

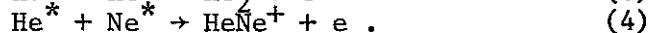
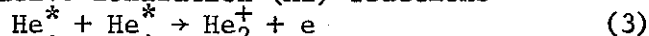
*Work supported by the National Science Foundation (Grant # ENG-76-10905)

LB-8

Penning and Associative Ionization in Systems of Two Metastable Reactants.* R. H. NEYNABER and S. Y. TANG, IRT Corp.--A merging-beams technique has been used to study chemi-ionization in the He^*-He^* and He^*-Ne^* systems. The He^* represents a composite of $\text{He}(2^1\text{S})$ and $\text{He}(2^3\text{S})$, and the Ne^* a composite of $\text{Ne}(3s\ ^3\text{P}_2)$ and $\text{Ne}(3s\ ^3\text{P}_0)$. Absolute and relative cross sections Q were obtained for the Penning-ionization (PI) reactions



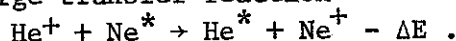
and the associative-ionization (AI) reactions



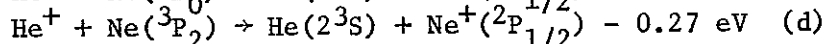
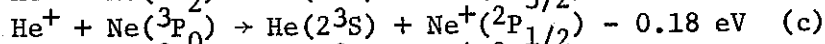
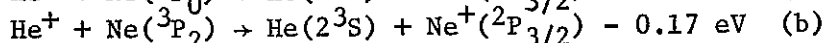
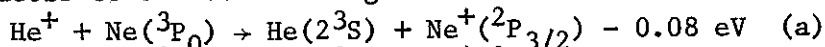
The measurements were made for a relative kinetic energy W of the reactants from nominally 0.01 to 10 eV. The data indicate that both systems are attractive, that Reactions (1) and (2) are directed, and that for $W < 0.1$ eV the ionization associated with each system is controlled by van der Waals forces. Well depths of each molecular system can be approximated from the measured energy distributions of the Penning ions.

*Research sponsored by the Air Force Office of Scientific Research and by the Office of Naval Research.

Charge Transfer in Collisions of He⁺ with Ne^{*}.[†]
S. Y. TANG and R. H. NEYNABER, IRT Corp.—Absolute and relative cross sections were made of the near-resonant, endothermic charge-transfer reaction



The studies were made by a merging-beams technique for a relative kinetic energy W of the reactants from threshold (0.08 eV) to 500 eV. The Ne^{*} represents a composite of Ne(3s ³P₂) and Ne(3s ³P₀), and is generated by passing Ne⁺ through Na vapor. In the range $W < 50$ eV the following channels appear to be the only significant contributors to the overall signal



Above 50 eV there are other contributing channels. In addition to presenting cross-section data we will show some measured laboratory energy distributions of the product Ne⁺ from which information on angular scattering in the c.m. system can be deduced.

[†]Supported by the Office of Naval Research.

Reactions of metastable excited ions of O, O₂ and NO with O, N₂, CO, CO₂, NO, H₂ and Ar at thermal energies, J. GLÓSIK, A. RAKSHIT and N.D. TWIDDY, U.C.W., Aberystwyth, and N.G. ADAMS and D. SMITH, U. of Birmingham, U.K.—A SIFT¹ system employing an ion source having a high yield of the metastable ions O^{+(2D)}, O^{+(2P)}, O₂^{+(a⁴Π_u)} and NO^{+(a³Σ⁺)} has been used to measure the reaction rates of these ions with atmospheric gases. In most cases, the ground states of these ions do not react with the neutrals (endothermic) but when g.s. reactions are possible, the excited ion reaction is usually much faster and is comparable to the Langevin limit. In reactions in which there is more than one ion product, branching ratios have been estimated and in some cases additional product ions are observed in the metastable ion reaction. In a number of cases, collisional electronic state quenching is faster than the reaction with the neutral and the quenching rate constants have been measured using an ion monitor method. The implications of these data to ionospheric chemistry will be briefly discussed. Good agreement is obtained with results of Lindinger et al² for O₂^{+(a⁴Π_u)}.

¹N. G. Adams and D. Smith, Int. J. Mass. Spectrum Ion Phys. 21, 349 (1976).

²W. Lindinger, Albritton, McFarland, Fehsenfeld, Schmeltekoff and Ferguson, J. Chem. Phys. 62, 4101 (1975).

	K _{gs}	K [*]	K _L
O ⁺⁺ + N ₂ → N ₂ ⁺ + O (> 90%)			
↓			
NO ⁺ + N	1.4(-12)	1(-9)	1(-9) cm ³ s ⁻¹
O ₂ ⁺⁺ + N ₂ → N ₂ ⁺ + O ₂	endothermic	6(-10)	8(-10)
NO ⁺⁺ + CO → CO ⁺ + NO	"	8(-10)	8.6(-10)

LB-11

Flow-Drift Tube Studies of the Reactions of NO^{+*} with N₂, CO₂, CH₄, SO₂, and Ar.* I. DOTAN, D. L. ALBRITTON,

and F. C. FEHSENFELD, NOAA Aeronomy Laboratory, Boulder,

CO, 80302.---The reactions of metastable NO^{+*} ions with a variety of neutral molecules have been studied in the center-of-mass kinetic energy range of 0.04 to 2 eV. Because of the low ionization potential of NO, these reactions are endothermic for ground-state NO⁺ ions. However, for metastable NO^{+*} ions, almost all of these charge-transfer reactions are fast; i.e., the rate constants are near their gas-kinetic limiting values. The reaction with Ar is an exception. The rate constant is $1.5 \times 10^{-10} \text{ cm}^3/\text{s}$ at room temperature and increases to $9 \times 10^{-10} \text{ cm}^3/\text{s}$ at 2 eV mean relative kinetic energy. The reaction of NO^{+*} with SO₂ has two ionic products: SO₂⁺ and SO⁺. At room temperature, the major product is SO₂⁺, since SO⁺ production is endothermic. However, at higher energies, SO⁺ is the dominant product ion.

* This research supported in part by DNA.

SESSION MA

8:30 AM - 10:00 AM, Friday, October 21

Room A

PHOTODISSOCIATION AND PHOTODETACHMENT

Chairman: J. LAUDENSLAGER,
JET PROPULSION LABORATORY

MA-1

Photofragment Spectroscopy of Ozone in the UV Region 270-310 nm and at 600 nm*. C.E. FAIRCHILD,[†] E.J. STONE,^{††} and G.M. LAWRENCE, LASP, Univ. of Colo.-- Both O(³P) and O(¹D) atom fragments are observed in the photofragment spectroscopy of O₃ in the Hartley Band absorption region 270-300 nm. In this wavelength interval the average quantum yield for O(³P) is 0.1. The dissociation partner for O(³P) is O₂(X ³Σ_u⁻) and that for O(¹D) is O₂(a ¹Δ_g). The O₂(X ³Σ_u⁻) fragment is populated in a range of vibrational levels from v = 0 to v ≈ 10. For the O₂(a ¹Δ_g) fragment, all energetically accessible vibrational levels are populated at each energy of bombardment. In the Chappius bands at 600 nm the O₂(X ³Σ_u⁻) photofragment is produced principally with v = 0,1. Photofragment angular distributions are measured in the uv for both O atom dissociation products at each wavelength of bombardment. A theoretical angular distribution for O(¹D) is derived; and the resultant prediction is in good agreement with the experimental results.

*Research supported by NSF Atmospheric Research Section, and by NASA Research Grant NGL 06-003-052.

[†]JILA-LASP Visiting Fellow, 1975-76.

^{††}Present address: NOAA-ERL, Mail Code R448, Boulder, CO 80302.

MA-2

Photofragment Spectroscopy of OC10 in the Wavelength Region 300-340 nm.* C.E. FAIRCHILD[†] and G.M. LAWRENCE, LASP, Univ. of Colo.--Photofragment time-of-flight spectra obtained from the photodissociation of OC10 in the region 300-340 nm indicate that the dissociation products are O(³P) + ClO(X²Π), with considerable vibrational excitation of the ClO fragment. Photofragment angular distributions are also observed; and these results will be compared with the models for the near uv dissociation of OC10.

*Research supported by the NSF Atmospheric Research Section, and by NASA research grant NGL 06-003-052.

[†]Summer Visiting Fellow, 1977. Permanent address: Physics Dept. Ore. St. Univ., Corvallis, Ore., 97331.

MA-3

Predissociation and Photofragment Spectroscopy of Quartet States of O_2^+ .* J.T. MOSELEY, M. TADJEDDINE, B.A. HUBER, R. ABOUAF, and P.C. COSBY, Molecular Physics Center, SRI International--The near-threshold photo-predissociation originating with the metastable $a^4\Pi_u$ state of O_2^+ has been investigated using a new coaxial-beams photofragment spectrometer.¹ When the wavelength is scanned near 5800 Å while observing photofragment O^+ ions of selected energy, sharp peaks in the O^+ count rate are observed. From such photofragment spectra obtained as a function of wavelength from 5730 to 5870 Å for discrete dissociation energies varying from 0 to 100 meV, and for both perpendicular and parallel laser polarizations, experimental peaks can be related to transitions between specific vibrational, rotational and fine structure levels of the $a^4\Pi_u$ and $b^4\Sigma_g^-$ states of O_2^+ . Peaks are also observed that are identified with transitions between ($a^4\Pi_u, v=4$) and $f^4\Pi_g$.

*Research supported by NSF and ARO.

1. B.A. Huber, T.M. Miller, P.C. Cosby, H. D. Zeman, R.L. Leon, J.T. Moseley, and J.R. Peterson, Rev. Sci. Inst. 10 (1977).

MA-4

Photodestruction of Ions Formed in O_2/SO_2 Gas Mixtures.* J. A. VANDERHOFF, Ballistic Research Lab.
--Measurement of the photodestruction cross sections for three thermalized ions; SO_2^- , SO_4^- , and SO_4^+ have been performed in gas mixtures (approximately 1 part SO_2 to 7000 parts O_2) over a photon energy range of 1.6 to 2.7 eV. The photodetachment cross section for SO_2^- varied smoothly from 0.9 to $1.7 \times 10^{-18} \text{ cm}^2$ over this energy range. No evidence of photodestruction was observed for SO_4^- and an upper limit for the photodestruction cross section was estimated as $1 \times 10^{-19} \text{ cm}^2$. SO_4^+ was found to photodissociate over the energy range 1.8 to 2.7 eV with a photodissociation cross section of approximately $1 \times 10^{-17} \text{ cm}^2$.

*Work supported by DNA.

MA-5

Photodestruction Cross Sections of Atmospheric Negative Ions.* G. P. SMITH, L. C. LEE, P. C. COSBY, J. R. PETERSON, and J. T. MOSELEY, Molecular Physics Center, SRI International--Photodissociation and photodetachment cross sections for most parent and first-hydrate negative ions of atmospheric importance have been measured between 1.5 eV (8250 Å) and 2.4 eV (5100 Å) using a drift tube mass spectrometer and tunable dye laser. Thresholds were determined for $\text{CO}_3^- \cdot \text{H}_2\text{O}$ (1.7 eV), $\text{O}_3^- \cdot \text{H}_2\text{O}$ (2.0 eV), O_4^- (1.6 eV), and O^- (E.A. = 1.60 eV). Upper limits on the photodissociation cross sections of less than $1 \times 10^{-19} \text{ cm}^2$ were obtained for NO_2^- , NO_3^- , HCO_3^- , CO_4^- , and their first hydrates. Structure observed in the $\text{O}_3^- \cdot \text{H}_2\text{O}$ and $\text{O}_3^- \cdot 2\text{H}_2\text{O}$ cross sections resemble that observed for O_3^- photodissociation. To better determine the absolute magnitudes of these cross sections, which are put on an absolute scale by normalization to O^- and/or O_2^- , the photodetachment cross sections for O^- and O_2^- were measured relative to D^- between 7000 and 8500 Å.

*Research supported by BRL through Army Research Office.

MA-6

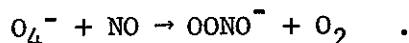
Photodissociation of Atmospheric Positive Ions.* P. C. COSBY, G. P. SMITH, J. T. MOSELEY, and L. C. LEE, Molecular Physics Center, SRI International--Photodissociation cross sections have been measured for 15 positive molecular cluster ions over the wavelength range of 8600-5300 Å using a drift tube mass spectrometer and tunable dye laser. The symmetric cluster ions O_4^+ , NONO^+ , CO_2CO_2^+ , and N_4^+ are observed to photodissociate into their parent diatomic ions and neutrals. The wavelength dependence of each cross section is similar to that for the direct photodissociation of homonuclear diatomics, apparently reflecting dissociation via a purely repulsive potential surface. Photodissociation of CO_4^+ and $\text{O}_2^+ \cdot \text{H}_2\text{O}$ is also observed. The cluster ions $\text{NO}^+ \cdot \text{M}$ ($\text{M} = \text{H}_2\text{O}, 2\text{H}_2\text{O}, \text{N}_2, \text{CO}_2, \text{N}_2\text{O}$) and $\text{H}_3\text{O}^+ \cdot (\text{H}_2\text{O})_n$ ($n = 0, 1, 2$) are not observed to photodissociate at these wavelengths. These results indicate the importance of electron exchange forces in the bonding of many positive ion clusters.

*Research supported by U.S. Army Research Office.

MA-7

Formation and Photodissociation of Peroxy NO₃⁻.*

J.T. MOSELEY, P.C. COSBY, J.R. PETERSON, and G.P. SMITH, Molecular Physics Center, SRI International--Ion-molecule reaction rate studies¹ have demonstrated that an isomeric form of NO₃⁻, usually written OONO⁻, is formed by reactions such as



We have studied the photodestruction of NO₃⁻ formed in NO/O₂, NO₂/O₂, NO₂/Ar, and O₂/N₂O mixtures. Ions formed in the first three mixtures are not observed to photodissociate or photodetach in the visible, indicating that they are normal, ground state NO₃⁻. However, NO₃⁻ formed in the O₂/N₂O mixture is observed to photodissociate into O₂⁻ and NO, indicating that this ion is the peroxy isomer. The wavelength dependence for this photodissociation has been measured, as has that for the first hydrate of peroxy NO₃⁻. Possible formation mechanisms for these ions and ionospheric chemistry implications will be discussed.

*Research supported by BRL through Army Research Office.

1. F.C. Fehsenfeld and E. E. Ferguson, J. Chem. Phys. 61, 3181 (1974).

MA-8

Zero Core-Contribution Calculation of Photodetachment of Atomic Negative Ions Having an Outermost d-Orbital.* W. B. Clodius, R. M. Stehman, and S. B. Woo, University of Delaware--The zero core-contribution model was applied to study the photodetachment of atomic negative ions having an outermost s or p orbital¹ and obtained good agreement with experimental data. This method is now applied to study the photodetachment of atomic negative ions having an outermost d-orbital as is the case with some transition metal negative ions. The absolute photodetachment cross section as a function of photon energy and differential cross section as a function of angle are calculated. Contrary to s and p orbital cases, the cross section of d-orbital ions is found to rise slowly to a peak amplitude of about $5 \times 10^{-17} \text{cm}^2$, in orders of magnitude, and is usually located at least 1.5 eV beyond the threshold. The anisotropy factor, β , varies between 0.2 and -1.0 in the visible photon energy range for almost all the cases considered.

*Supported in part by NSF.

¹R. M. Stehman and S. B. Woo, Bull. Am. Phys. Soc. 22, 191 (1977).

MA-9

Zero Core-Contribution Calculation of Photodetachment of O_2^- and S_2^- * R.M. Stehman, Northeastern Illinois University and S.B. Woo, Univ. of Delaware--Using a one-electron wave function which is a linear combination of atomic orbitals of a form appropriate for a π_g electron moving in a region of constant potential, the photodetachment cross section, σ , of O_2^- and S_2^- are calculated. The results for O_2^- agree with experimental data for the differential cross section and the relative total σ . The method determines the absolute σ within a factor of two. It also yields relative photodetachment transition probabilities between vibrational levels that are in excellent agreement with the results of LPES experiment for O_2^- and S_2^- , if a +1% change is made to the O_2^- internuclear distance reported as a result of LPES measurements. The zero core-contribution method assumes that the extra electron of the negative ion is bound by a potential well in a core region defined by the parent neutral. The contribution to σ from the core region is assumed zero. The information needed to determine σ is the symmetry of the highest occupied molecular orbital of the anion, the equilibrium internuclear distance, the size of the neutral atoms, the vertical detachment energies and the Frank-Condon factors for each vibrational transition.

*Supported in part by NSF.

MA-10

High Resolution Photodetachment Cross Section of a Dipolar Molecular Ion. P. L. JONES, S. E. NOVICK, J. H. FUTRELL* and W. C. LINEBERGER,† Dept. of Chemistry, U. of Colo. and JILA, U. of Colo. & NBS/Boulder.--The relative cross section for the photodetachment of OH^- has been measured in the threshold region between 14300 cm^{-1} to 14700 cm^{-1} with a resolution of 0.5 cm^{-1} . A mass analyzed, near thermal ($\sim 700^\circ\text{K}$) beam of OH^- formed in a drift ion source was crossed with the intracavity beam of an argon ion laser pumped tunable dye laser. Individual thresholds corresponding to rotational channel openings have been resolved in selected regions of the P, Q and R branches. The energy dependences of the thresholds in the photodetachment cross section vary with rotational branch. The data provide information on the influence of a rotating molecule with a permanent dipole moment on the threshold photodetachment process. Discussion of these results and a refined value of the electron affinity of OH will be presented.

Research supported by NSF and ARO.

*JILA Visiting Fellow 1976-77, on leave from University of Utah.

†Camille and Henry Dreyfus Teacher-Scholar.

SESSION MB

8:30 AM - 10:00 AM, Friday, October 21

Room B

PROCESSES IN CO₂ LASERS

Chairman: G. FOURNIER, O.N.E.R.A.

MB-1

A 16 μm CO₂ Laser Kinetics Model.* L. H. Taylor, Y. S. Evangelista, D. W. Feldman and W. H. Kasner, Westinghouse R&D Center--A laser kinetics model has been developed for pulsed 16 μm CO₂ lasers in mixtures of CO₂, N₂, He, H₂O, and H₂. The lowest six excited vibrational levels of CO₂ are treated in detail. The rotational manifold for each vibrational state is treated as an energy reservoir with each rotational level involved in lasing being treated individually. The gas temperature is described by an energy balance equation and the effects of external mirrors are treated by a laser photon flux equation. Eight E/N-dependent electrical excitation rates and eighteen temperature-dependent collisional relaxation rates are included. Computer solutions have been compared with experimental results and exhibit the same qualitative behavior: the electrical excitation of the gas must be followed by a time delay of about 1 ms to allow the 01¹0 laser level to relax collisionally. After this time delay a 9.4 μm optical pump pulse can then populate the 02⁰0 laser level, thereby causing an inversion and lasing at 16 μm .

*Partially supported by LASL/ERDA Contract EY-77-C-04-3914.

MB-2

Megawatt Operation of an (0,0⁰,2) \rightarrow (1,0⁰,1) Sequence-Band High-Pressure CO₂ Laser. Robert A. Fisher, B. J. Feldman, C. R. Pollock, S. W. Simons, & R. G. Tercovich, LASL[†].--We report megawatt operation of an 1800 torr 170 kV uv preionized double-discharge CO₂ laser on the (0,0⁰,2) \rightarrow (1,0⁰,1) sequence band. The gain medium is 154 cm long and the interelectrode spacing is 3.5 cm. Sequence band lasing in this device is possible because of the high ν_3 vibrational temperatures we measured (3000 $^\circ\text{K}$ at a 0.881:0.095:0.024 mix of He:N₂:CO₂). Single-line sequence band lasing on lines P(9)² thru P(27) was obtained by putting the gain medium in a grating-tuned cavity which contained a 57-cm-long cell of hot CO₂ and a 1.1-m-long low-pressure pulsed discharge. As in Ref. 1, the hot CO₂ prevented conventional (0,0⁰,1) \rightarrow (1,0⁰,0) lasing. Rapid pulsing of the low-pressure cell allowed quick cavity alignment, and pulsing it just prior to the high-pressure discharge generated a temporally smooth output pulse with power $\sim 10^7$ times that reported previously.¹ This provides new lines in the 10 μm region which are suitably powerful for isotope separation, multiphoton absorption, laser-pumped molecular lasers, and a variety of nonlinear optics experiments.

[†]Work performed under the auspices of the US ERDA.

1. J. Reid & K. Siemsen, Appl. Phys. Lett. **29**, 250 (1976)

MB-3

Acoustic Instability Model for High Power CWEDL Lasers.* D.KORFF, S.L.GLICKLER, J.D.DAUGHERTY. --High energy CWEDL lasers are subject to a mode medium interaction which produces an instability in output flux. The instability can be modelled by a circuit analysis approach of a photo-acoustic-kinetic interaction, which couples gain, flux, kinetic, and density perturbations - in a form analogous to the Stutz-deMars treatment of relaxation oscillations. The coupling results in a non-uniform heat deposition and density variation. In contradistinction to the usual case (no density variations) instabilities are predicted for various ranges of cavity parameters. Experimental results will be shown.

*Supported by IRAD and the Air Force Weapons Laboratory.

MB-4

Attachment and Electrode Surface Field Effects on Arc Formation in Laser Glow Discharges.* L.J.DENES, L.E.KLINE, R.R.MITCHELL and R.J.SPREADBURY, Westinghouse R&D Center--We have studied the glow discharge energy density required for arc formation, and the spatial distribution of arcing, in atmospheric pressure mixtures with no attachment ($\text{CH}_3\text{F}:\text{Ar}:\text{He}$), weak attachment ($\text{CO}_2:\text{N}_2:\text{He}$) and strong attachment ($\text{SF}_6:\text{Ar}:\text{He}$). The volume of the 1-2 μsec , spatially uniform cylindrical discharges was ~ 1 liter. The arc formation energy is >100 J in the CH_3F and CO_2 mixtures and ≤ 5 J in the SF_6 mixtures. When $E_p \leq 1.15E_a$ the arcs are randomly distributed within the glow discharges. E_p and E_a are the peak and nominal values of the calculated vacuum electrostatic field ($E_a = \text{voltage}/\text{electrode spacing}$). The arcs occur outside the glow discharge, near the location of E_p when $E_p \geq 1.15E_a$, even though the current and energy density there are well below the current and energy density in the central glow discharge. These observations suggest arc initiation by the enhanced field when $E_p > 1.15E_a$. However streak photographs of the final stages of arc formation are very similar for both types of arcs.

*Supported in part by the U.S. Army Missile Command.

MB-5

PLASMA AND CHEMICAL PROCESSES IN CO₂ VOLUME DISCHARGES, W.J. Sarjeant and C. Willis,

National Research Council of Canada, Ottawa, Canada, KIA 0R6. -- Quantitative data, on the plasma and chemical changes in electrical discharge media, necessary for a more comprehensive understanding of gas discharge and laser kinetics has been obtained for CO₂ lasers. The significant electrical parameter was determined to be the electrical energy deposited in the gas, obtained by measurement of time-resolved electric field and current density. The overall decomposition yield measurement showed that approximately 30% of the deposited energy is directed into the chemical potential of the primary decomposition products. Experiments with a commercial TEA CO₂ laser produced identical decomposition yields for CO₂-He mixtures, independent of the composition of the gas mixture in the range 1-5% CO₂. Detailed results for both systems will be presented and the significance of this technique for the general study and understanding of gas discharge lasers will be discussed.

MB-6

A Simulated High-Repetition Rate TEA CO₂ Laser,

R. TURNER and R. A. MURPHY, Applied Physics Laboratory, Johns Hopkins Univ.* - A sealed TEA CO₂ laser (2.2 x 1.3 x 40 cm) is operated with two current pulses (50 nsec FWHM), separated by 0-100 msec, to study the sources of arcing encountered at high-repetition rate operation. The laser output energy and wavelength, electron density, gas resistance, visible emission spectrum (CO, CO₂, He, etc.) and the effects of CO, O₂ and H₂ additives on the above, have been measured as a function of current pulse separation. The minimum separation before arcs form depends critically on the preionization. In general, however, the laser power and gas resistance decreases, the emission delay increases, and the wavelength remains P(18), as the current separation is decreased to the point of arcing. The addition of CO and H₂ improve laser performance; O₂ degrades performance. The slow build up of CO, determined spectroscopically and from the delayed CO₂ laser emission as CO transfers energy to CO₂, and other contaminants do not significantly affect these results. Arcing appears mainly due to local heating and inhomogeneities in the gas.

*Work supported by U.S. Navy.

MB-7

Calculation of the Transport Coefficients of Molecular Species in Laser Discharges. R.M. THOMSON, Leeds University, U.K.* - Transport coefficients (conductivity, diffusion, viscosity) are required for spatially dependent modelling of gas laser discharges (CO₂ waveguide lasers, stability analysis of lasing media, etc.) Transport coefficients have been calculated using a theory which includes explicitly the contribution from molecular vibrational energy, which may not be in equilibrium with the gas temperature; and also includes the effect of electron impact excitation of molecular vibrational states. Calculated values for the transport coefficients are in agreement with experimental values, and the effect of the electrical excitation of gases on the transport coefficients is discussed.

* Supported by Procurement Executive, Ministry of Defence sponsored by DCVD.

SESSION NA

10:15 AM - 12:20 PM, Friday, October 21

Room A

ION MOLECULE REACTIONS

Chairman: J. LEVENTHAL, UNIVERSITY OF
MISSOURI-ST. LOUIS

Ion-Molecule Reactions at Thermal Energies Studied Using the SIFT. N.G.ADAMS, D.SMITH and D.GRIEF, U of Birmingham, England-- The Selected Ion Flow Tube (SIFT) technique which we have successfully exploited to study a large number of reaction rates and product ion distributions at thermal energies will be described 1-6. Data, much as yet unpublished, will be presented to illustrate the versatility of the technique including reactions of the ions CH_n^+ ($n=0$ to 4)³⁻⁵ and H_nCO^+ ($n=0$ to 3)⁷ with several molecules and the implications of these data to chemical synthesis in interstellar gas clouds⁸ and to the Earth's ionosphere⁶ will be briefly discussed. A greatly improved version of the SIFT, which has recently been constructed, will be described.

1,2 N.G. Adams and D. Smith, Int. J. Mass Spectrom. Ion Phys. 21, 349 (1976); J. Phys. B. 9, 1439 (1976)

3 D. Smith and N.G. Adams, Int. J. Mass Spectrom. Ion Phys. 23, 123 (1977)

4 D. Smith and N.G. Adams, Chem. Phys. Letts. 47, 145 (1977)

5 N.G. Adams and D. Smith, Chem. Phys. Letts. 47, 383 (1977)

6 D. Smith, N.G. Adams and D. Grief, J. Atmos. Terres. Phys. 39, 513 (1977)

7 N.G. Adams, D. Smith and D. Grief, Int. J. Mass Spectrom. Ion Phys. (in press)

8 D. Smith and N.G. Adams, Astrophysical Journal (in press)

A Study of the Binary and Ternary Reactions of CH_3^+ Ions at Thermal Energies. D.SMITH and N.G.ADAMS, U. of Birmingham-- In the simple hydrocarbon ion series CH_n^+ studied in a SIFT apparatus at 300 K, we have observed that the behavior of CH_3^+ is atypical¹ in its reactions with a series of diatomic and polyatomic molecules, e.g., with H_2S and CH_4 , only fast binary product channels are observed; with other molecules, e.g., NH_3 and H_2CO , simultaneous fast binary and pressure saturated ternary association reactions are observed; whereas for several other molecules, e.g., H_2 , CO , CO_2 , and H_2O , only the ternary association product results. In some cases the ternary reaction rate coefficient is extremely great ($>10^{-26}$ cm⁶/sec) and thus the reaction rate is pressure independent at pressures greater than 0.2 torr in the flow tube, implying a long lifetime for the excited intermediate associated ion. The ternary coefficients k have in some cases been determined at both 300 K and ~220 K and assuming a law of the form $k = f(T^{-n})$, it is shown that, as expected, n is dependent on the atomicity of the associated product ion. The rapid increase of k with reducing temperature has interesting implications regarding synthesis of molecules in interstellar clouds.

1. D. Smith and N.G. Adams, Int. J. Mass Spectrom. Ion Phys. 23, 123 (1977).

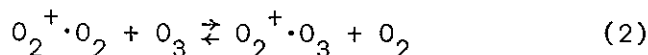
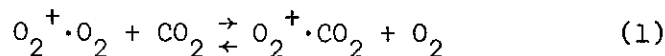
NA-3

Some Positive Ion-Molecule Reactions of Stratospheric Interest. N.G. ADAMS, D. SMITH, and T.M. MILLER, U. of Birmingham--Rate coefficients and product-ion distributions have been determined at 300 K for several stratospheric "primary" ions, e.g., N^+ , N_2^+ , O^+ , O_2^+ and "secondary" ions, e.g., N_4^+ , with several minor neutral constituent stratospheric molecules, e.g., H_2O , CO_2 , CH_4 , H_2CO , in order to search for clues to the identity of the recently observed positive ions in this region.¹ The experiments were carried out in a SIFT apparatus.² The reactions studied are generally fast, in some cases exceeding the ADO theoretical predictions, and multiple products are often observed. For example, the $N^+ + H_2CO$ reaction has a rate of $3.25 \times 10^{-9} \text{ cm}^3/\text{sec}$ and the products are H_2CO^+ (74%), HCO^+ (25%), and NH^+ (1%).

1. F. Arnold, D. Krankowsky, and K.H. Marien, *Nature* **267**, 30 (1977).
2. N.G. Adams and D. Smith, *Intern. J. Mass Spectrom. Ion Phys.* **21**, 349 (1976), and *J. Phys. B* **9**, 1439 (1976).

NA-4

The Reactions of $O_2^+ \cdot O_2$ with CO_2 , O_3 and CH_4 and $O_2^+ \cdot O_3$ with CH_4 and H_2O *. I. DOTAN, F. C. FEHSENFELD, and D. L. ALBRITTON, NOAA Aeronomy Laboratory, Boulder CO, 80302.---The equilibrium constants for the reactions



have been measured in a variable-temperature flowing after-glow. These measurements yield thermochemical values for the above reactions: $\Delta H_{273}^{\circ}(1) = 0.3 \pm 1.0 \text{ kcal mole}^{-1}$, $\Delta S_{273}^{\circ}(1) = 4.3 \pm 3.0 \text{ cal mole}^{-1} \text{ K}^{-1}$, $\Delta H_{273}^{\circ}(2) = -2.7 \pm 1.0 \text{ kcal mole}^{-1}$, $\Delta S_{273}^{\circ}(2) = 8.0 \pm 4.0 \text{ cal mole}^{-1} \text{ K}^{-1}$. In addition the rate constants for the reactions of $O_2^+ \cdot O_3$ with H_2O and $O_2^+ \cdot O_2$ and $O_2^+ \cdot O_3$ with CH_4 have been measured. These measurements will be reported and their implication to the ion chemistry of the stratosphere discussed.

* This research supported in part by DNA.

NA-5

Theory of He-X gas mixture plasma afterglow and its application to ion-molecule reaction measurements by a pulsed-flowing afterglow technique, JEN-SHIH CHANG, R.M. HOBSON, G.L. OGRAM, R.H. PRINCE and A. SALEM, York University, Canada -- The theory of the medium pressure plasma afterglow has been studied for He-X gas mixtures taking into account diffusion, volume recombination, charge transfer and ion-molecule reactions. Experiments have also been initially conducted in order to confirm the validity of the pulsed-flowing afterglow technique (PFA). The shock-wave heated gas and also the cooled gas in the expansion flow of the PFA method enables one to measure a wide range of gas temperature dependences of the rate coefficient of ion-molecule reactions. In the He-O₂ gas mixture plasma afterglow, charge transfer reactions, $\text{He}_2^+ + \text{O}_2 \xrightarrow{k_1} \text{O}_2^+ + 2\text{He}$ and $\text{He}_2^+ + \text{O} \xrightarrow{k_2} \text{O}^+ + 2\text{He}$, $\text{O}^+ + \text{O}_2 \xrightarrow{k_3} \text{O}_2^+ + \text{O}$, and volume recombination $\text{O}_2^+ + e \xrightarrow{\beta} \text{O} + \text{O}$ are considered. Correlating theory and initial experimental results we obtain $k_1/k_2 \approx 3.5$ and $k_1 + k_2 = 1.05 \times 10^{-9} \text{ cm}^3 \text{ molecule}^{-1} \text{ sec}^{-1}$ at a gas pressure of 11 torr at a calculated temperature of 240°K in the expansion flow of the flow tube.

NA-6

Measurement of the Rate Coefficients for the Bimolecular and Termolecular Charge Transfer Reactions of He₂⁺*. C.B. COLLINS and F.W. LEE, Univ. of Texas at Dallas--This work continues¹ the measurement in afterglows of e-beam discharges into high pressure gas mixtures of reaction rate coefficients for charge transfer reactions of He₂⁺ with twelve gases selected to have varying values of polarizability and dipole moment. The bimolecular components of reaction obtained compare favorably with the NOAA results² at low pressures and with the ADO theory.³ Termolecular components measured from 9×10^{-30} for H₂ to $140 \times 10^{-30} \text{ cm}^6 \text{ sec}^{-1}$ for HBr and agree with a model developed to estimate the rates at which third-body collisions change glancing encounters into inwardly spiraling orbits.

*Research supported by NSF Grant ENG 74-06262.

1. F.W. Lee, C.B. Collins and R.A. Waller, J. Chem. Phys., 65, 1605 (1976).
2. D.K. Bohme, N.G. Adams, M. Mosesman, D.B. Dunkin, and E.E. Ferguson, J. Chem. Phys. 52, 5094 (1970).
3. T. Su and M.T. Bowers, Int. J. of Mass Spect. and Ion Phys., 12, 347 (1973).

NA-7

Charge Transfer Studies of Ne-N₂ by Proton Excitation.* C. H. CHEN, J. P. JUDISH, and M. G. PAYNE, Oak Ridge National Laboratory.--Pulses of 2-MeV protons were injected into a reaction cell containing Ne-N₂ mixtures, producing ion pairs and excited atomic states. Fluorescence photons from the transition $N_2^+(B^2\Sigma_u)_{v=0} \rightarrow N_2^+(X^2\Sigma_g)_{v=1}$ pass through a quartz window and enter a uv-visible monochromator and then are detected by a time-resolved single photon counting technique. Our experimental data give indirect evidence of the existence of Ne₃⁺. The overall quenching rates for Ne⁺ and Ne₂⁺ by N₂ at room temperature were obtained (7.2×10^{-11} and 5.3×10^{-10} cm³ sec⁻¹, respectively). The termolecular quenching rate was obtained as 2.3×10^{-29} cm⁶ sec⁻¹. The fluorescence efficiency of Ne-N₂ at 4278 Å is only 18% of that for He-N₂ mixtures. Possible laser application will be discussed briefly.

* Research sponsored by the Energy Research and Development Adm. under contract with Los Alamos Scientific Lab. and under subcontract with Oak Ridge Nat'l. Lab., operated by Union Carbide Corp.

NA-8

Product Distributions for Some Thermal Energy Charge Transfer Reactions of Rare Gas Ions. J. B. LAUDENSLAGER, V. G. ANICICH, and W.T. HUNTRESS, JR. Jet Propulsion Laboratory, Pasadena, CA and J.H. FUTRELL, Univ. of Utah.--Ion Cyclotron resonance mass spectrometry methods were used to measure the product distributions for thermal energy charge transfer reactions of He⁺, Ne⁺, and Ar⁺ ions with N₂, O₂, CO, NO, CO₂, and N₂O. Except for the He⁺-N₂ reaction, no molecular ions were produced by thermal energy charge transfer from He⁺ and Ne⁺ with these target molecules. The propensity for dissociative ionization channels in these highly exothermic charge transfer reactions at thermal energies contrasts with the propensity for formation of parent molecular ions observed in photoionization experiments and in high energy charge transfer processes. This difference can be explained in terms of the more stringent requirements for energy resonance and favorable Franck-Condon factors which appear to be necessary for efficient charge transfer at thermal ion velocities.

NA-9

Measurements of Ion-Molecule Reaction Rates in a High Temperature Drift Tube - Mass Spectrometer Apparatus.* A. K. CHEN, R. JOHNSEN, and M. A. BIONDI, Univ. of Pittsburgh. -- The variation of several ion-molecule rate coefficients with ambient gas temperature has been determined in a high temperature drift tube mass spectrometer apparatus. Measurements of the reactions $O^+ + O_2$, $O^+ + N_2$, and $He^+ + N_2$ in the temperature range 300 - 900 K give results in good agreement with rate coefficients inferred from the E/N dependences measured with drift tube apparatus and those observed in heated flowing afterglow systems. The agreement indicates that in this temperature range the effects of internal energy of the reactant molecules are not very important. While higher temperatures are easily attainable in the present apparatus, problems such as unwanted thermionic emission and surface ionization have so far prevented measurements above 900 K.

*This research was supported, in part, by the U.S. Army Research Office (DNA) (DAAG-29-76-C-0343).

NA-10

Reactions of $CO_2CO_2^+$, CO_2^+ and $COCO^+$ with the Oxides of Nitrogen in CO_2 , J. L. MORUZZI and P. COXON, Univ. of Liverpool. -- Using a high pressure drift tube mass spectrometer reactions involving CO_2^+ , $CO_2CO_2^+$ and $COCO^+$ with the oxides of nitrogen have been studied. Rapid ion molecule reactions were observed for all the systems examined and in some cases two reacting channels were detected. The rates of these reactions have been measured as a function of ion energy by varying E/N, the ratio of electric field strength to gas density.

NA-11

Ion Mobility "Resonance" in High Pressure Helium Plasmas Produced by Beta Particles. C. C. LEIBY, JR. RADC/ESO, Hanscom AFB, MA 01731--Current-voltage (i/v) characteristics were measured in helium plasmas at pressures of 1, 2, and 3 atm. The plasmas were produced by a 2x4 cm, 100 mCi, Ni-63 beta source ($E_{\max}=66$ Kev). The test cell contained 10 guarded ss electrodes spaced at one cm intervals. The i/v characteristic at $x=8$ mm from the beta source exhibited very strong peaks in the range of $E/p_0 \sim 30$ to ~ 50 volts/cm-atm. The peaks shifted to lower E/p_0 and diminished in height with increasing x . At a fixed x , the peaks increased in height and shifted to lower E/p_0 with increasing pressure. The peaks were extremely temperature sensitive, shifting to higher E/p_0 and decreasing in height with slight increases in gas temperature. Although ion identification was not possible, the i/v characteristics are understandable if, in addition to a majority He_2^+ ion, there exists a minority ion with a very high mobility (He^{++} ?) whose concentration decreases exponentially with increasing drift energy. Using such a model, the inferred ion densities of our beta-produced plasmas range from 10^7 to 10^8 /cc. These results indicate that Ni-63 should be a very effective source of preionization for gas lasers.

NA-12

Ion Mobilities in Dense Helium Vapor. B. L. HENSON, Univ. of MO-St. Louis.--Measurements of the zero-field mobilities of helium ion swarms in dense helium vapor using time-of-flight techniques indicate that large positive ion complexes are formed that may contain well over a hundred atoms and have radii as large as 16A in some cases. The apparent sizes of the ions are observed to be dependent on both the density and the temperature of the vapor. These mobility data can be satisfactorily explained using a kinetic theory type mobility equation with a hard sphere type cross-section for the clustered ion in the temperature range from 2°K to 5°K. However, near the liquid-vapor critical point, the mobilities are anomalous in that additional effects are required for explanation. Both positive and negative charge carriers show discontinuous changes in their mobility between 5.0°K and 5.05°K.

SESSION NB

10:15 AM - 11:35 AM, Friday, October 21

Room B

CO LASERS

Chairman: R. CENTER, MATHEMATICAL
SCIENCES NORTHWEST

NB-1

Spark Photoionization of Nitric Oxide and Ethylene in Carbon Monoxide Laser Mixtures.* D. R. SUHRE, Westinghouse R&D Center, Pittsburgh, PA.--Photoionization as a function of distance from a spark was measured using charge collection in various CO laser mixtures seeded with NO and C₂H₄. Single-step photoionization was found to dominate, and the data was analytically approximated as a simple exponential function of distance and seedant density for a given gas mixture. Photoionization efficiencies relative to input electrical spark energy were calculated from the data, and were typically about 1%. The spark current and gap width were varied, and photoionization scaling relationships were developed from these results. By obtaining data at reduced temperatures, it was also verified that the photoionization process is independent of temperature, provided that the seedant density remains constant.

* Work sponsored by DARPA and monitored by AFWL under contract F29601-76-C-0086.

NB-2

UV-Sustained Carbon Monoxide Laser Plasma.* D. R. SUHRE and S. A. WUTZKE, Westinghouse R&D Center, Pittsburgh, PA.--A high current UV-spark array was used to irradiate a transverse discharge apparatus for several microseconds in which the discharge potential was substantially less than the self-sustained glow voltage. Current densities in excess of 2 A/cm² were obtained, corresponding to electron densities $>2 \times 10^{12}$ cm⁻³. The electron production was shown to be entirely by photoionization. Low ionization potential seedants, such as NO or C₂H₄, were needed to obtain the high photoionization levels. The specific energy loading of the plasma was shown to be comparable to conventional self-sustained discharges while the discharge electric field to particle density ratio (E/N) was kept at $\sim 1 \times 10^{-16}$ V-cm², a value more suitable for efficient laser excitation. At higher energy loadings, the photoionizer energy was comparable to the main discharge input energy. The UV-sustained mode of discharge is suitable for CO laser excitation at cryogenic temperatures when the appropriate seedants are used.

* Work sponsored by DARPA and monitored by AFWL under contract F29601-76-C-0086.

NB-3

V-I Characteristics of Self-Sustained CO Laser Discharges* R. R. MITCHELL, L. E. KLINE, D. R. SUHRE, and S. A. WUTZKE, Westinghouse R&D Center -- Numerical solutions of the Boltzmann equation were used to obtain electron-CO collision cross sections which are consistent with measured electron transport coefficient values over a wide E/N range. These cross sections were then used, together with available N₂ and He cross sections, to calculate electron transport coefficients for CO:N₂:He mixtures. A discharge analysis based on a rate equation model predicts that recombination is the dominant electron loss. Electron loss by dissociative attachment is offset by fast associative electron detachment. The predicted positive volt-ampere (V-I) characteristic is in good agreement with experiment for $10^{-1} \lesssim j/N \lesssim 10$ A/Amagat cm². The theory predicts that superelastic collisions between electrons and vibrationally excited CO and N₂ heat the electrons and result in enhanced ionization and a negative V-I characteristic for $j \gtrsim 10$ A/cm².

*Work sponsored by DARPA and monitored by AFWL under Contract F29601-76-C-0086.

NB-4

Electrical Characteristics and Vibrational Excitation in a Supersonic CO Electric Discharge* A. C. STANTON, R. K. HANSON, and M. MITCHNER, Stanford University.-- The performance of a continuous glow discharge in a small-scale supersonic flow facility has been studied. The discharge, which is sustained by auxiliary sources of ionization at the cathode, is used to excite CO in mixtures with Ar or N₂. Probe measurements of ion density and E/N have been made, and the CO vibrational distribution has been determined from the first overtone emission. The probe measurements show a sharp decrease in ion density in the direction away from the cathode. This result is qualitatively consistent with a model in which electrons are fed into the main discharge from the cathode region through ambipolar diffusion and convective processes. Initial results from the overtone emission experiments show a vibrational excitation efficiency greater than 60%, with calculated small-signal gains of approximately 0.01 cm⁻¹. Higher gain is anticipated as the input power is increased.

The authors wish to acknowledge contributions to this work by J. H. Blom, Eindhoven University of Technology, The Netherlands, and D. J. Bender, Lawrence Livermore Lab.

*Research supported by NSF Grant ENG-75-11156.

NB-5

Poker-Controlled Pulsed Discharges in Supersonic CO Flows. W. M. MOENY, SSDC, and J. P. O'LOUGHLIN, AFWL, Kirtland AFB, NM-- An experimental and theoretical study has been made of 'Poker' controlled pulsed discharges in static and supersonic CO gas mixtures. 'Poker' is a non-e-beam discharge control technique using short, repetitive, high-voltage pulses superimposed on a DC electric field to control a laser discharge. The poker pulser used here is capable of 50-100 nsec wide pulses, with a peak voltage of 35 kV (high impedance load), 300 amps peak current (low impedance load), and a PRF of 500 KHz. This pulser and a DC electric field are used to produce 1 liter static and supersonic ($M = 3.5$) 15-30 μ sec pulsed discharges in 0.1 to 0.3 amagat CO/He gas mixtures at E/N 's of 1.0 to 2.0×10^{-16} v-cm². The effect of circuit parameters, density, and gas mixture on discharge characteristics is discussed.

NB-6

Performance of a CW Pulser-Sustainer Carbon Monoxide Electric-Discharge Supersonic Laser. D.J. Monson and G. Srinivasan*, NASA-Ames Res. Ctr.--A CW carbon monoxide electric-discharge supersonic laser has been successfully operated using a pulser-sustainer discharge¹ in 0.8 liter volume, Mach 3 supersonic flow. Like an electron-beam stabilized discharge, the pulser-sustainer discharge is stable and uniform at high power loadings, and provides independent control over electron energy and density for optimum discharge efficiency. Energy loadings exceeding 100 KJ/lb of mass flow, output power exceeding 6 KWatts and electro-optical efficiencies exceeding 10% have been achieved in CO/He and CO/N₂/He laser mixtures for discharge times of 1 msec (equivalent to 10 cavity gas flow exchange times). The effects on the discharge and laser performance of the pulser parameters, gas density and temperature, gas mixture and additives, and location of optical cavity are discussed.

* Contractor

¹A. E. Hill, Appl. Phys. Lett., 22, pp. 670-673 (1973).

NB-7

Parametric Evaluation of Collisional Processes in an E-Beam Sustained CO Laser.* D. J. PISTORESI and D. J. NELSON, Boeing Aerospace Company, Seattle, WA.-- Evaluation of CO molecular and electron/molecular processes by comparison of CO kinetics model predictions with experimental results shows laser efficiency and after-spiking behavior as a function of E/N for electron excitation cross sections of Hake and Phelps, Schulz, Ehrhardt, as well as combinations thereof. Laser efficiency predictions demonstrate a stronger dependence on E/N for the Hake and Phelps low energy cross sections as compared with those of Schulz, and Ehrhardt. The predicted after-spike characteristics are shown to depend on the strong electron down pumping occurring for the higher level superelastic collisions. Experimental results from a supersonic CO pulsed electrical discharge laser agree well with the functional dependence of the values predicted by combining the low energy Hake and Phelps cross sections with the high energy Ehrhardt cross sections.

*Submitted by W. Maher.

NB-8

Experimental Findings on the Glow-Arc Transition in Discharges in the Supersonic CO Laser.* M. F. WEISBACH and D. J. NELSON, Boeing Aerospace Company -- Although the measurable quantities, which characterize the onset of the glow to arc transition in electric discharges, vary considerably as the discharge parameters (gas density, e-beam current density, pulse length, gas mixture) are changed, several features have been observed, in the supersonic CO laser, which may aid in assessing theories pertaining to the cause of the discharge instability. (1) The behavior (as characterized by E/N and J) is essentially independent of the physical size of the discharge. (2) Although the average electron energy at which the glow to arc transition occurs varies with the discharge parameters, it is independent of the makeup of the noble gas diluent mixture. (3) There are two distinct time scales involved in the rise of the discharge current density. The first, which is associated with electron collision processes requires 1-2 μ sec; this is followed by a much more gradual temporal increase, which continues for approximately 100 μ sec, with a slope that increases with increasing E/N.

*Work supported in part by AFWL.

INDEX TO ABSTRACTS

- Abouaf, L. JA9, JA10
 Abouaf, R. MA3
 Adams, N. G. LB10, NA1, NA2, NA3
 Albritton, D. L. LB11, NA4
 Alcock, A. J. DA4
 Ali, A. W. LA9
 Allis, W. P. GB3
 Ambrose, J. G. JB2
 Amme, R. C. JB5
 Anderson, J. A. JA7
 Anderson, J. H. LA2
 Anderson, R. J. GA3
 Anderson, R. S. LA7
 Anderson, R. W. DB1
 Anicich, V. G. NA8
 Bacal, M. FA11
 Bailey, W. F. HB4
 Bakker, M. KA3
 Bardsley, J. N. KB3
 Barnard, A. J. AB8
 Bastien, F. KA3
 Bearman, G. H. JB8
 Beaty, E. C. HA11
 Bedford, R. HB10
 Benedict, R. P. FB7
 Benenson, D. M. DB6
 Bergman, R. S. AB2, GB2
 Bhattacharya, A. K. GB1
 Biblarz, O. HB1
 Biondi, M. A. KB6, KB7, NA9
 Bischel, W. K. LB2
 Bleekrode, R. AB6
 Blevin, H. A. FA10
 Bohn, W. L. LA4
 Boness, M. J. W. FA3, I
 Bonifield, T. D. JA1
 Boody, F. P. LA2
 Borzileri, C. HB10
 Boulmer, J. HA6
 Boxman, R. CB7
 Boyer, J. K. LA10
 Brau, C. A. CA6, E1
 Bricks, B. G. LA7
 Brion, C. E. GA8
 Brunner, W. HB10
 Burnham, R. AA3
 Burrage, L. M. CB8
 Burrow, P. D. GA1, GA4, I
 Buttler, W. LB1
 Carroll, J. M. LA8
 Cartwright, D. C. BA1, GA7
 Center, R. E. AA6
 Champagne, L. F. CA1, CA5
 Chang, J-S. HB8, NA5
 Chang, R. S. F. LB5
 Chantry, P. J. FA1
 Chen, A. K. NA9
 Chen, C. H. E, NA7

Chen, C. L. BB4, BB5, CB4, E, FA1.
 Chen, H-L. HB10
 Chen, S. T. HA2
 Cherrington, B. E. DA5, I
 Chien, Y-K. DB6
 Church, M. J. KB1, KB2
 Cleary, M. J. HB3
 Clodius, W. B. MA8
 Cohen, J. S. BA1
 Collins, C. B. JA7, LA8, NA6
 Collins, G. J. FB2, LA10
 Compton, R. N. FA4, JB11
 Cosby, P. C. BA5, MA3, MA5, MA6, MA7
 Coxon, P. NA10
 Crispin, Y. HB1
 Crompton, R. W. FA6
 Cunningham, A. J. LB6
 Daugherty, J. D. MB3
 Davies, D. K. CB4
 Day, R. L. GA3
 de Groot, J. J. AB4
 Dehmer, J. L. BA3
 Dehmer, P. M. BA3
 Delcroix, J. L. LA11
 Delpech, J.-F. HA6
 Denes, L. J. MB4
 Dettmer, J. W. HB4
 Devos, F. HA6
 de Vries, C. P. HB9
 Dotan, I. LB11, NA4
 Doucet, H. J. FA11
 Driscoll, J. F. DB1, DB3
 Drummond, D. L. FB6, FB7
 Dunning, T. H. AA1
 Ecker, G. H. AB9, KA5
 Eckhardt, G. CB3
 Eden, J. G. AA5
 Eliasson, B. DB4
 Ernie, D. W. LB7
 Evangelista, Y. S. MB1
 Ewing, J. J. JA4, JA5, LB3
 Fairchild, C. E. MA1, MA2
 Falconer, W. E. JB3
 Farrall, G. A. CB9
 Feeney, R. K. HA12
 Fehsenfeld, F. C. LB11, NA4
 Feldman, B. J. MB2
 Feldman, D. W. LA5, LA6, MB1
 Feldman, R. B. LA5
 Finn, T. F. CA1
 Fisher, C. H. AA6
 Fisher, R. A. MB2
 Flannery, M. R. E4, I
 Fletcher, J. FA7, FA8, FA9, FA10
 Flinsenberg, H. J. AB3
 Foltyn, S. R. FA7, FA8, FA9
 Fournier, G. HB5
 Franklin, R. D. CA8, JA4, JA5
 Freeman, R. R. JA6
 Froelich, H. R. KB5

Futrell, J. H. MA10, NA8
 Gallagher, A. FB3, FB4, FB5, HA2
 Garrett, W. R. FA5
 Garscadden, A. HB4, I
 George, E. V. JA2
 Glickler, S. L. MB3
 Glosik, J. LB10
 Goble, J. H. LB4
 Golden, D. HA10
 Goldhar, J. BA8
 Goldman, M. KA1
 Goldsmith, S. CB7
 Greene, A. E. CA6
 Grief, D. NA1
 Griffin, S. DA5
 Haas, R. A. CA8, I, JA4, JA5
 Hackmann, J. KA8
 Haddad, G. N. HA10
 Hall, R. J. FA2
 Hanson, R. K. NB4
 Harmann, G. KA2
 Harris, L. P. CB2
 Hartman, D. C. LB4
 Haugsjaa, P. BB1, BB2
 Hawryluk, A. CA4
 Hay, P. J. AA1, BA1
 Hayes, M. HB10
 Heberlein, J. V. R. CB5
 Hefferlin, R. FB11
 Henson, B. L. NA12
 Hickman, A. P. GA5
 Hirsh, M. KA1, KA2
 Hobbs, R. H. BA2
 Hobson, R. M. HB8, NA5
 Homsey, R. J. LA7
 Hong, S. P. HA11
 Howton, C. BA6
 Hozack, R. S. JB3
 Hsia, J. CA4
 Huang, C. M. KB7
 Huber, B. A. MA3
 Hudda, F. G. CB9
 Huebner, R. H. GA1, GA2
 Huestis, D. L. AA2, FB1, FB10, JA10
 Hughes, W. M. AA4
 Hunter, R. O. BA6
 Hunter, S. R. FA7, FA8, FA9, FA10
 Huntress, Jr., W. T. NA8
 Hyman, H. A. HA3
 Ingold, J. H. AB2, GB2
 Isaacs, G. G. KA6
 Jacob, J. H. CA2, CA3, CA4
 James, P. B. JB2
 Jensen, S. W. HA4, HA5
 Johnsen, R. KB7, NA9
 Johnson, D. CB6
 Johnson, S. G. GB6
 Johnston, R. H. CB9
 Jolly, J. LA11
 Jones, P. L. MA10
 Jones, W. W. LA9

Jordan, D. L. KA6
 Jordan, K. D. GA4
 Judish, J. P. E, NA7
 Kallne, E. AB8
 Karras, T. W. LA7
 Kasner, W. H. DA3, MB1
 Katayama, D. H. BA4
 Keijser, R. A. J. GB5
 Kempe, E. E. GB8
 Kligler, D. LB2
 Kline, L. E. DA3, GB4, MB4, NB3
 Klots, C. E. FA4
 Kofoid, M. J. KA4
 Korff, D. MB3
 Laframboise, J. G. HB8
 Lake, M. L. I
 Langhoff, S. FB9
 Laskowski, B. FB9
 Laudenslager, J. B. NA8
 Lawrence, G. M. MA1, MA2
 Lecuiller, M. HB5
 Lee, F. W. NA6
 Lee, L. C. BA5, MA5, MA6
 Leep, D. FB3, FB4
 Leiby, Jr., C. C. NA11
 Leopold, K. E. DA4
 Leventhal, J. J. JB2, JB8
 Liao, P. F. JA6
 Liebermann, R. W. BB4, BB5
 Lighthart, F. A. S. GB5
 Lineberger, W. C. MA10
 Little, W. L. LA10
 Liu, C. H. DB5
 Liu, C. S. LA5, LA6
 Long, Jr., W. H. BA7, DA2, GB9
 Lorents, D. C. FB1, JA9, JA10
 Lucas, R. HB5
 Maier, W. B. JB7
 Mandl, A. LB3
 Mangano, J. A. CA2, CA3, CA4, I
 Mani, S. A. LA3
 Margevicius, J. A. FB1, JA9, JA10
 Marode, E. KA3
 Mathur, B. P. JA8
 Maya, J. FB8
 Michejda, J. A. GA4, I
 Michels, H. H. BA2
 Miley, G. H. LA2
 Miller, T. M. BA5, KB2, NA3
 Milloy, H. B. GA6
 Mitchell, J. B. A. KB5
 Mitchell, R. R. MB4, NB3
 Mitchner, M. NB4
 Mitterauer, J. CB1
 Moeny, W. M. NB5
 Monson, D. J. NB6
 Moran, T. F. JB6
 Morgan, W. L. CA8, FB5, I, JA5
 Moruzzi, J. L. NA10
 Moseley, J. T. MA3, MA5, MA6, MA7

Murphy, R. A. MB6
 Murray, J. R. BA8
 Myers, G. D. JB2, LB6
 McAfee, K. B. JB3
 McArthur, D. A. LA1
 McClure, D. J. JB3
 McCusker, M. V. BA6, FB1, JA9, JA10
 McGowan, J. W. KB5
 McNeill, W. BB1, BB2
 Nagalingam, S. J. S. LA2
 Nagamatsu, H. T. DB2
 Nelson, D. J. NB7, NB8
 Neynaber, R. H. LB8, LB9
 Nicolopoulou, E. FA11
 Nighan, W. L. DA1, FA2, I
 Novick, S. E. MA10
 Nygaard, K. J. FA7, FA8, FA9
 Ogram, G. L. HB8, NA5
 Oldenettel, J. BA6
 O'Loughlin, J. P. NB5
 Oskam, H. J. HB9, LB7
 Oster, L. HB2
 Pack, J. L. DA3
 Palmer, A. J. HB7
 Palumbo, L. J. CA1
 Partlow, W. D. GB4
 Paulson, J. F. BA4, JB9
 Payne, M. G. E, NA7
 Peterson, J. R. MA5, MA7
 Pfender, E. CB6, DB5
 Phelps, A. V. FB3, FB5
 Pigache, D. HB5
 Pistoresi, D. J. NB7
 Poe, R. T. HA5
 Pollock, C. R. MB2
 Popescu, D. JA7
 Popescu, I. JA7
 Powell, H. T. JA3, JA4
 Prelas, M. A. LA2
 Prince, R. H. NA5
 Pritchard, D. LB2
 Quigley, G. P. AA4
 Rakshit, A. B. LB10
 Rambow, F. H. K. JA1
 Reck, J. JA8
 Regan, R. BB1, BB2
 Register, D. F. HA4, HA5
 Reid, I. D. FA6
 Rhodes, C. K. LB2
 Robb, W. D. HA1
 Rogoff, G. L. DA3
 Rokni, M. CA2, CA3, CA4
 Roman, W. C. BB3
 Rose, T. L. BA4
 Rothe, D. E. CA7
 Rothe, E. W. JA8
 Rothwell, H. L. FB4, JB5
 Futherford, J. A. JB4
 Salem, A. NA5
 Sarjeant, W. J. DA4, MB5
 Sayle, W. E. HA12

Schade, E. DB4
Schearer, L. D. KB4
Schenck, P. K. HB6
Schlie, L. A. FB6, FB7
Schlotter, N. E. AA2
Schuessler, H. A. JB1
Searles, S. K. AA3
Setser, D. W. E2, LB5
Sharpton, F. A. GA3
Shay, T. FB2
Shiu, Y-J. KB6
Shuker, R. FB5
Simmons, M. DA5
Simons, S. W. MB2
Smith, D. KB1, KB2, LB10,
NA1, NA2, NA3
Smith, F. T. GA5
Smith, G. P. BA5, MA5, MA6, MA7
Smyth, K. C. HB6
Spence, D. GA1, GA2, HA7, HA8, HA9
Spreadbury, R. J. MB4
Srinivasan, G. NB6
Stallcop, J. FB9
Stamm, M. R. HB4
Stanton, A. C. NB4
Stehman, R. M. MA8, MA9
Steph, N. HA10
Stockdale, J. A. D. JB11
Stockton, M. HB3
Stone, E. J. MA1
Suhre, D. R. NB1, NB2, NB3

Sutcliffe, V. C. HA10
Szoke, A. JA2, JA3
Tadjeddine, M. MA3
Tan, K. H. GA8
Tang, S. Y. LB8, LB9
Taylor, G. W. LB5
Taylor, K. N. LA8
Taylor, L. H. LA5, MB1
Taylor, S. A. HB3
Tercovich, R. G. MB2
Thomson, R. M. MB7
Trainor, D. W. FA3, LA3
Trajmar, S. HA4, HA5
Tuma, D. T. CB4
Turner, R. MB6
Twiddy, N. D. LB10
Uhlenbusch, J. KA8
Utterback, N. G. JB10
Van den Hoek, W. J. AB7
Vanderhoff, J. A. MA4
Van der Leeuw, Ph. E. GA8
Van der Wiel, M. J. GA8
van Gemert, M. J. C. GB7
van Vliet, J.A.J.M. AB4
Van Zyl, B. JB5, JB10
Velazco, J. E. FB2
Verbeek, T. G. GB7
Verdeyen, J. T. DA5
Visser, J. A. AB7
Vriens, L. GB5
Vroom, D. A. JB4

Pellen 282-3847
678 Corbett Av.

Wadehra, J. M. KB3
Wadt, W. R. BA1
Walters, G. K. JA1
Warmack, R. J. JB11
Wasserstrom, E. HB1
Waszink, J. H. AB3
Waynant, R. W. AA5
Weaver, L. A. LA6
Weber, E. W. LB1
Weisbach, M. F. NB8
Werner, C. W. JA5
West, J. B. BA7
Whealton, J. H. KA7
Whitaker, M. KB7
Whitson, J. C. KA7
Wilcox, J. B. JB6
Willis, C. MB5
Winn, J. S. LB4
Witting, H. L. DB7
Wong, S. F. I
Woo, S. B. MA8, MA9
Wutzke, S. A. NB2, NB3
Wyner, E. F. AB5
Yang, T. P. E
Zabielski, M. F. BB3
Zollweg, R. J. AB1
Zondervan, K. L. DB1
Zondervan, K. P. DB1

30th ANNUAL GASEOUS ELECTRONICS CONFERENCE

October 18-21, 1977
Palo Alto, California

PARTICIPANTS

Adams, Nigel G., University of Birmingham
Akerman, Al, Union Carbide Nuclear Div.
Albritton, Daniel Lee, NOAA .
Allen, M., Yale University
Allis, W. P., MIT
Allison, John, Stanford University
Amme, Robert C., University of Denver
Anderson, Jon, University of Texas at Dallas
Arendt, Paul, Exxon Research

Bacal, Marthe, Ecole Polytechnique
Baily, Philip, Hughes Aircraft Co.
Bardsley, J. N., Los Alamos Scientific Laboratory
Barnard, A. J., University of British Columbia
Barreto, Ernesto, State University of N.Y.
Bearman, Gregory, University of Missouri
Behringer, Robert E., Office of Naval Research
Bender, Charles, Lawrence Livermore Laboratory
Benedict, Rett, Air Force Weapons Laboratory
Benenson, David M., State University of New York
Benson, R. C., Johns Hopkins University
Bergeman, Tom, Fordham University
Bergman, Rolf S., Cleveland Heights, Ohio
Bernhardt, David, State University of New York at Albany
Betts, Jeanette A., TRW
Beverly, R. E., Battelle Columbus Laboratories
Bhattacharya, A. K., General Electric Lighting
Bhaumik, M. L., Northrop Research & Technology Center
Biblarz, Oscar, Naval Postgraduate School
Bigio, Irving, Los Alamos Scientific Laboratory
Binns, Robert, McDonnell Douglas Research Laboratories
Biondi, M. A., University of Pittsburgh
Bischel, William, SRI International
Bokor, Jeffrey, SRI International
Boness, M. John, Avco Everett Research Laboratory
Bonifield, Thomas, Rice University
Boyer, Kirk, Colorado State University
Boxman, Raymond, Tel Aviv University
Bradford, Jr., R. S., Hadron
Brau, Charles, Los Alamos Scientific Laboratory

Bricks, B. Gerard, General Electric Co.
Brion, C., University of British Columbia
Buczek, Carl, United Technologies Research Center
Bullis, Robert H., United Technologies Research Center
Burckel, William, Air Force Weapons Laboratory
Burnham, Ralph, Naval Research Lab
Burrage, Lawrence M., Thomas A. Edison Technical Center
Burrow, Paul D., Behlen Laboratory

Cartwright, David C., Los Alamos Scientific Laboratory
Center, R. E., Mathematical Sciences N.W.
Champagne, Louis, Naval Research Laboratory
Chang, Robert S. F., Kansas State University
Chanin, L. M., University of Minnesota
Chantry, Peter J., Westinghouse Research Labs
Chen, C. H., Union Carbide Corporation
Chen, C. L., Westinghouse Research Lab
Chen, Hao-Lin, Lawrence Livermore Laboratories
Cherrington, Blake, University of Illinois
Chien, Kuei-Ru, TRW
Childress, II, John W., Northrop Research & Technology Center
Chou, Mau-Song, Exxon Research
Christensen, Paul, University of Southern California
Coggiola, Michael J., SRI International
Collins, Carl B., University of Texas at Dallas
Collins, George, Colorado State University
Cooper, Gary, University of Wisconsin
Cosby, Philip C., SRI International
Cramer, William H., National Science Foundation
Crandall, David H., Oak Ridge National Laboratory
Crane, John, University of Illinois
Crompton, Robert W., Australian National University
Curtis, Earl C., Rocketdyne

Davies, D. K., Westinghouse R&D Center
Dehmer, Patricia M., Argonne National Laboratory
Delcroix, J. L., University of Paris
Delpech, Jean F., University of Paris
Denes, Louis J., Westinghouse R&D Center
De Temple, Thomas A., University of Illinois
Dettmer, John W., USAF
de Vries, C., University of Minnesota
Dotan, I., NOAA
Dowell, Jerry T., IRT Corporation
Dreyfus, Russell W., IBM Research
Driscoll, James F., University of Michigan
Duzy, Carolyn, Avco Everett Research Laboratory

Eckhardt, Gisela, Hughes Research Laboratories
Eckstrom, Donald J., SRI International
Eden, J. Gary, Naval Research Laboratory
Eggelston, John, SRI International
Eimerl, David, Lawrence Livermore Laboratories
Ernie, Douglas, University of Minnesota
Ewing, J. J., Lawrence Livermore Laboratories
Fahlen, T. S., San Jose, California
Fairchild, Clifford E., Oregon State University
Farrukh, Usamah, Applied Sciences Technology Inc.
Fehsenfeld, F. C., NOAA
Feldman, D. W., Westinghouse R&D Center
Feldman, R. B., Pittsburgh
Filcoff, John, Air Force Weapons Laboratory
Finn, Tom, Naval Research Lab
Fisher, Charles H., Mathematical Sciences N.W.
Fisher, Edward R., Wayne State University
Fisher, Leon H., Atherton, Ca.
Fisher, Robert A., Los Alamos Scientific Laboratory
Fitaire, Marc, University of Paris
Fitzsimmons, William, National Research Group
Flamm, Daniel L., Bell Laboratories
Flannery, Ray, JILA
Foltyn, Steve, University of Missouri-Rolla
Fournier, Gerard, ONERA
Franklin, R. D., Lawrence Livermore Laboratory

Gaily, T. Dean, SRI International
Gallagher, Alan, JILA, NBS
Gardner, Phillip, GTE Sylvania
Garrett, W. R., Oak Ridge National Laboratory
Garscadden, Alan, Air Force Aeropropulsion Lab
Gatland, Ian R., Georgia Institute of Technology
Gerardo, J. B., Sandia Laboratories
Gerber, R. A., Sandia Laboratories
Gillen, Keith T., SRI International
Glickler, Sheldon, Avco Everett Research Lab
Golden, David, University of Oklahoma
Golden, S. A., Rocketdyne
Goldhar, Julius, Lawrence Livermore Lab
Gower, M. C., NASA-Ames Research Center
Graham, Walter J., Naval Surface Weapons Center
Green, B. David, Physical Sciences Inc.
Greene, Arthur, Los Alamos Scientific Laboratory
Griffin, Steven T., University of Illinois
Gutcheck, Robert, Palo Alto, Ca.

Haas, Roger, Lawrence Livermore Laboratory
Hackmann, Jobst, University of Dusseldorf
Hadley, S. G., Rocketdyne
Hargrove, Steve, Lawrence Livermore Laboratory
Harris, L. P., General Electric Co.
Harwell, Roger, Air Force Weapons Laboratory
Haugsjaa, Paul, GTE Laboratories
Hay, P. Jeffrey, Los Alamos Scientific Labs
Hays, G. N., Sandia Laboratories
Hazi, Andrew, Lawrence Livermore Laboratory
Heberlein, Joachim, Westinghouse Electric Corp.
Hefferlin, Ray, Southern Missionary College
Henson, Bob L., University of Missouri-St. Louis
Hewes, Ralph, General Electric
Hickman, A. P., SRI International
Hill, Robert, SRI International
Hirsh, Merle N., University of Minnesota
Hodgson, Rod, IBM Research
Hoff, Paul W., Department of Energy
Hohnstreiter, Glenn, Bell Laboratories
Hong, Siu-Ping, JILA
Hopper, Darrel, Science Applications Inc.
Hsia, James, Avco Everett Research Laboratory
Huang, Chou-Mou, University of Michigan
Hudson, David F., Naval Surface Weapons Center
Huestis, David L., SRI International
Hunter, Scott, University of Missouri
Husain, Javed, Stanford University
Hyde, Rod, Lawrence Livermore Laboratory
Hyman, Howard A., Avco Everett Research Laboratory

Jacob, Jonah, Avco Everett Research Laboratory
James, Douglas J., Lumonics Research
Jensen, Steve, University of California-Riverside
Johnsen, R., University of Pittsburgh
Johnsen, Russell H., Florida State University
Johnson, A. Wayne, Sandia Laboratories
Johnson, Dean C., University of Minnesota
Johnson, Stephen G., GTE Sylvania
Jones, P. L., JILA
Jones, Walter, Naval Research Lab
Jordan, David, Royal Signal and Radar Establishment
Judd, O., Los Alamos Scientific Laboratory
Junker, B. R., Office of Naval Research

Kan, Tehmau, Lawrence Livermore Laboratory
Karny, Ziv, Stanford University
Karras, Thomas W., General Electric Co.
Kasdan, Abraham, Exxon Research & Engr. Co.
Katayama, Daniel H., Air Force Geophysics Laboratory
Kempe, Ernest E., Naval Research Laboratory
Keyser, Rob. A. J., Philips Research Lab
Kiang, Teddy, Stanford University
Kligler, Daniel, RI International
Kline, L. E., Westinghouse R&D Center
Klots, Cornelius, Oak Ridge National Lab
Kofoid, Melvin J., Seattle, Washington
Kolpin, Marc, TRW
Konrad, G. T., Stanford Linear Accelerator Center
Korff, David, Avco Everett Research Laboratory/Univ. Lowell
Kramer, Jerry, GTE Labs
Kunkel, Wulf B., Lawrence Berkeley Laboratory

Lake, Max L., Universal Energy Systems
Lancashire, Richard, NASA-Lewis
Lane, Neal F., Rice University
Laskowski, Bernard, NASA-Ames
Laudenslager, James, Jet Propulsion Laboratory
Lawton, Stan, University of Illinois
Lee, Francis, University of Texas
Lee, L. C., SRI International
Leiby, C. C., RADC/ESO
Lengel, Russell, Stanford University
Levatter, Jeff, University of California-San Diego
Leventhal, J. J., University of Missouri-St. Louis
Levron, David, JILA
Lewittes, Mark, Colorado State University
Liao, Paul F., Bell Laboratories
Liebermann, Richard W., Latrobe, Pa.
Lin, Chum C., University of Wisconsin
Lippmann, B. A., Physics International
Little, Wendell, Colorado State University
Liu, C. S., Westinghouse Research Labs
Liu, Frank, Owens-Corning Fiberglas
Loeb, Leonard B., University of California
Long, Jr., W. H., Northrop Research & Technology Center
Loree, Thomas R., Los Alamos Scientific Laboratory
Lorents, Donald C., SRI International
Lubell, Michael S., Yale University

Maier, W., Los Alamos Scientific Laboratory
Mandl, A., Avco Everett Research Laboratory
Mangano, Joseph, Avco Everett Research Lab
Manikopoulos, C. N., State University of New York-Buffalo
Margevicius, Joseph, SRI International
Marode, E., CNRS
Maya, Jakob, GTE Sylvania
McAfee, Kenneth B., Bell Laboratories
McArthur, David A., Sandia Laboratories
McClure, Gordon W., Sandia Laboratories
McCusker, Michael V., SRI International
McGeoch, Malcolm, Avco Everett Research Laboratory
McKenzie, Robert L., NASA-Ames
McNeill, William, GTE Laboratories
Meson, John K., DARPA
Meyerott, Roland
Michejda, J. A., Yale University
Michels, H. Harvey, United Technology Research Center
Mickish, Roger A., Rocketdyne
Miller, Charles, Stanford University
Miller, John, Lawrence Livermore Laboratory
Miller, Thomas M., SRI International
Mitchell, Robert, Westinghouse Research Center
Mitterauer, Johannes, University of Technology Vienna
Moeny, William M., Albuquerque, N.M.
Mondelli, Alfred, Maxwell Laboratories
Monson, Daryl, NASA Ames Research Center
Morgan, Wm. Lowell, JILA
Morris, James, University of California-San Diego
Moruzzi, J. L., University of Liverpool
Mosburg, Earl R., National Bureau of Standards
Moseley, John T., SRI International
Muller, Clifford, University of California-Santa Barbara
Murray, John R., Lawrence Livermore Laboratory

Naaman, Ron, Stanford University
Nagamatsu, Henry T., Schenectady, New York
Nesbet, R. K., IBM Research
Neynaber, R. H., IRT Corporation
Nighan, William L., United Technologies Research Center
Nygaard, Kaare J., University of Missouri-Rolla
Nightingale, John, Exxon Research

Ogram, Geoffrey, York University
Olson, Robert A., SRL, Inc.
Osgood, Jr., R. M., MIT Lincoln Laboratory
Oskam, H. J., University of Minnesota
Oster, Ludwig, JILA
Ostermayer, Jr., Frederick W., Bell Laboratories
Ozenne, Jean-Bernard, SRI International

Pacala, Thomas, University of Southern California
Palmer, A. Jay, Hughes Research Laboratory
Palumbo, Louis, Naval Research Laboratory
Paquette, Guy, University of Montreal
Parks, Joel, Avco Everett Research Laboratory
Parton, William, Westinghouse Research
Patterson, E. L., Sandia Laboratories
Patterson, Paul L., Varian Instrument Division
Paulson, John F., Air Force Geophysics Laboratory
Pence, William H., JILA
Perry, B. E., SRI International
Pfender, E., University of Minnesota
Phelps, A. V., JILA
Pichler, Goran, JILA
Pilloff, H. S., Office of Naval Research
Pleasance, Lyn D., Lawrence Livermore Laboratory
Powell, Howard, Lawrence Livermore Laboratory
Prelas, Mark, University of Illinois
Preston, R. K., Lawrence Livermore Laboratory
Prosnitz, Donald, Lawrence Livermore Laboratory
Pummer, Herbert, SRI International
Quigley, G. P., Los Alamos Scientific Laboratory

Rambow, Frederick H. K., Rice University
Rapoport, William, Lawrence Livermore Laboratory
Reck, Gene, Wayne State University
Register, David, Jet Propulsion Laboratory
Rehder, Ludwig, Philips Research Laboratory
Reid, Ray, Colorado State University
Rescigno, T., Lawrence Livermore Laboratory
Rice, J. K., Sandia Laboratories
Rich, Joseph A., General Electric
Rich, Joseph William, Calspan Corporation
Robb, W. D., Los Alamos Scientific Laboratory
Roberts, Stuart, Leeds University
Roberts, Victor, General Electric Company
Rockwood, Steve, Los Alamos Scientific Laboratory
Rogoff, G. L., Westinghouse R&D Center

Rokni, Mordechai, Avco Everett Research Laboratory
Roman, Ward, United Technologies Research Center
Rothe, D. E., Northrop Research & Technology Center
Rothwell, Harold, University of Denver
Rumble, John, JILA
Rutherford, John A., IRT Corporation

St. John, Robert M., University of Oklahoma
Salop, Arthur, SRI International
Sandstrom, Richard, University of California-San Diego
Sarjeant, Jim, National Research Council
Saxon, Roberta P., SRI International
Schearer, Laird D., JILA
Scheps, Richard, Westinghouse R&D Center
Schlie, La Verne, Air Force Weapons Laboratory
Schlotter, N. E., SRI International
Schuebel, W. K., Air Force Avionics Laboratory
Schuessler, Hans A., Texas A&M University
Setser, D. W., Kansas State University
Sharp, Terry E., Lockheed Research Laboratory
Sharpton, Francis A., Northwest Nazarene College
Shay, Tom, Colorado State University
Shiu, Yueh-Jaw, University of Pittsburgh
Shuker, Reuben, JILA
Slanger, T. G., SRI International
Smith, David, University of Birmingham
Smith, Felix T., SRI International
Smith, G. P., SRI International
Smith, Kenneth, Leeds University
Smyth, Kermit C., National Bureau of Standards
Snow, William R., Rice University
Spence, David, Argonne National Laboratory
Srinivasan, G., NASA-Ames Research Center
Srivastava, Basuki, Avco Everett Research Laboratory
Stallcup, James R., NASA-Ames Research Center
Stanton, Alan C., Stanford University
Stockdale, John, Oak Ridge National Laboratory
Stockton, Marilyn, Dartmouth College
Stone, P. M., Department of Energy
Suhre, Dennis, Westinghouse R&D Center
Sutter, L. V., Hughes Aircraft
Sze, R. C., Los Alamos Scientific Laboratory
Szoke, Abraham, Lawrence Livermore Laboratory

Taillet, Joseph, ONERA
Tang, Kenneth Y., Maxwell Laboratories
Tang, S. Y., IRT Corporation
Taylor, Lyle H., Murrysville, Pa.
Taylor, Raymond, Physical Sciences Inc.
Thiess, Paul, Catholic University
Thomson, R. M., Leeds University
Thweatt, Weldon, U.S. Air Force
Tiernan, T. O., Wright State University
Tio, T. K., University of California-San Diego
Tisone, G. C., Sandia Laboratories
Trainor, Daniel W., Avco Everett Research Laboratory
Trenchard, Herbert A., Westinghouse Electric Corp.
Trivelpiece, Alvin W., Maxwell Laboratories
Turner, Jr., Charles E., Lawrence Livermore Laboratory
Turner, Robert, Johns Hopkins University
Twiddy, N. D., University College, Wales
Utterback, Nyle G., TRW Inc.

Vanderhoff, John A., Aberdeen Proving Ground
Van Gemert, Martin J. C., Philips Research Laboratory
Van Zyl, Bert, University of Denver
Velazco, J. Enrique, Colorado State University
Verdeyen, Joseph, University of Illinois
Von Rosenberg, Jr., C. W., Avco Everett Research Laboratory
Vroom, David, IRT Corporation
Wadehra, J. M., Los Alamos Scientific Laboratory
Watt, Willard R., Los Alamos Scientific Laboratory
Wakalopoulos, George, Hughes Aircraft Co.
Walker, Keith G., Bethany Nazarene College
Walters, G. K., Rice University
Wang, Charles, Aerospace Corporation
Warmack, Robert J., University of Tennessee
Warner, Bruce, University of Colorado
Watt, William, U.S. Naval Research Laboratory
Weber, E. W., Stanford University
Weisbach, Michael F., Seattle, Wn.
Wells, William, Miami University
West, John B., Northrop Research & Technology Center
West, William P., University of California-Santa Barbara
Wexler, Bernard L., Naval Research Laboratory
Wharmby, D. O., Thorn Lighting Ltd.
Whealton, J. H., Oak Ridge National Laboratory
White, Jonathan, Stanford University
Wiegand, Walter, United Technologies Research Center
Williams, Frazer, Texas Tech University

Winans, J. Gibson, Buffalo, N.Y.
Winn, John, University of California-Berkeley
Winter, N., Lawrence Livermore Laboratory
Witting, Harald L., General Electric
Wong, S. F., Yale University
Wright, Michael D., Stanford University
Wu, Richard L. C., Wright State University
Wutzke, Steve, Westinghouse R&D Center
Wyner, Elliot, GTE Sylvania
Yadavalli, S.
Zollweg, Robert J., Westinghouse R&D Center

Van Den Hoek, W. J., Philips Research, Light Division

Bohn, Willy L, DFVLR, Stuttgart
Bortner, M. H., GE, Valley Forge, PA
Douglas-Hamilton, D. H., AVCO-Everett
Giguere, Robert, Aerospace Corp.
Gunton, Rupert, Lockheed, Palo Alto
Huntess, Wesley T., JPL, Pasadena
Moran, T. F., Chem. Dept., Georgia Tech.
Pistoressi, D., The Boeing Co., Seattle
Stehman, R. M. Northwestern, Ill. University
Taylor, Kenneth, University of Texas, Dallas
Thomas, J. K., UCLA
Wong, J., Hughes Aircraft Co.
Woo, Shien-Biau, University of Delaware